КОЛЛОИДНЫЙ
ЖУРНАЛ

5

WITHDRAWN
POSTMASTER:
IF NOT DELIVERABLE NOTIFY
Chemical Abstracts
OHIO STATE UNIV., COLUMBUS 10, O.
AND POSTAGE WILL BE [illegible]
REC'D. MAR 21 1958
ABSTRACTOR
PLEASE RETURN PROMPTLY TO
CHEMICAL ABSTRACTS
OHIO STATE UNIV., COLUMBUS 10, O.

COLLOID JOURNAL

(KOLLOIDNY ZHURNAL)

(1957)

IN ENGLISH TRANSLATION

VOL. 19 NO. 2

CONSULTANTS BUREAU, INC.
227 WEST 17TH STREET, NEW YORK 11, N. Y.
an agency for the interpretation of international knowledge

COLLOID JOURNAL

(KOLLOIDNY ZHURNAL)

Journal of Theoretical and Applied Physics and
Chemistry of Colloids

Volume XIX

(Number 2, March-April, 1957)

Editor

A. V. Dumansky

Editorial Board

P. N. Antipov-Karataev, B. V. Deryagin, B. A. Dogadkin (Deputy Editor), A. V. Dumansky,
V. A. Kargin, S. M. Lipatov, P. A. Rebinder, I. P. Serdobolsky (Secretary), M. P. Volarovich

Publication of the Academy of Sciences of the USSR

IN ENGLISH TRANSLATION

Copyright, 1957

CONSULTANTS BUREAU, INC.
227 West 17th Street
New York 11, N. Y.

Printed in the United States

Annual Subscription	$ 80.00
Single issue	20.00

Note: The sale of photostatic copies of any portion of this copyright translation is expressly prohibited by the copyright owners. A complete copy of any paper in this issue may be purchased from the publisher for $ 7.50.

ON THE FIFTIETH BIRTHDAY OF

Valentin Alekseevich Kargin

January 23, 1957 was the fiftieth birthday of the eminent Soviet scientist and social worker, Valentin Alekseevich Kargin. The fruitful scientific and organizing activity of V. A. Kargin in the fields of physical and colloid chemistry is well known to the scientific community.

V. A. Kargin began his working life at the age of fifteen. In 1924, as a youth of seventeen, he commenced scientific work in the L. Ya. Karpov Physicochemical Institute, and his first scientific paper, on analytical chemistry, was already published in 1926. Without leaving his research work, V. A. Kargin studied at the Moscow State University, where he graduated in 1930. During the same period V. A. Kargin worked in Academician A. E. Fersman's group on radioactive ores, and also in the laboratory of the "Russian Gems" Trust, and by the time of his graduation he had published more than ten original scientific researches. V. A. Kargin's subsequent activity developed mainly in the fields of colloid chemistry and the physical chemistry of high polymers. Being already at that time an eminent specialist in the field of analytical chemistry, well acquainted with rare minerals, V. A. Kargin took part in the discovery of valuable mineral deposits in his capacity of geochemist to the Pamir expedition in 1932-1934.

In 1936 V. A. Kargin's creative scientific activity was recognized by the award, without presentation of a dissertation, of the degree of Doctor of Chemical Sciences. From 1937 to the present day he has been the head of the Colloid Chemistry Laboratory at the L. Ya. Karpov Physicochemical Institute. In 1946 he was elected an associate member, and in 1953 a full member of the Academy of Sciences USSR. His work has been rewarded by three Stalin prizes and two Bakh prizes. He has received the Order of Lenin and the Order of the Red Banner of Labor.

V. A. Kargin, jointly with his pupils and associates, has published about 200 papers. Kargin's earlier papers mainly dealt with research into hydrophobic colloids. In these papers he demonstrated the erroneous nature of the views, prevalent at that time, on the causes of stability in colloid systems, and proved experimentally the need for studying the chemistry of the phenomena in such systems. He proved that reactions between various colloids occur in true solutions, and not by coalescence of the particles. In addition to this work, V. A. Kargin carried out original research on the preparation of metal organosols and studied the properties of these systems. A large series of his papers dealt with studies of the properties of soil colloids. In recent years he has taken up work on the mechanism of formation of aluminosilicate systems, using the results of his earlier investigations on the mechanism of formation of colloidal particles.

V. A. Kargin made wide use of electrochemical methods for studying colloidal systems and developed a number of new techniques. Among these mention must be made of the use of high-voltage electrodialysis for purification of colloidal systems, multichamber electrodialysis for synthesis of colloidal systems and for separation of different substances, and the development of an electrochemical method for evaluation of anti-corrosion coatings.

In the 1930's V. A. Kargin began his research in the field of high polymers. In his earlier papers in this field it was shown that polymer solutions are true equilibrium, thermodynamically stable systems. By using electrochemical methods, he succeeded for the first time in making a detailed study of the chemical composition of viscose, and its changes during the ripening process. By the combined use of X-ray and electronographic methods V. A. Kargin established the amorphous nature of cellulose structure, despite the existing views on its microcrystalline structure. V. A. Kargin's further work on high polymers has been in connection with the relationships between the structure and the mechanical and physicochemical properties of polymers. Of this extensive series of investigations covering many years, mention must be made of the work on the properties of amorphous linear polymers, in which the glassy, high-elastic, and viscofluid states of these polymers were studied in detail and the relationships between these states and the chain structure of the molecules were demonstrated. A further development of this line of investigation has been the extensive study, during recent years, of the properties of crystalline polymers; in this work V. A. Kargin was able to demonstrate the erroneous nature of the application to such systems of the theories developed for low-molecular crystalline substances, and to indicate the future development of the theory of the crystalline state in polymers.

Of the other directions of V. A. Kargin's research on polymer properties we shall mention only the work on the properties of gels, in which the mechanism of gel formation was revealed, and studies of the mechanism of flow of structurized polymer systems, which have provided an approach to studies of polymer processing. V. A. Kargin is carrying out extensive work in organizing research on high polymers, correlating theoretical work in this field with concrete production problems.

V. A. Kargin is directing scientific control over important problems on the production and processing of polymers on an All-Union scale; he is the chairman of the Commission on High Polymers at the Academy of Sciences USSR,; and is closely associated with the chemical institutes of the Academies of Sciences of the Uzbek and Georgian SSR, and a large number of branch institutes. In the technology of production of processing of polymers, V. A. Kargin has shown new and original routes which have led to many important results utilized in our industry.

During the years of V. A. Kargin's scientific activity a group of scientific workers, developing the lines of research created by him, has arisen. The work of V. A. Kargin and his school has exerted a great influence on the development of Soviet physical and colloid chemistry. He organized and directed the Department of High Polymers at the Moscow State University.

In addition to his scientific, teaching, and organizing work, he has numerous social activities, being a deputy at the Moscow City Council of Deputies for several terms, working for many years as a member of the Plenum of the Higher Certification Commission at the Ministry of Higher Education of the USSR, and participating in the work of scientific societies.

V. A. Kargin has been a member of the Editorial Board of Colloid Journal for many years.

With all our hearts we wish our beloved Valentin Alekseevich Kargin health, strength, and creative successes in his varied fruitful activities for the good of our great Fatherland.

Z. Ya. Berestneva and G. L. Slonimsky

~~THE~~ STRUCTURE OF LINEAR POLYMERS

V. A. Kargin, A. I. Kitaigorodsky, and G. L. Slonimsky

As is known, long chain molecules are flexible and therefore become coiled under the influence of thermal motion. This is the reason for the appearance of high-elastic properties in polymers, and for the anomalies in their physical properties. The ability of chain molecules to change their configuration is especially prominent in orientation effects during deformation of amorphous and crystalline polymers, and during flow of polymer solutions. The hypothesis of the easy coiling of chain molecules has been finally confirmed by the recent investigations of the configuration of chain molecules, by the possibility of obtaining a number of linear polymers in globular form, and by other experimental data. This has provided the basis for the development of modern views on the arrangement of chain molecules in amorphous polymers and on orientation in crystallization of polymers. This has given rise to the concept of polymers as systems of chaotically entangled, coiled chain molecules. However, modern data on the structure of matter lead to the conclusion that the packing of chaotically coiled chain molecules, having flexibility owing to rotation about the C – C bonds, cannot be dense enough to account for the experimentally observed densities of polymers.

On the other hand, electron-microscopic observations show that the arrangement of chain molecules in polymers corresponds in some cases to systems of molecules coiled on themselves into globules, and in others to systems of chain bundles, in which each chain has largely the same neighbors.

Thus the generally accepted picture of the molecular arrangement in amorphous polymers must be reviewed.

In our view, amorphous polymers are composed either of chains coiled into globules, or of packets of uncoiled chains. The mechanical and other physical properties of polymers consisting of packets of chains can be satisfactorily explained by this model because of the inevitable flexibility, with several possible structural mechanisms, of the packets themselves. Examples of such mechanisms may be the untwisting of a region of the packet within which the chains are twisted into spirals, or coordinated rotation of one region of the packet relative to another, about C – C bonds. Further structural investigations of this question are, of course, necessary. It is also necessary to develop a statistical theory of deformation of elastic polymers based on this model. It should be pointed out that the above views on the structure of amorphous polymers refer not only to the high-elastic and glass states, but also to the viscofluid state. Indeed, as is known, liquids consisting of rodlike molecules of low molecular weight contain packets of molecules: each molecule is surrounded by other molecules, predominantly arranged with the same axial orientation. Although these packets (sometimes termed "swarms") are not thermodynamically stable formations, they are nevertheless always present in such liquids. This applies in greater force to polymers. It must be stressed that, in consequence of the well known slow nature of mechanical relaxation processes in polymers, the life of a packet of long chain molecules must be exceptionally long, while in the glassy state the bundles will remain practically unchanged.

These concepts of the structure of amorphous polymers naturally necessitate a revision of the views on the structure of crystalline polymers. The picture, widely accepted at the present time, of the structure of a crystalline polymer as a system of small ordered domains linked by common chains passing successively through regions of oriented and disordered parts of the chains, cannot be valid in the form in which it is usually presented. This follows even on purely geometrical considerations: on the basis of the quite well known dimensions of the ordered domains and the distances between them it is impossible to construct a polymer model in which the chains would leave an ordered domain, become twisted, and then again form an ordered domain. There is no doubt that any one chain passes through several domains of order and disorder. However, the chain does not leave the limits of its packet, and largely retains its same neighbors along its entire length.

In the proposed model, the degree of order of a polymer is determined by the structure of the packets of chain molecules, since all the packets are of the same type. The order of the packet depends on the degree of lateral order of its molecules and on the alternation of ordered and disordered domains along the packet. The latter is associated with the mechanical stresses which invevitably arise within the packet with growth of the ordered domains. These stresses, which oppose further growth of the ordered domains, can be appreciably diminished only by alternation of the domains of order and disorder along the packet. The proposed model for the molecular structure of amorphous and crystalline polymers must be amplified by structural investigations and analysis of various physical properties of polymers. The structure of polymer systems consisting of individual molecules coiled into globules must be considered separately.

SUMMARY

1. Consideration of modern data on the structure of matter and the latest results of polymer research makes it necessary to review the generally accepted views on the arrangement of molecules in amorphous and crystalline polymers.

2. A new model for the molecular structure of amorphous and crystalline polymers is proposed.

The M. V. Lomonosov State University, Moscow
The Institute of Elementoorganic Compounds Acad. Sci. USSR
Moscow

Received December 28, 1956

MOLECULAR CONFIGURATION AND STRUCTURE FORMATION IN POLYACRYLATE SOLUTIONS

V. A. Kargin and N. F. Bakeev

Determination of the configuration and relative disposition of macromolecules in polymers presents perhaps one of the most interesting and important problems. The existing views on polymer structure are, unfortunately, largely speculative, and not confirmed by direct experimental data. The structure of amorphous polymers is generally regarded as comprising quite randomly and chaotically twisted polymer chains, having the configuration of irregularly coiled globules resulting from their flexibility.

The answer to the question of configuration and relative disposition of macromolecules should in the first instance be sought by the use of structure analysis and direct observations of molecules. The low resolving power of optical microscopy (maximum 2000 A) does not allow of its use for studying the structure of polymers, although their molecules are of enormous size. It is also difficult to determine the arrangement and configuration of a polymer chain molecule along its entire length by means of structure analysis, since the magnitudes of the distances given by structure analysis are not great. Apparently the best method is that of electron microscopy, which has been widely used for studying high polymers. By the use of the electron microscope in high polymer studies it has been possible to see individual macromolecules [1], the dimensions of which proved to be within the resolution limits of the electron microscope, and also to study the elements of "secondary structure" in high polymers.

We have therefore used electron microscopy for studying the configuration of polyelectrolyte macromolecules, and the nature of their aggregation and structure formation in solutions. By a gradual increase in the concentration of the polymer solution, we passed from observations of individual isolated molecules to their aggregates, since use of the electron microscope for investigations of condensed systems of polymers cannot reveal their structure because of the high density of the object under examination.

The materials chosen for the study were polyacrylic acid and its salts: the barium, sodium, cesium, and quaternary ammonium salts. The choice was determined by the known structure of the polyacrylic acid chain and the ease with which its configuration may be varied in different media. The universal electron microscope UEM-100 was used for the investigations. The material was prepared by the method described in the literature [2], by application of a drop of the solution onto a supporting film placed on a gauze. To eliminate the influence of the support, two types of support were used in parallel investigations: collodion and structureless quartz. The electron microscopy was carried out with direct electron-optical magnification of 20,000-25,000 with subsequent photographic enlargement. To test the reproducibility of the results each solution used was prepared a number of times. Numerous electron micrographs (100-150 for each solution) were taken for each series of solutions. The results of this investigation are therefore based on repeatedly checked and completely reproducible data. The polyacrylic acid used was prepared by polymerization of acrylic acid, the molecular weight of the fractionated acid was determined viscosimetrically, using the constant $K_m = 2.9 \cdot 10^{-4}$, found by Staudinger [3] for aqueous polyacrylic acid solutions. The molecular weights found for several samples of polyacrylic acid were within the range of 1,000,000-3,000,000.

A micrograph of pure polyacrylic acid is shown in Fig. 1,1. Single isolated globules of spherical shape, and always symmetrical, can be seen. The size of the individual globules is in the range of 100-150 A. The molecular dimensions were calculated from the molecular weight of the polyacrylic acid used, on the assumption that each chain constitutes a coiled globule and that the density of the globule is equal to the density of the polymer mass. The calculated diameter of such a globule is approximately 100 A. Hence it may be concluded that most of the globules seen in the photographs are individual molecular chains. Formation of "secondary" structures was observed on increase of the acid concentration. These are fairly compact structures, formed by individual symmetrical globules joined together without interpenetration.

Barium polyacrylate (Fig. 1, 2), like pure polyacrylic acid, is characterized by "secondary" structures of a globular type, formed by union of symmetrical globules of molecular globule dimensions (80-100 A). Symmetrical globules which are not involved in secondary structure formation correspond in size to coiled molecular chains. The diameter of such globules are also about 80-100 A.

The analogous behavior of pure polyacrylic acid and of its barium salt, seen in the formation of similar secondary structures and single symmetrical globules, consisting of coiled molecular chains, is explained by the similar configuration of the long chain polyions in solution. Polyacrylic acid is a weak polymeric electrolyte. The weak acid is ionized only partially in the pure solvent (water in this case), and the intramolecular forces of electrostatic repulsion between the ionogenic (carboxyl) groups, covalently linked to the molecular chain, are small and not sufficient to straighten the molecule. The flexible polyion assumes a random ring configuration under the action of thermal forces. Of course, such a polymer globule will have a more diffuse structure than barium polyacrylate, where the thermal forces are augmented by large intramolecular forces caused by the presence of bivalent barium and its interaction with the carboxyl group, pulling the globule into a more dense formation. The viscosities found for polyacrylic acid and barium polyacrylate confirm the more diffuse structure of the molecular globules of polyacrylic acid in comparison with its barium salt.

It appeared of considerable interest to study the molecular configuration of polyacrylic acid after introduction of univalent cations, capable of increasing the degree of dissociation of the carboxyl groups, into its side chains. In this case it is to be expected that intramolecular forces of electrostatic repulsion between the charged segments of the chain should lead to increased rigidity and straightening of the molecular chains. The following salts were studied: polyacrylates of sodium, cesium, and quaternary ammonium bases. The relationship between polyacrylate viscosity and the degree of neutralization was investigated. This relationship could be represented by the type of curve shown in Fig. 2 for all the salts. The viscosity rises sharply on addition of alkali and reaches a maximum at pH 6.5, which corresponds to approximately 80 % neutralization. Further additions of alkali decrease the viscosity, and with excess alkali the viscosity reaches a definite limiting value.

The salts used for the electron microscopy were neutralized to pH 6.5, corresponding to maximum viscosity, and therefore to maximum molecular asymmetry.

Electron micrographs of sodium polyacrylate are shown in Figs. 1, 3, 4 and Fig. 3,1. The micrographs of sodium polyacrylate do not resemble those of pure polyacrylic acid or its barium salt. The secondary structures of sodium polyacrylate have totally different configuration and structure. The structure is unfolded, composed of curved threads of varying density and length; it is a typical fibrillar structure in which the fibrils are joined in the most random manner. The transverse dimensions of the fibrils lie in the range of 60-120 A. These fibrils are apparently formed from several molecular chains joined together in a definite manner into "packets" which participate in that form in the formation of secondary structures. From the dimensions of the molecule of maximum asymmetry, the distances between them (approximately 7.5 A), and the fibril dimensions (60-120 A), we may conclude that from 8 to 16 molecular chains are involved in the formation of one fibril. In dilute solutions, single isolated particles are also found; these are either strongly convoluted isolated "packets" formed from molecular chains, or, as in the case of polyacrylic acid and its barium salt, they are individual symmetrical globules, corresponding in size to single coiled molecular chains (90-100 A).

The secondary structures seen in the case of cesium polyacrylate (Fig. 3,2) are even more unfolded than those in sodium polyacrylate. As in the case of sodium polyacrylate, the structure is formed by convoluted long fibrils which do not penetrate into each other. However, the fibrils participating in the formation of secondary structures of cesium polyacrylate are smaller than those in sodium polyacrylate structures; their transverse dimensions are in the range of 40-80 A. These are not greatly convoluted "worms" but longer and straighter threads. They are probably also formed analogously by union of molecular chains into packets. However, in this case the molecular chains are straighter and join in smaller numbers. The average number of molecular chains joined together to form a fibril is 5-11.

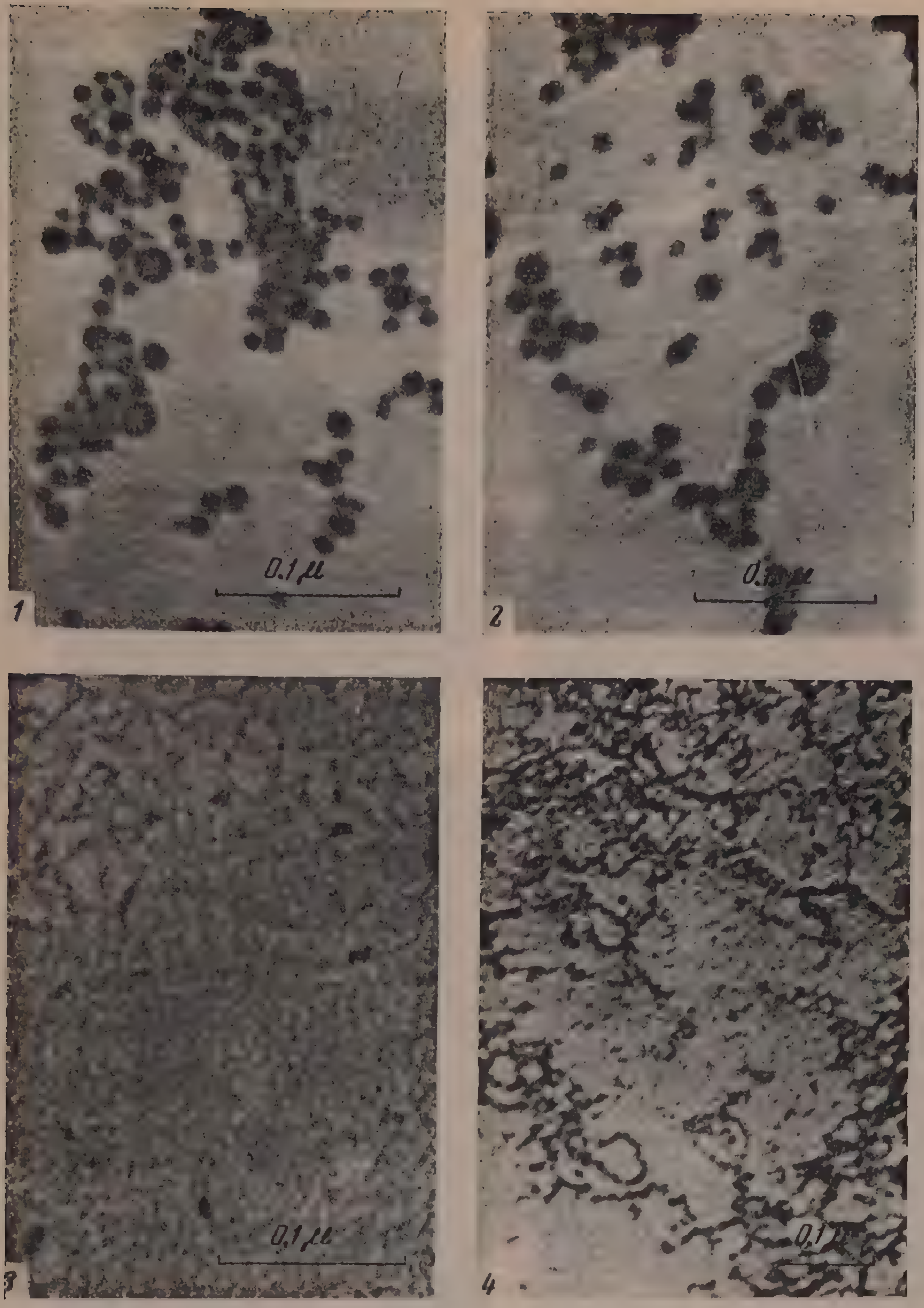

Fig. 1. Electron micrographs: 1) polyacrylic acid (X 250,000); 2) barium polyacrylate (x 250,000) ; 3) sodium polyacrylate (x 250,000); 4) sodium polyacrylate.

Quaternary ammonium polyacrylates (tetramethylammonium, Fig. 3,3 and triethylphenylammonium, Fig. 3, 4) show chain aggregation analogous to that in cesium polyacrylate. The secondary structures formed from chain aggregates are typical fibrillar structures. The individual fibrils, to judge by their transverse size of 40-90 A, are formed from 5-12 asymmetric molecular chains joined in parallel into packets.

The presence of strongly branched secondary structures in sodium, cesium, and quaternary ammonium polyacrylates is to be expected if the configuration of flexible polyions in solution is considered in terms of the relationship between the thermal forces tending to coil the chain into a globule and the electrostatic forces between the charged chain segments, resulting in increased rigidity. In fact, in a weak polymeric

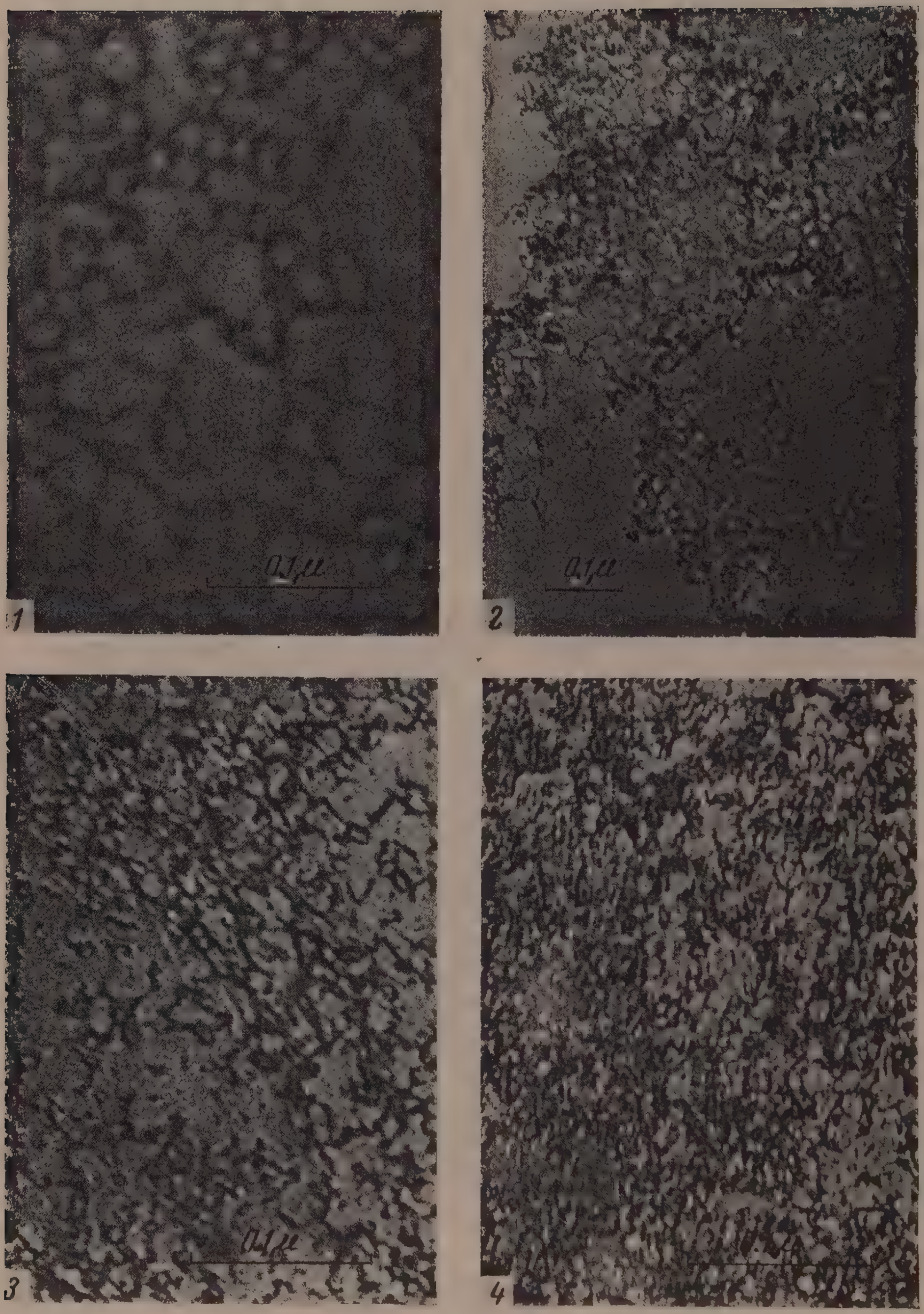

Fig. 3. Electron micrographs of polyacrylates: 1) sodium (x 250,000); 2) cesium (x 100,000); 3) tetramethylammonium (x 250,000); 4) triethylphenylammonium (x 250,000) .

electrolyte (as was shown above for polyacrylic acid in aqueous solution), the molecules of which are only partially ionized, the polyion is in the form of a compact or more or less diffuse globule, since the intramolecular electrostatic repulsion forces are not large, and are not sufficient to straighten the molecule, but merely expand the globule. When cations favoring increased dissociation of the ionogenic group, and therefore also favoring an increase in the effective charge of the chain, are introduced into the weak electrolyte chain, an increase of the intramolecular repulsion forces, and therefore of chain rigidity, is to be expected. When these forces begin to exceed the thermal forces, the molecular chain begins to straighten and attain the form of an elongated rigid rod. Therefore, the molecular chains in solutions of sodium, cesium, and quaternary ammonium polyacrylates will be of maximum straightness. Further, molecular chains with maximum asymmetry form aggregates by joining together in parallel to form fibrils, which interwine to form networks — the secondary structures. The transverse diameters of the single fibrils lie in the range of 40-120 A. From the distances between compactly arranged molecular chains (3 A) and the transverse dimensions of the molecular chains themselves (4.5 A), in the case of maximum asymmetry, when the molecules are in the form of elongated rods, it may be assumed that the fibrils are composed of 5-16 molecular chains joined together in bundles or packets. It should be noted that in very dilute solutions, in which secondary structures are not formed because of the low concentrations of the substances, the packets do not dissociate; they continue to exist, acquiring a greatly convoluted configuration owing to their flexibility.

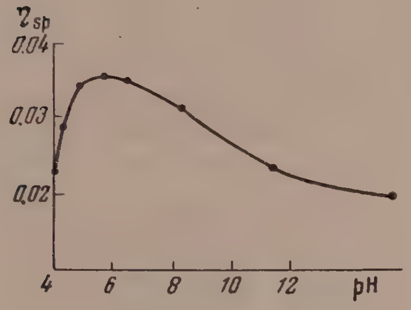

Fig. 2. Viscosity of sodium polyacrylate as a function of the degree of neutralization.

Solutions of pure polyacrylic acid and of its barium salt contain individual molecular chains, which coil into compact globules by the action of thermal and strong intramolecular forces. Interpenetration of such globules, naturally, cannot occur because of the considerable density of the globular formations. Such symmetrical globules become joined together without interpenetration and form secondary structures of another type, analogous to the globular structures in biological systems.

SUMMARY

1. Two types of structure in polyacrylic acid and its salts, the character of which is determined by the configuration of the long-chain polyion, have been established:

a) Typical fibrillar structures, in which the fibrils are molecular chains of maximum asymmetry, formed by parallel aggregation into "packets" of 5-16 molecular chains.

b) Typical globular structures, formed by the joining of molecular chains coiled into symmetrical globules, without interpenetration.

2. In the case of sodium polyacrylates both types of structure were found simultaneously: coiled globular and fibrillar; no intermediate type was found. It seems that this type of aggregation, i. e., coiling of the molecular chain into a globule and further structure formation by cohesion of the globules without interpenetration, and parallel (although not strictly so) joining of straightened chains into flexible packets is the only and the regular type for polyacrylates.

3. The existence of globular and fibrillar structures in biological systems in natural polyelectrolytes and proteins suggests that this type of aggregation and mutual arrangement of polymer chains is of a more general character.

Moscow State University Faculty of Chemistry

Received December 28, 1956

LITERATURE CITED

[1] B. Siegel, D. Johnson, H. Mark, J. Polym. Sci. 5, 111 (1950).

[2] A. A. Lebedev, Electron Microscopy (Tech. Theoret. Lit. Press, 1954).

[3] H. Staundinger, High-Molecular Organic Compounds (State United Sci.-Tech. Press, 1935).

THE FORMATION OF CRYSTALLINE ALUMINOSILICATES

Z. Ya. Berestneva, M. B. Konstantinopol'skaya, and V. A. Kargin

It is known that aluminosilicates of various compositions are widely distributed in nature and form the main mass of the soil. The crystal structures of the minerals contained in soils have been studied by means of x-ray analysis. However, in order to understand the nature of soil formation processes, it is necessary to synthesize the minerals. Since formation of soil minerals occurs under normal conditions of the earth's surface, at low temperatures and pressures, aluminosilicates should be synthesized under these conditions also. The formation of crystalline aluminosilicates in alkaline media when aqueous solutions of sodium silicate and aluminate are mixed is well known. By saturating the resultant precipitates with magnesium salts, Sedletsky [1] approached nearer to a neutral medium, but aluminosilicates have not been prepared in a neutral medium.

The natural conditions of aluminosilicate formation are entirely different; large volumes of aqueous salt solutions are not involved. The process of aluminosilicate formation in natural conditions can be regarded as occurring by interaction of minerals of the aluminum hydroxide group with silicic acid. To determine the mechanism of this process, we studied the interaction of aluminum hydroxide both with colloidal silicic acid and with aqueous suspensions of finely ground silica gel and quartz.

The EM-3 electron microscope was used for the investigations.

As is known from the previous paper [2], freshly prepared aluminum hydroxide has an amorphous structure, and crystallization occurs progressively. Both freshly prepared amorphous and crystallized aluminum hydroxide were used for studying the interaction between aluminum hydroxide with silicic acid sol, silica gel, and quartz. The plate shows electron micrographs of aluminosilicates formed by the interaction of freshly prepared amorphous aluminum hydroxide with silicic acid (1), silica gel (2), and quartz (3). All three photographs present practically the same picture – they all show small spherical particles forming cellular structures, and having an amorphous structure in agreement with electron diffraction data. Aluminosilicates prepared from crystallized aluminum hydroxide and silicic acid sol, silica gel, and quartz, are shown in Micrographs 4,5, and 6 respectively. A different picture is seen in this case – crystals of aluminum hydroxide surrounded by silicic acid, constituting cellular structures, are clearly visible. However, here also all three micrographs are similar regardless of whether silicic acid sol, silica gel, or quartz was mixed with aluminum hydroxide.

Thus it is found that in all cases, regardless of the form of the silicic acid (sol, silica gel, or quartz), the results of its interaction with aluminum hydroxide appear the same under the electron microscope. To find the reasons for this, silicic acid sol, and aqueous suspensions of silica gel and quartz, were studied separately. The silica gel and quartz were first ground to a fine dust in an agate mortar. In this case the specimens were subjected to oblique chrome shadowing to increase contrast. The micrographs of silicic acid (7), silica gel (8), and quartz (9) were very similar, although in the case of silica gel and quartz amorphous formations can be seen together with spherical particles.

The only explanation for this is that colloidal silicic acid solution [3], like aqueous suspensions of silica gel [4] and quartz [5] always contain silicic acid in a state of true solution; in aqueous suspensions of silica gel and quartz the colloidal solutions may be formed as the result of evaporation of water and temperature fluctuations, so that in all three cases (sol, silica gel, and quartz) the processes of interaction are of the same nature, consisting of reactions between true silicic acid solution and aluminum hydroxide, and therefore the same result is obtained in each case by electron microscopy.

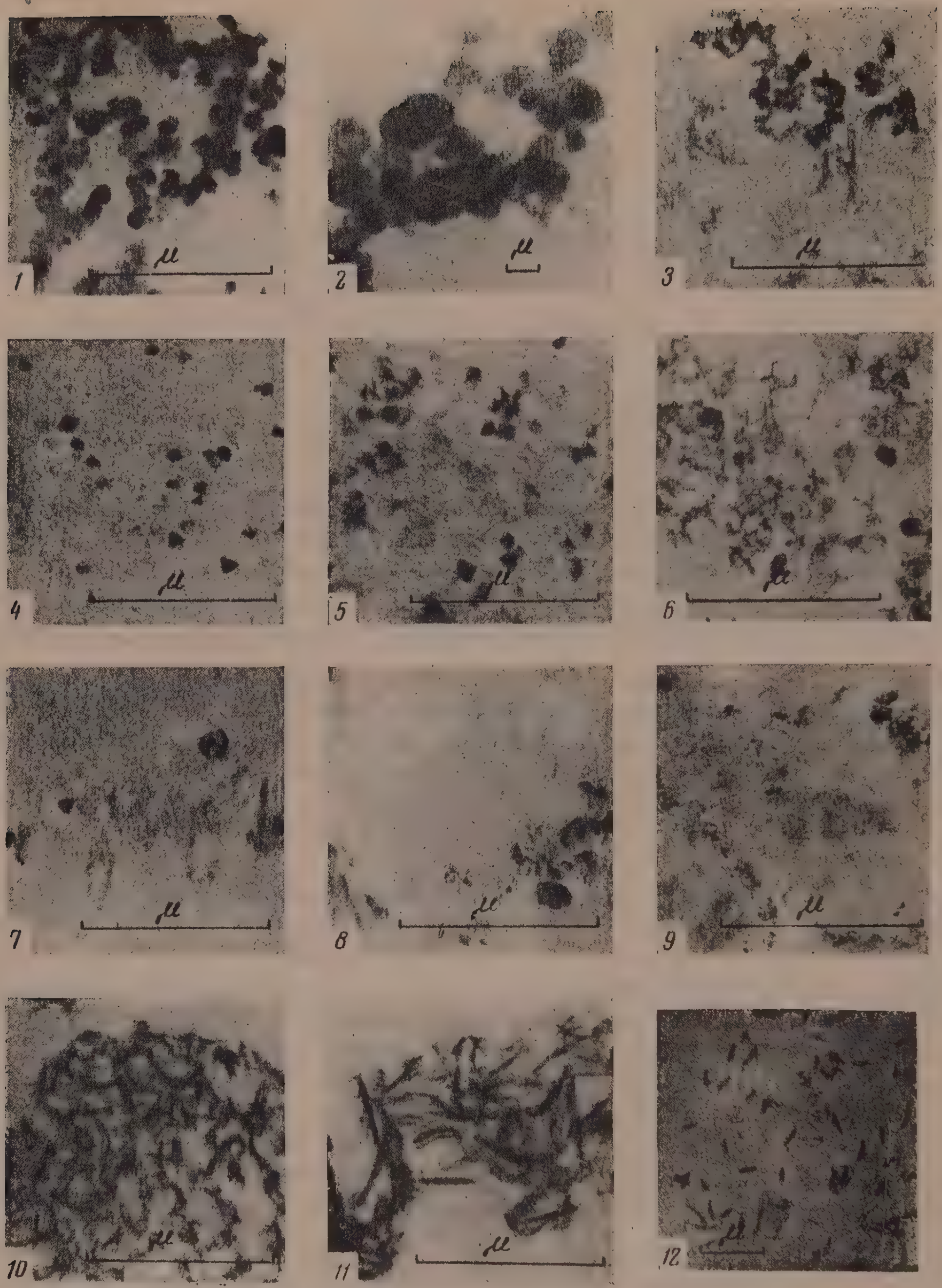

Electron micrographs of aluminosilicates (explanation in text).

Thus, the reaction between colloidal solutions of silicic acid and aluminum hydroxide occurs in true solution, as is the case in a number of other colloidal systems [6]. The rate of aluminosilicate formation when aluminum hydroxide sols react with silicic acid sols or with aqueous suspensions of silica gel or quartz, if the reaction occurs in true solution, will evidently be determined by the diffusion rates of the corresponding ions. However, the amount of substances in true solution in these cases are so small that the formation of aluminosilicates will proceed exceedingly slowly.

The migration of dissolved substances can be accelerated by application of an electric field. We used five-chamber electrodialysis [7] for this purpose.

The central and the two end compartments were filled with redistilled water. The second compartment was filled with silicic acid sol, and the fourth, with aluminum hydroxide sol. On application of an electric field (potential gradient 300-400 v/cm) across the membranes separating the compartments, two streams of ions (aluminum and silicate) move toward each other into the central compartment, interact, and form aluminosilicates.

As the membrane is not permeable to colloid particles, these remain in the second and fourth compartments. Application of an electric field accelerates the formation of aluminosilicates considerably. For example, samples taken from the central compartment after 300-350 hours give an electron micrograph shown in the Figure, 10. This clearly shows the crystalline form of the particles, which have a needlelike structure and form fairly large aggregates. Electron diffraction data also indicate that the particles formed have a crystalline structure.

In our previous investigation [8] we made unsuccessful attempts to obtain crystalline aluminosilicates under normal conditions by mixing 0.1 N true solutions of aluminum nitrate and sodium metasilicate. Neither variations of the $Al_2O_3 - SiO_2$ ratio, nor changes in the pH of the medium, had any effect on the structure of the aluminosilicate gels formed. The gels were amorphous in all cases. Only as the result of prolonged heating at high temperatures was it possible in a few cases to obtain aluminosilicates with a crystalline structure.

It is evident that in this case crystallization is exceedingly slow, as was shown by Sedletsky [1].

The interaction of true solutions of aluminum nitrate with sodium silicate may give aluminum hydroxide sols, silicic acid sols, and mixed aluminosilicate gels. We do not know the kinetics of formation of each of these substances in the given conditions. The electron microscope in this case reveals spherical particles of various sizes, from which the chemical composition of the resultant formation cannot be deduced, while electron diffraction data indicate that the substances formed are of an amorphous structure. The 0.1 N solutions used in the preceding investigation are concentrated relative to the true solutions of silicic acid or aluminum hydroxide which are present in the corresponding sols or suspensions. Experiments were therefore carried out with 0.001 N solutions of aluminum nitrate and sodium metasilicate. Mixing of these solutions at room temperature gave the same results as for 0.1 N solutions. However, if the solutions were mixed at the boiling point an aluminosilicate was formed which gave an electron micrograph quite analogous to that found for the aluminosilicate synthesized by electrodialysis (Micrographs 11 and 12). Further investigations showed that an aluminosilicate of crystalline structure, with $Al_2O_3 - SiO_2$ ratio of 3:1, is formed in the temperature range between 85-90 and 100°. The aluminosilicate gels formed at lower temperatures had amorphous structure and formed spherical particles. Evidently at higher temperatures the rate of formation of aluminosilicates is considerably higher than the formation rate of aluminum hydroxide and silicic acid sols. Micrograph 12 shows that the aluminosilicate crystals formed appear to be enclosed within larger spherical particles. Probably, larger amorphous particles are formed first, and crystallization then takes place within them, but the rate of this process is so high that the original particles can be seen under the electron microscope. The higher crystallization rate is probably the consequence of the higher temperature. Thus aluminosilicates of crystalline structure can be obtained at elevated temperatures in dilute solutions.

SUMMARY

1. It is shown that formation of aluminosilicates in the interaction of aluminum hydroxide with silicic acid sols or aqueous suspensions of quartz or silica gel occurs in true solutions.

2. Aluminosilicate with a crystalline structure has been synthesized by means of five-chamber electrodialysis.

3. From dilute solutions of aluminum nitrate and sodium silicate at high temperatures an aluminosilicate was prepared having a crystalline structure and given the same type of electron micrograph as the aluminosilicate synthesized by means of five-chamber electrodialysis.

The L. Ya. Karpov Physicochemical Institute
Moscow

Received July 12, 1956

LITERATURE CITED

[1] I. D. Sedletsky, Proc. Acad. Sci. USSR, 17,371 (1937).

[2] Z. Ya. Berestneva, T. A. Koretskaya, and V. A. Kargin, Colloid J., 13, 323 (1951).

[3] Z. Ya. Berestneva, T. A. Koretskaya, and V. A. Kargin, Colloid J., 11,369 (1949); H. Brinzinger and B. Troemer, Z. Anorg. Chem. 181, 237 (1929).

[4] V. Lehner, H. Merill, J. Am. Chem. Soc. 39, 2630 (1917).

[5] E. J. King, G. McMurray, Biochem. J. 32, 476 (1938); P. D. Ritchie, P. B. Demster, Nature 169, 538, (1952); D. W. Clellang, W. M. Cumming, P. D. Ritchie, J. Appl. Chem. 2, 31, (1952).

[6] V. A. Kargin and R. E. Chernitskaya, J. Phys. Chem., 9,461, 471, 481 (1937).

[7] V. A. Kargin, T. A. Matveeva, Proc. Acad. Sci. USSR, 105,294 (1955); O. I. Dmitrienko and V. A. Kargin, Colloid J., 13,259 (1951).

[8] Z. Ya. Berestneva and V. A. Kargin, Colloid J., 17,196 (1955).

STUDY OF THE TRANSITION OF AMORPHOUS AND CRYSTALLINE POLYMERS FROM THE SOLID ~~INTO~~ INTO THE FLUID STATE ON ADDITION OF SUBSTANCES OF LOW-MOLECULAR WEIGHT

V. A. Kargin, G. L. Slonimsky, and L. Z. Rogovina

In recent years the effects of temperature and molecular weight on the deformation of linear amorphous and crystalline polymers has been studied in detail [1]. In addition, the effects of plasticizers on the glass and flow transition temperatures have been studied [2]. However, no investigations of this type have yet been carried out over a wide range of plasticizer concentrations, covering the transition from a solid (glassy or crystalline) polymer to its dilute solution *. Study of this transition was the purpose of the present work.

The materials studied were glassy polymers – polyvinyl chloride and polymethyl methacrylate, and also a crystalline polymer – a mixed polyamide formed by joint polycondensation of caprolactam and salts of hexamethylenediamine and adipic and azelaic acids. Polyvinyl chloride of two different molecular wieghts (80,000 and 120,000) was used, so that it was possible to study the influence of molecular weight on the transition of the polymer into solution. The plasticizer used for both amorphous polymers was dibutyl phthalate, chosen as being the most common plasticizer of low volatility; meta-cresol was used for the polyamide. The mixing of the polymer with the plasticizer was effected by the swelling method at ~140° with stirring. Specimens with little or no plasticizer were molded for the tests; specimens which were in the form of gels or solutions were poured into aluminum basins. The specimens with different plasticizer contents were studied over a wide temperature range (from – 70 to +200°) by means of the dynamometric balance. The deformation produced by uniaxial compression of the specimens in 15 seconds, at constant stress of 0.05 kg / cm^2, was studied as a function of the temperature. In view of the possibility of flow, which can occur especially easily in systems of low concentrations, the measurements were started at low temperatures.

Polyvinyl chloride (PVC). Fig. 1 shows thermomechanical curves obtained by the method outlined above for specimens of PVC containing different amounts of dibutyl phthalate. In agreement with earlier results [4], the original PVC does not show residual deformation at any temperatures, i. e., it does not exhibit true flow; at a definite temperature large deformations are produced in it, which can be easily mistaken for flow (this is seen in the graph in the sharp upward turn of the curve). However, additional investigation showed that these deformations are reversible.

A similar result is found for a system containing 33.5 wt. % of dibutyl phthalate, which is also incapable of flow. However, in this case two temperature regions of softening are found (~40 and 120°). With 50 wt. % the system softens slightly even at -10°, and again at 70-80°. In this case further increase of temperature leads to true flow at 110°. It must be pointed out that the temperature at which flow begins does not coincide with the start of large deformations. Thus, in the case of plasticized PVC there are two softening resions and one flow region, which we shall term the first and second glass (softening) temperatures and the flow temperature respectively. Consequently, when glassy plasticized PVC is heated, elastic deformations arise in the first glass region; the magnitude of these remains constant over a certain temperature range. Then, in the second glass region, the deformability increases sharply, although flow only occurs at still higher temperatures.

---

* Chumakova-Ivanova and Rebinder [3] studied the mechanical properties of polyisobutylene and its solutions over a very wide concentration range, but this investigation was confined to the high-elastic and viscofluid states.

Increase of the plasticizer content softens the system and lowers the first and second glass temperatures, and also the flow temperature. At dibutyl phthalate concentrations above 82 wt. % the flow and second glass temperatures coincide. Further dilution of the polymer leads to a contraction of the high elastic region, which vanishes completely at a concentration of ~ 90%. More dilute systems behave as liquids of low molecular weight. It must be stressed that the transition from systems which are elastic gels to fluid systems – solutions – occurs in a very narrow concentration range, from 86 to 90% dibutyl phthalate; at 90% the flow in still accompanied by elastic deformations, but 95% dibutyl phthalate content PVC already forms a true solution, with only one flow temperature. The transition toward solutions for the PVC specimen of higher molecular weight is in general similar to that described.

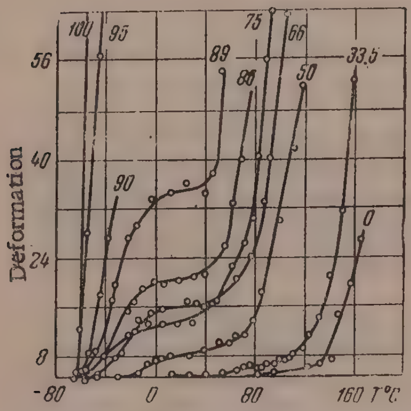

Fig. 1. Effect of temperature on the deformation of polyvinyl chloride with various contents of dibutyl phthalate plasticizer (the numbers on the curves represent dibutyl phthalate concentrations in wt. %).

The features common to both PVC specimens are: 1) displacement of the region of high elasticity into the region of lower temperatures; decrease of the elasticity modulus (elevation of the plateau in the graph); expansion of the temperature range in which elasticity is present at low plasticizer contents, and narrowing of this range, down to complete disappearance, at high plasticizer contents; 2) existence of a considerable region of the gel state, up to very high dilutions, the transition to solution occurring in a narrow range of temperatures and concentrations; 3) existence of two glass (softening) temperatures, not coordinated with transition into the region of high deformations and with appearance of flow.

The differences in the transition to solutions, associated with the molecular weight of the polymer are as follows: 1) transition to solutions in specimens of higher molecular weight is more sharp (thus, with 96% dibutyl phthalate the system is still a gel, and at 98% it is a fluid solution); 2) in the specimens of higher molecular weight there is a greater divergence between the temperature at which residual deformations arise and the temperatures at which large deformations appear.

Polymethyl methacrylate (PMMA). The transition to solutions is much more gradual in PMMA, as can be seen in Fig. 2. The temperatures at which true residual deformations appear and large deformations arise, coincide for all specimens of plasticized PMMA. As was to be expected, the glass and flow temperatures depend on the plasticizer concentration. With 50 and 66% of dibutyl phthalate the specimens are gels over a considerable temperature range. Transition into the solution region begins from 75%, as is shown by the gradual degeneration of the region of high elasticity and the convergence of the glass and flow temperatures. With 90% of dibutyl phthalate the region of high elasticity disappears completely and the system becomes an ordinary fluid solution.

Polyamide (PA). The curves for the crystalline polyamide are given in Fig. 3 . The original polyamide passes directly from the solid into the viscofluid state, and a region of high elasticity is not observed at all. Fusion, as in other crystalline polymers, does not occur at one definite temperature, but over a narrow temperature range (125-140°).

On addition of cresol to the polyamide, in contrast to the amorphous polymers considered above, the system passes into solution at room temperatures even at relatively low plasticizer concentrations, from 50% of cresol. The behavior of the polyamide on addition of 0 to 75% of cresol was therefore studied. On addition of 9% of cresol the thermomechanical curve is on the whole of the same form as for the original polyamide, but the fusion temperature rises somewhat and the bend in the curve becomes sharper. Moreover, an increase in the PA deformability is seen over a narrow temperature range before fusion, although these deformations are not large enough to make it possible to speak of an elastic state. On additions of 23 and 28% of cresol the fusion temperature decreases correspondingly, the fusion region becomes increasingly diffuse, and a small temperature region of weak elasticity appears, which becomes more prominent on application of greater forces of deformation. Specimens containing 33 and 43% of cresol are elastic at room temperature and become viscous liquids on slight heating. With 50% of cresol the system is a normal but viscous solution even at room temperature. Increase of the cresol content to 75% converts the system into an easily flowing liquid, which thickens at low temperatures.

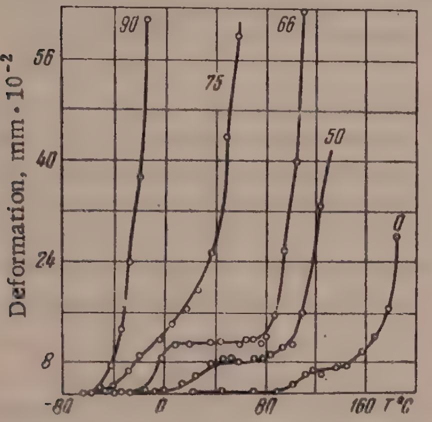

Fig. 2. Effect of temperature on the deformation of polymethyl methacrylate with various contents of dibutyl phthalate plasticizer (the numbers on the curves represent dibutyl phthalate concentrations in wt. %).

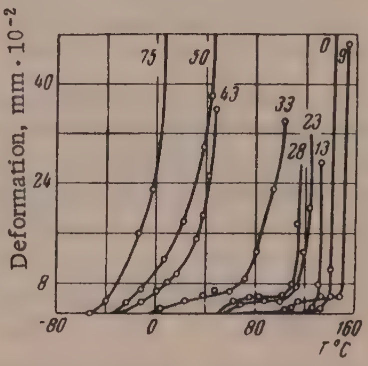

Fig. 3. Effect of temperature on the deformation of polyamide with various contents of m-cresol plasticizer (the numbers on the curves represent m-cresol concentrations in wt. %).

DISCUSSION OF RESULTS

Polyvinyl chloride. First ut must be noted that addition of a substance of low molecular weight has little effect on the properties of the solid polymer up to the softening region. The softening region lies in a relatively narrow concentration range, in which the polymer passes from the solid to the high-elastic state. Thus, the variation in the properties of any polymer on dilution is not uniform, but is analogous to the variation in the polymer properties on heating, and therefore the deformation – concentration graph is of characteristic form (Fig. 4).

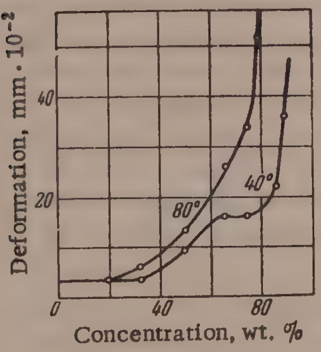

Fig. 4. Deformation of polyvinyl chloride plasticized with dibutyl phthalate as a function of the dibutyl phthalate concentration at 40 and 80°.

The absence of true flow in PVC, the existence of a wide concentration region of gel formation, up to very high degrees of dilution (95-98% of dibutyl phthalate), and the sudden transition to solutions in a very narrow concentration range – all this can only be explained on the assumption that PVC, which is usually regarded as a linear polymer, nevertheless forms a spatial network owing to intermolecular interaction. Structure formation by PVC molecules during heating has been detected previously [5], when it was attributed to the presence of thermoreactive groups, the origin of which is not clear, in PVC.

The second transition temperature in the region of large deformations does not correspond to the temperature at which flow appears, and therefore these large reversible deformations must arise when some other, stronger bonds are overcome at a definite temperature.

Thus, the existence of two glass temperatures indicates that the network is formed by two types of bonds, which are respectively broken at two different temperatures. Bonds of the first type are evidently formed between CHCl and CH_2 groups of two adjacent molecules; they are not very stable and when the energy of thermal motion on increase of temperature becomes comparable to the energy of these bonds the first softening occurs, and the polymer passes into the state of high elasticity. However, during deformation in this state bonds of the second type still retain the molecules in a partially glassy state. On further increase of temperature thermal motion overcomes these bonds also, and the deformation then begins to increase rapidly, corresponding to the second softening region. The question arises, what is the nature of the bonds which determine the second softening. It may be postulated that they are caused by the presence of strongly polar groups which appear in PVC as the result of oxidation processes.

It has been shown for polyisobutylene [3] that in polymers which cannot form networks under any conditions the transition from the high-elastic to the fluid state on dilution is quite gradual. It is seen that not all polymers show transition of this type. When PVC passes from the solid into the fluid state there are two sudden jumps in the variation of the physical properties of the system: one corresponds to transition to the state of high elasticity, and is not very sharp; subsequently the elasticity of the system remains of the same order of magnitude over a wide concentration range, and the second jump in the transition into the fluid state is very sharp. This type of transition to solution is probably found in all polymers capable of forming relatively stable spatial networks.

The discrepancy between the second softening and the flow temperatures arises because PVC flows only when the viscosity of the polymer is low enough; therefore the flow temperature need not be related to the temperature at which rupture of intermolecular bonds of either type takes place.

Polymethyl methacrylate (PMMA). The fairly narrow region of gel formation and the absence of a second softening indicate that PMMA contains only one type of intermolecular bonds, which are easily overcome on heating; this correspond to softening. The transition into the solution region is therefore much more gradual; in this respect PMMA occupies an intermediate position between linear polyisobutylene and polyvinyl chloride, which forms a spatial network.

Polyamide. The appearance of a state of high elasticity in the polyamide on addition of small amounts of the low-molecular substance and the simultaneous small rise in the fusion temperature appear unnatural at first sight. The rise of the fusion temperature suggests that when a crystalline polymer is swollen in a low-molecular substance the polymer crystals become more regular. A similar effect has been discovered recently [6], when it was shown that as the temperature approaches the melting point of a crystalline polymer the reflexions become sharper on the X-ray diagram.

This effect may be explained as follows: a crystalline polymer consists of amorphous and crystalline regions; the nonequilibrium stressed state of the crystals is manifested in the decrease of the fusion temperature and the existence of a fusion region rather than a melting point. When a substance of low molecular weight is added, it is dissolved in the amorphous portion, i. e., the latter is plasticized. Because of this, stresses are diminished both in the amorphous and the crystalline regions, and the crystalline regions of the system therefore become more ordered. Thus, with small amounts of solvent introduced into the polymer, the amorphous regions are changed first. This is in entire agreement with the appearance of a region of high elasticity in this range of solvent concentration: if the amorphous regions begin to play an important role in the behavior of the polymer, its characteristic state of high elasticity will appear. The experiments show that the height and extent of this elasticity plateau on the thermomechanical curve are not great, as the fraction of the amorphous regions is not large.

The observed rise in the fusion temperature of the polyamide on addition of 9% of cresol is a natural consequence of the increased crystal order. With a higher cresol content in the mixture the solubility of the crystals in it increases and as a result the temperature at which the crystals disappear is lower. At high degrees of swelling the crystals dissolve so rapidly on heating that the flow temperature decreases considerably. Thus, while in amorphous polymers the decrease of the flow temperature on plasticization is the result of decreased viscosity of the system, plasticization of crystalline polymers leads to a decrease of the flow temperature owing to loss of the crystalline state by solution of the polymer crystals in the plasticized amorphous portion. In absence of plasticizer, flow begins in the crystalline polymer only after fusion of the crystals.

SUMMARY

1. The transition from the pure solid polymer to its fluid solution has been studied for two glassy and one crystalline polymer, and the characteristics associated with phase state and molecular structure have been demonstrated.

2. The transition of a polymer from the glassy or crystalline state into a fluid solution is effected by addition of a solvent in the same way as on heating; i. e., the solid polymer, with increasing dilution, passes through a state of high elasticity, with a definite concentration region for each particular polymer, and then passes into a fluid solution.

3. Polyvinyl chloride does not pass directly from a high-elastic into a viscofluid state, but remains in gel form over a wide concentration range. Thus, two transitional stages were found during solution of polyvinyl chloride. The appearance of a second transitional stage on dilution of PVC, and also of a second glass temperature, are the results of the existence of two types of intermolecular forces, differing in magnitude, in PVC. It may be assumed that the second type of bonds is formed by strongly polar groups which arise as the result of oxidation of PVC.

4. In the case of polymethyl methacrylate the transition to solutions is intermediate in nature between that found for ideal linear polyisobutylene and for polyvinyl chloride, which forms a spatial network.

5. The characteristics of the transition from a crystalline polymer (polyamide) to its solution depend on the development of crystal order in presence of small amounts of plasticizer, the development and growth of a state of high elasticity within the limits of existence of the crystalline state, and the decrease of flow temperature as the result of increased solubility of the ordered regions (crystals) in the plasticized amorphous portion.

The L. Ya. Karpov Physicochemical Institute
Moscow

Received November 20, 1956

LITERATURE CITED

[1] P. Kobeko, E. Kuvshinsky, and G. Gurevich, Bull. Acad. Sci. USSR, Phys. Ser,, No. 3, 329 (1937); A P. Aleksandrov and Yu. S. Lazurkin, J. Tech. Phys., 9,1249 (1939); V. A. Kargin and T. I. Sogolova, J. Phys. Chem., 23,530 (1949); 27,1039, 1208 (1953).

[2] S. N. Zhurkov, Proc. Acad. Sci. USSR, 47,493 (1945); 49,201 (1945); S. N. Zhurkov and R. I. Lerman, Proc. Acad. Sci. USSR, 47,109 (1945); V. A. Kargin and Yu. M. Malinsky, Proc. Acad. Sci. USSR, 73,967 (1950).

[3] L. I. Chumakova-Ivanova and P. A. Rebinder, Colloid J., 18,429 (1956).

[4] V. A. Kargin and T. I. Sogolova, Proc. Acad. Sci. USSR, 108,662 (1956).

[5] V. A. Kargin and M. N. Shteding, J. Chem. Ind., No. 3, 137 (1956).

[6] V.A. Kargin and G. S. Markova, J. Phys. Chem., 29, 1273 (1955).

ADSORPTION OF POLYSTYRENE LATEXES IN RELATION TO THE SIGN OF THE PARTICLE CHARGE AND THE SORBENT

E. M. Aleksandrova and N. S. Razumikhina

The ability of colloidal systems to be adsorbed on extraneous surfaces is of great practical importance in such processes as dyeing, leather tanning, sizing and impregnation. According to Peskov [1], adsorptive fixation of colloid particles is a special form of coagulation (heterocoagulation), differing from ordinary coagulation in that an extraneous phase is required for it. The mechanism of the process is that the extraneous surface adsorbs the stabilizer of the colloidal particles, and the destabilized particles coagulate on the adsorbing surface.

The colloidochemical theory of sizing was developed by Voyutsky [2], the basis being the fact that the fiber and sizing material are colloid systems. The sizing process is regarded as coagulation of the sizing agent on the fiber surface, i. e., as heterocoagulation. Heterocoagulation occurs as the result of destabilization of the colloidal particles by means of some coagulant, or by direct interaction between the surface layers of the fiber and the stabilizer (molecular or micellar).

The heterocoagulation process occurs most effectively if the charges on the colloidal particles and on the adsorbing surface are of opposite sign. If the particles and the surface are similarly charged, heterocoagulation usually does not occur.

It is known that electrolytes are added when fibrous materials are treated with negatively charged latexes. We followed the same procedure, combining positively charged adsorbents and latexes. The need to add electrolytes for the adsorption of colloidal particles has been demonstrated not only for latexes [3]. Considerably earlier, Peskov and Moryganov [4] added electrolytes in studying the adsorption of dyes. Recently Koganovsky and Rovinskaya [5] performed analogous experiments on the adsorption of humic acid micelles on graphite.

The probable explanation for the action of electrolytes is that they cause some desolvation of the colloidal particles, although the system remains aggregatively stable until the adsorbent is introduced.

Considerable interest in relation to impregnation and sizing attaches to the use of positively charged latexes, which have been obtained by charge reversal of negatively charged latexes [2] and directly by emulsion polymerization of styrene [6].

The stability of such latexes was studied by Aleksandrova and Kertes-Mureshan [7]. The colloidochemical properties of latexes, as of other sols, are largely determined by the properties of the stabilizing component.

The stabilizers used by us for preparation of latexes were cation-active colloidal electrolytes.

These substances form semicolloidal systems in aqueous solution. The distribution of the substance between the phases is determined by the temperature and especially by the concentration. Micelles are formed in large amounts only in a relatively narrow range of concentrations —at the so-called critical concentration of micelle formation (CCM).

The stabilizing action of cation-active substances, making them effective stabilizers, depends on their tendency to form colloidal solutions, their structuromechanical properties, and their considerable surface activity.

Two cation-active substances were studied: Leveling Agent A (LA), and octadecyloxymethylpyridinium chloride (OOPC). The cationic agent sold as Leveling Agent A was first synthesized by Lapina [8], and is widely used in the textile industry, in dyeing fur, woolen, and felt goods, and as a detergent; its general formula is

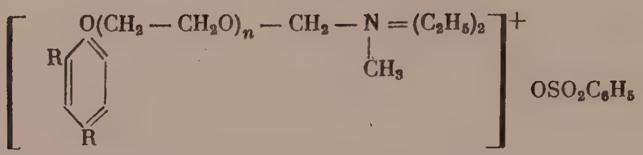

where n can vary from 3 to 30; R is C_8H_{17}.

The molecular weight varies, according to n, over a wide range from M = 634 when n = 3, to M = 1246 when n = 30. We used Leveling Agent A (n = 12.9) the colloidochemical properties of solutions of which has been studied by Kertes [7] .

The other stabilizer, octadecyloxymethylpyridinium chloride (OOPC), of molecular weight 397.7, has the structure

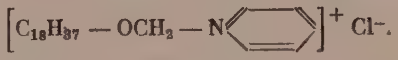

It is sparingly soluble in water at room temperature; 0.1% solutions of OOPC are strongly opalescent; its colloidal properties were also studied by Kertes [7] . The surface activities of both stabilizers are of the same order of magnitude.

Investigations of the adsorption of latexes were preceded by studies of adsorption of the stabilizers themselves. The adsorbent was filter paper, which is negatively charged at the water interface.

The reasons for this choice were the purity of filter paper (ash content 0.01%), its standard quality, relatively high adsorptive activity, and also the practical importance of the adsorption of latex particles on fibrous materials.

The adsorption of LA was also studied on active carbon, which also has a negative surface charge. The degree of adsorption was determined from the decrease of solution concentration. The equilibrium concentrations of LA and OOPC stabilizers were determined by an optical method developed by A. S. Kryukova. The principle of the method is that when the dye Acid Blue K is added to solutions of the stabilizers LA and OOPC, they are colored violet at low concentrations and blue at high concentrations. These solutions obey Beer's law over a definite concentration range. Calibration curves (Figs. 1,2) are obtained by plotting the optical density of the solutions ($D_{\lambda = 619}$) against the concentration (c) . The optical densities were measured by means of the MF universal photometer.

The results obtained were used to plot adsorption isotherms (Figs. 3,4) the amounts of adsorbed substance in millimoles per gram of sorbent (a) being plotted against the equilibrium concentrations (in millimoles per liter). Both stabilizers are well adsorbed by ashless filter paper and active carbon. The adsorption on carbon reaches almost the same values as in experiments with CH_3COOH or isoamyl alcohol. The adsorption on paper is less, owing to its different structure. The adsorption is, as a rule, reversible.

The experiments show that both stabilizers have considerable surface activity at the adsorbent – aqueous solution interface. There are therefore grounds to expect effective heterocoagulation in latexes stabilized by these cation-active agents.

The latexes were prepared by the emulsion polymerization method described by Mochalov [3] and Kertes [7] .

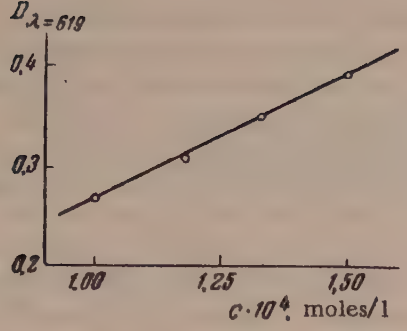

Fig. 1. Calibration curve for determination of the concentration of leveling agent LA from the optical density.

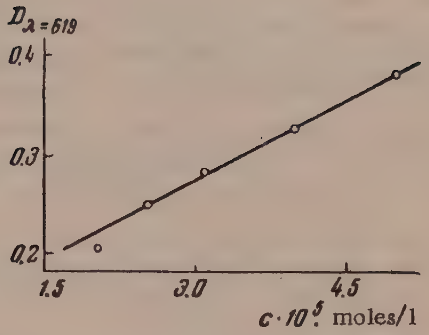

Fig. 2. Calibration curve for determination of the concentration of leveling agent OOPC from the optical density.

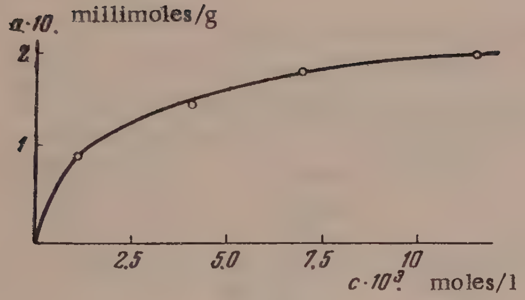

Fig. 3. Adsorption isotherm for LA on carbon.

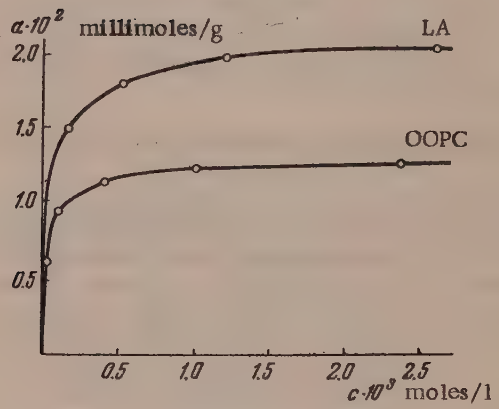

Fig. 4. Adsorption isotherm for LA and OOPC on paper.

Latex with stabilizer LA (latex LA) was stable to dilution and to addition of electrolytes (K_2SO_4, $BaCl_2$, K_3PO_4) even at very high concentrations of the latter. The dry solids content was 168 g/liter. The latex was positively charged; its electrokinetic potential was 42 mv.

Latex with stabilizer OOPC (latex OOPC) was stable to electrolytes in the amounts usually added for coagulation of hydrosols with solvated ion stabilization; its aggregative stability is only destroyed by salting out of the stabilizer on addition of large amounts of electrolytes (KCl – 1 millimole/liter, K_2SO_4 – 0.5 millimole/liter). The dry solids content was 52.8 g/liter; the electrokinetic potential was + 40 mv.

The adsorption of latex LA was studied on ashless filter paper and on active carbon, which has a negatively charged surface at the water interface. The results of the experiments are given in Table 1.

The experiments showed that positively charged latex LA is adsorbed on negatively charged surfaces without addition of electrolyte. As Table 1 shows, not only heterocoagulation but also homocoagulation took place. Particularly strong homocoagulation was observed at low latex concentrations (from 0.5 to 2 g/liter). Stabilizer LA passes almost completely to the sorbent surface, with resultant total destabilization of the latex particles. At latex concentrations between 4 and 12 g/liter mainly heterocoagulation occurs, the extent of homocoagulation being very small. Only some isolated particle aggregates were visible under the microscope.

TABLE 1

Adsorption of Latex LA on Paper and Carbon
(Volume of latex 50 ml, weight of adsorbent 1 g)

Initial concentration of LA latex in g/liter	Latex concentration after adsorption for		Amount of latex adsorbed in mg/g
	5 days	9 days	
	Latex LA on paper		
11.6	11.16	11.12	24
5.76	5.32	5.30	23
2.68	2.24	2.20	24
1.24	coagulation		–
0.68	coagulation		–
	Latex LA on carbon		
8.72	7.4	7.32	70
4.32	3.52	3.48	42
1.04	coagulation		–
0.68	coagulation		–

TABLE 2

Effect of Electrolyte Additions on Adsorption of Latex
(Volume of latex 40 ml, weight of adsorbent 1 g)

0.1 N NaCl added, ml	Concentration of latex LA in g/liter		Amount of latex adsorbed in mg/g
	initial	after 3 days	
–	4.65	4.08	22.8
1	4.65	3.96	27.6
2	4.65	3.90	29
5	4.65	3.90	29

Both types of coagulation are the result of transfer of the stabilizer from the latex particles to the adsorbent, and destabilization of the latex particles; this is confirmed by the increase in the optical density of the latexes. After the adsorption the optical density did not decrease, as was to have been expected, but increased owing to growth of the destabilized particles. Moreover, the latex coagulum formed in the presence of the adsorbent loses its hydrophilic properties and is not wetted by water, while the powder obtained when the latex is dried in air is easily wetted, as the stabilizer remains on the particle surfaces and makes them hydrophilic. Addition of electrolyte to the positively charged latex LA at a concentration below the coagulation threshold results in a very slight increase of adsorption of the latex on paper (Table 2), but addition of the same electrolyte to a negatively charged latex increases adsorption sharply [3].

In the adsorption of latex OOPC on ashless filter paper with a negatively charged surface the result was quite analogous to that in the adsorption of latex LA on paper and carbon (Table 3).

TABLE 3

Adsorption of Latex OOPC on Paper
(Volume of latex 50 ml, weight of adsorbent 1 g)

Concentration of latex OOPC in g/liter			Amount of latex adsorbed in mg/g
initial	after 5 days	after 9 days	
11.8	11.34	11.20	30
8.68	8.12	8.04	32
5.0	4.37	4.36	32
3.32	2.68	2.68	32
1.86	coagulation		–
0.66	coagulation		–

TABLE 4

Effect of Concentration of Stabilizer OOPC on the Adsorption of Latex OOPC
(Volume of latex 50 ml, weight of adsorbent 1 g)

Initial concentration of latex OOPC in g/liter	0.1 N solution of OOPC added, ml	Volume of H_2O, ml	Equilibrium concentration of latex after		Amount of latex adsorbed in mg/g
			4 days	10 days	
4.32	–	10	3.60	3.60	36
4.24	3	7	3.90	3.90	17
4.68	10	3	4.50	4.40	8

TABLE 5

Adsorption of Latexes in Relation to the Sign of the Charge on the Particles and the Adsorbent

Change on adsorbent	Change on latex	Addition of electrolyte	Result
+	+	Required	Heterocoagulation
+	–	Not required	"
–	+	Not required	"
–	–	Required	"

It is seen from Table 3 that latex OOPC undergoes volume coagulation at concentrations from 0.66 to 2 g/liter, while at concentrations from 3 g/liter upward both types of coagulation occur, homocoagulation being slight, and detected only by the slight increase of optical density.

If excess of stabilizer OOPC is added to latex OOPC, the adsorption of the latex diminishes sharply. With a large excess the adsorption may cease altogether, as the surface of the adsorbent will be shielded by a layer of the stabilizer (Table 4).

An experiment was performed on the adsorption of latex OOPC on paper with a positively charged surface, obtained by charge reversal by the use of a cation-active substance, sapamine:

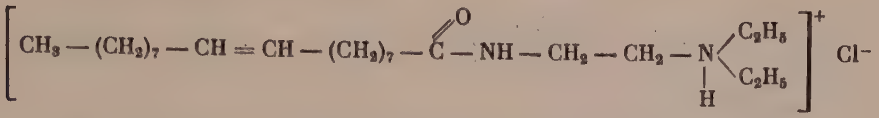

$$\left[CH_3-(CH_2)_7-CH=CH-(CH_2)_7-\overset{O}{\overset{\diagup}{C}}-NH-CH_2-CH_2-\underset{\underset{H}{|}}{N}\begin{smallmatrix}\diagup C_2H_5\\ \diagdown C_2H_5\end{smallmatrix}\right]^+ Cl^-$$

The charge on the paper surface was determined by the electroosmotic method.

Positively charged latex OOPC was not adsorbed on the positively charged surface, but addition of electrolytes induced adsorption. The results of experiments on the influence of the sign of the charge on the particles and the adsorbent on the adsorption of polystyrene latexes are given in Table 5.

SUMMARY

1. The adsorption of polystyrene latexes, in relation to the sign of the charge on the colloid particles and latexes, has been studied. It is shown that cation-active stabilizers are adsorbed on negatively charged adsorbents.

2. With like charges, appreciable adsorption of the latex occurs only on addition of electrolytes to the system.

3. With like charges, addition of electrolytes is not required for heterocoagulation, but if dilute latexes are used ($\leqslant$ 1 g/liter), volume coagulation of the latexes (homocoagulation) occurs instead of adsorption (heterocoagulation) .

The D. I. Mendeleev Institute of Chemical Technology
Moscow

Received June 28, 1956

LITERATURE CITED

[1] N. P. Peskov, Symposium "Modern Problems of Colloid Chemistry and the Leather Industry" (Mendeleev All-Union Chem. Soc. Press, Moscow, 1937).

[2] S. S. Voyutsky, Colloid Theory of Paper and Cardboard Sizing (Light Ind. Press, 1946).

[3] P. V. Mochalov, Dissertation (Moscow, 1952); E. M. Aleksandrova and P. V. Mochalov, Colloid J., 16, No. 3,161 (1954); No. 6, 401 (1954.).

[4] N. P. Peskov, Bull. Textile Ind., No. 5,25 (1926); P. V. Moryganov and V. E. Rostovtsev, Cotton Ind., No. 11,36 (1938).

[5] A. M. Koganovsky and T. M. Rovinskaya, Colloid J., 17, No. 2, 81 (1955).

[6] A. P. Sheinker (Dissertation, Moscow, 1954); E. V. Zabolotskaya (Dissertation, Moscow, 1954).

[7] Yu. Kertes-Mureshan, Dissertation (Moscow, 1954); E. M. Aleksandrova and Yu. Kertes-Mureshan, Proc. Acad. Sci. USSR, 103, No. 2,269 (1955).

[8] P. A. Lapina (Dissertation, Moscow, 1955).

THE RELATIONSHIP BETWEEN THE STRUCTURE OF EMULSIFIERS OF THE ALKYLAROMATIC ACID TYPE AND THE POLYMERIZATION OF UNSATURATED COMPOUNDS

4. SALTS OF DI-SEC-BUTYLNAPHTHALENESULFONIC ACID WITH UNIVALENT CATIONS

N. P. Apukhtina and A. M. Lyagalova

In the previous papers we demonstrated the dependence of the solubilization of α-methylstyrene and of the copolymerization of divinyl with α-methylstyrene on the butyl group contents of alkyl aryl sulfonates [1], and on the contents of univalent cations [2] and anions [3]. It was shown that all these factors have a great influence on the emulsifier properties. It was found [2] that, in presence of alkyl aryl sulfonates with different cations in the same equivalent concentrations, the rates of polymerization are different, both in presence and in absence of salts.

The present study deals with certain colloidochemical properties of alkaline di-sec-butylnaphthalenesulfonates with K^+, Na^+, Li^+ and NH_4^+ cations (di-NP K, di-NP Na, di-NP Li, and di-NP NH_4).

The solubilities in water, the surface tensions of the aqueous solutions, and the influence of these compounds on the solubilization and polymerization of divinyl were determined.

Starting materials. The emulsifiers were prepared by neutralization of di-sec-butylnaphthalenesulfonic acid with potassium, sodium, lithium, and ammonium hydroxides. The compounds obtained were purified to remove mineral salts and hydrocarbons. The purity of the products was determined from the sulfur contents of the emulsifier molecules.

Method of investigation. The solubilities of the emulsifiers were determined from the saturated solutions at 20°. The surface tension was determined with the aid of the Rebinder apparatus from the maximum bubble pressure.

For the solubilization determinations, 25 g of aqueous emulsifier solution was placed in an ampoule fitted with an electromagnetic stirrer. The ampoule was evacuated and joined to a buret containing divinyl; the absorption of the latter was continued, with stirring, to constant volume, at 20° ± 0.2°. The solubilization of α-methylstyrene was determined refractometrically [1,4].

Divinyl was polymerized at 50° with potassium persulfate initiator; the pH of the medium was 11.8-12; the volume ratio of the hydrocarbon and aqueous phases was 1:1.

In the emulsifier solubility determinations it was noted that the saturated solutions differ in appearance according to the cation combined with the alkylnaphthalenesulfonic acid. For example, di-NP K forms turbid solutions, a fine suspension passing through the filter. Di-NP Na gives transparent saturated solutions with a solid phase in the form of loose flakes. Aqueous solutions of d-NP Li gelatinize readily.

The solubilities of the emulsifiers increase with decreasing cationic radius:

Emulsifiers	di-NP K	di-NP NH_4	di-NP Na	di-NP Li
Solubility in water, %	7-9	12-13	20-22	25-27

The absolute values of surface tension of aqueous solutions of the emulsifiers are fairly similar (Fig. 1), and all four $\sigma = f(c)$ curves can be classified as curves of the first type, in McBain's terminology [5]. In all cases the surface tension decreases sharply up to emulsifier concentrations of $4.0 \cdot 10^{-3} - 4.5 \cdot 10^{-3}$ g-equiv./1000 g; the curves flatten out on further increase of concentration. The surface tension of emulsifier solutions as a function of concentration decreases regularly with increasing heat of solvation of the cations, which form the following lyotropic series in order of surface tension decrease produced:

$$K^+ > NH_4^+ > Na^+ > Li^+.$$

The results are in agreement with Aickin's observations [6] on the influence of the nature of the cations in the electrolytes added to aqueous solutions of alkyl sulfonate esters.

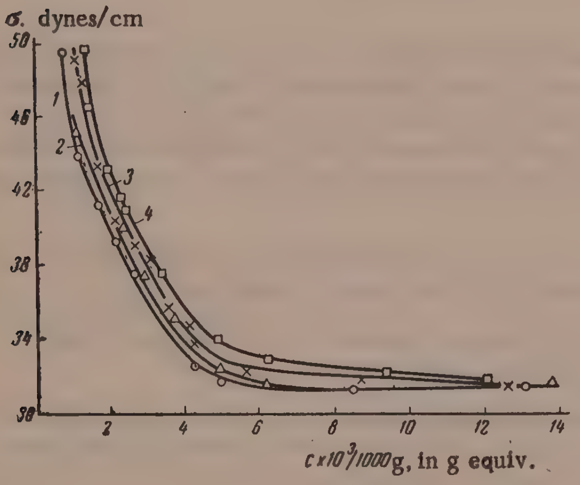

Fig. 1. Surface tension of aqueous emulsifier solutions: 1) di-NP K; 2) di-NP NH_4; 3) di-NP Na; 4) di- NP Li.

The solubilization of divinyl was studied over a wide range of emulsifier concentrations in dilute solutions and in saturated solutions (Figs. 2,3). In all cases with the exception of di-NP NH_4 the solubilization gradually increases with emulsifier concentration. In dilute solutions, approximately up to concentrations of 0.2 g-equiv./1000 g, the solubilization of divinyl is practically the same in all these cases. On further increase of emulsifier concentration* the solubilization varies linearly, di-NP K being the most effective, and di-NP Li the least. All the curves pass through a maximum at a concentration of ~0.7 g-equiv./1000 g; the solubilization of divinyl in di-NP Li solution falls sharply. The curve for the variation of divinyl solubilization with di-NP NH_4 concentration is of a different character (Fig. 2, Curve 4); the solubilization diminishes starting with an emulsifier concentration of 0.2 g-equiv./1000 g.

In Fig. 3 the solubilization is represented as the ratio of moles of divinyl to moles of emulsifier. The solubilization is constant at concentrations up to 0.6-0.7 g-equiv./1000 g in presence of all the cations with the exception of NH_4^+. In aqueous solutions of di-NP NH_4 the solubilization of divinyl falls steeply over the whole concentration range studied (Fig. 3, Curve 4).

Thus it may be concluded that emulsifier cations influence solubilization in the order of their positions in the lyotropic series: $K^+ > Na^+ > Li^+$; the NH_4 ion is exceptional, as it is the most effective at low concentrations (up to 0.2 g-equiv./1000 g), while on further increase of concentration it goes to the last place in the above series.

Earlier we determined the solubilization of α-methylstyrene as a function of the concentrations of K^+, Na^+, and Li^+ ions, added as chlorides of the univalent metals to an aqueous solution of sodium tri-sec-butylnaphthalenesulfonate. The cations in this case again formed the same lyotropic series [2].

---

* It should be noted that with the exception of di-NP Li the properties of all the emulsifiers were mostly studied in saturated solutions of these colloidal electrolytes, containing different amounts of the solid phase. Thus, in solutions of di-NP K, di-NP Na, di NP-Li, and di-NP NH_4, the solid phase was present at emulsifier concentrations in the water above 0.19, 0.45, 0.7, and 0.35 g-equiv./1000 g of the mixture respectively. Therefore in this paper the term "concentration" of the emulsifier represents its total content in the water both in the dissolved state and as the solid phase.

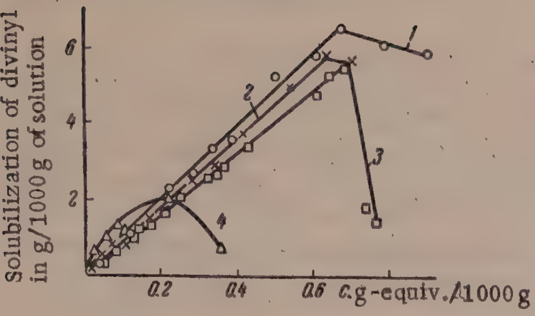

Fig. 2. Solubilization of divinyl in aqueous solutions of emulsifiers: 1) di-NP K; 2) di-NP Na; 3) di-NP Li; 4) di-NP NH_4.

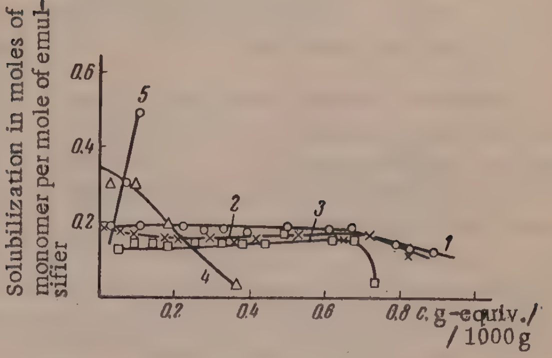

Fig. 3. Solubilization of hydrocarbons in aqueous emulsifier solutions: 1) di-NP K; 2 and 5) di-NP Na; 3) di-NP Li; 4) di-NP NH_4; 1,2,3,4) divinyl; 5) α-methylstyrene.

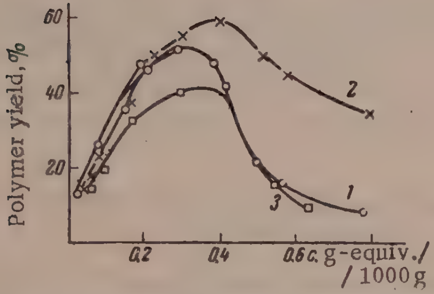

Fig. 4. Influence of emulsifier concentration on conversion of divinyl:
1) di-NP K; 2) di-NP Na; 3) di-NP Li.

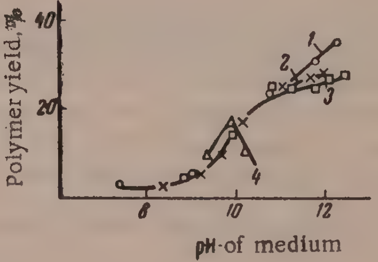

Fig. 5. Influence of the emulsifier cation on the yield of divinyl- α-methylstyrene polymer at different pH values:
1) di-NP K; 2) di-NP Na; 3) di-NP Li; 4) di-NP NH_4.

As has been shown by McBain and his associates [7], the nature of the solubilization curves depends on the emulsifier used and also on the added electrolytes. They showed that in aqueous solutions of emulsifiers of the ionic type (both anion-active and cation-active) aromatic hydrocarbons are solubilized to a far greater extent than aliphatic hydrocarbons, and in some instances the curves for solubilization as a function of concentration also differ in type.

We have also shown that solubilization of α-methylstyrene in aqueous solutions of di-NP Na is considerably greater than that of divinyl (Fig. 3, Curve 5), and that the curve for solubilization as a function of emulsifier concentration is of a different type. The complex character of monomer solubilization suggests the existence of micelles which vary in form and size according to the emulsifier concentration. McBain earlier reached a similar conclusion on the basis of data on transference numbers in laurylsulfonic acid solution [8] and X-ray investigations of highly concentrated solutions of surface-active agents [9].

Polymerization of divinyl. Contradictory data are found in the literature on the influence of cations on the polymerization process. For example, Fermor and Peizner [10, 11] studied the influence of alkyl aryl sulfonate and oleate anions on the polymerization of styrene and concluded that univalent K^+ and Na^+ cations exert an equal influence on the polymerization process, and also on the solubilization of styrene. According to their observations, the nature of the cation in salts of dibutylnaphthalenesulfonic acid does not influence the polymerization rate of styrene over a wide pH range.

We have shown that the polymerization rate of a mixture of divinyl and α-methylstyrene in presence of Li^+, Na^+, and K^+ cations is the same at pH from 7 to 11, while on further increase of pH the polymerization rate increases in the series from Li^+ to K^+; NH_4^+ sharply decreases the polymerization rate at pH 10 (Fig. 4).

Fermor and Peizner showed that the course of polymerization is different only in presence of emulsifiers containing NH_4^+ ions (in the case of oleates). The different effects of potassium and ammonium ions were attributed to different degrees of charge on the ionic micelles. It is difficult to believe that salts of dibutylnaphthalenesulfonic acid with different cations (which, according to these authors, have the same influence on styrene polymerization) have micelles of the same degree of charge, as the latter is probably closely related to the magnitude of the cationic charge which, in its turn, depends on the nature of the cation. In our opinion the authors failed to notice the clear influence of emulsifier cations on polymerization because only one emulsifier concentration was used (~4% by weight), and the polymerization rate was studied mainly as a function of pH at high degrees of conversion of styrene (80-100%).

According to our data, the influence of emulsifier cations on polymerization and certain colloidochemical properties of emulsifier solutions is seen most clearly if the investigations are performed over a wide range of emulsifier concentrations.

It should be noted that some of the authors' data [11] show a clear distinction between the influence of K^+, Na^+, and NH_4^+ ions. However, their conclusions contradict the results of our investigations [2], and the data obtained by others [12].

We have shown in the present investigation that the nature of the emulsifier cation has a significant effect on the polymerization of divinyl. For dilute solutions (up to 0.2 g-equiv./1000 g) it is possible to draw a complete analogy between the dependence of solubilization and of the polymerization rate of divinyl on the nature and concentration of the cation (Figs. 2 and 5); namely, that the effectiveness of the cation increases with increase of its radius. Other laws apply to concentrated emulsifier solutions; Na^+ ions have the greatest effect on the polymerization rate, while K^+ and Li^+ ions at concentrations above 0.4 g-equiv./1000 g have roughly the same effect on the conversion of divinyl.

Di-NP NH_4 is a poor emulsifier for polymerization in the conditions studied, and the highest degree of conversion of divinyl does not exceed 6% (emulsifier concentration 0.05 g-equiv./1000 g).

Polymerization is a more complex process than solubilization of monomers, which is associated with a number of different factors (nature of the monomer, emulsifier, and initiator, pH of the medium, phase ratio, stability of the monomer and polymer emulsions, etc); therefore a complete analogy between variations of polymerization rate and polymerization is hardly to be expected.

It is highly probable that the complex character of the relationship between polymerization rate and the nature of the cations in the region of high concentrations is related to the solubility of colloidal electrolytes in water. Thus, the maxima on the curves for the conversion of divinyl (Fig. 4) in presence of di-NP K and di-NP Na are near the region of maximum solubility of the emulsifiers. The sharp decrease of divinyl conversion in presence of di-NP K at high concentrations is probably caused by a salting-out effect. It is possible that the decreased effectiveness of di-NP Li is associated with the tendency of its solutions to gelation.

SUMMARY

1. The solubilities in water of the emulsifiers studied increase in the following order: di-NP K < < di-NP NH_4 < di-NP Na < di-NP Li.

2. The surface tensions of aqueous solutions of these emulsifiers increase from K^+ to Li^+ in the above series.

3. At emulsifier concentrations up to 0.2 g-equiv./1000 g the solubilization and the polymerization rate of divinyl increase linearly with emulsifier concentration. In this concentration region the cations form the following series according to their effectiveness: $K^+ > Na^+ > Li^+$. The NH_4^+ ion occupies a special position. The solubilization of divinyl, expressed in moles of the monomer per mole of emulsifier, does not change for lithium, sodium, and potassium salts, at concentrations of the latter up to 0.7 g-equiv./1000 g, which

suggest that the micelle structure is also constant in this concentration region.

The S. V. Lebedev Scientific Research Institute
for Synthetic Rubber

Received July 14, 1956

LITERATURE CITED

[1] N. P. Apukhtina and A. M. Lyagalova, Colloid J., 17,337 (1955).

[2] N. P. Apukhtina and A. M. Lyagalova, Colloid J., 17,415 (1955).

[3] N. P. Apukhtina and A. M. Lyagalova, Colloid J., 18,3 (1956).

[4] A. I. Yurzhenko, Trans. III Conf. Acad. Sci. USSR on High Mol. Compounds (Moscow, 1945).

[5] J. W. McBain et al., Koll.-Z. 78, I, (1937); J. Am. Chem. Soc. 58, 379, (1936).

[6] Aickin, J. Soc. Dyers Colorists, 60,36 (1944).

[7] J. W. McBain, K. J. Lissant, J. Phys. Coll. Chem. 55, 655, (1951).

[8] M. E. L. McBain, Phys. Chem. 47, 196, (1943).

[9] J. W. McBain, O. A. Hoffman, J. Phys. Coll. Chem. 53, 39, (1949).

[10] N. A. Fermor and A. B. Peizner, Colloid J., 15,292 (1953).

[11] N. A. Fermor and A. B. Peizner, Colloid J., 15,459 (1953); 16,297 (1954).

[12] K. Berezan, A. Dobromyslova, and B. Dogadkin, Bull. Acad. Sci. USSR, Chem. Ser., 2,409 (1936); C.F. Fryling and T. G. John, Trans. Faraday Soc., 49,980 (1953).

INVESTIGATION OF THE AQUEOUS PROPERTIES OF PEAT BY MEANS OF RADIOACTIVE ISOTOPES

M. P. Volarovich, N. V. Churaev, and B. Ya. Minkov

Ever increasing use is now being made of radioactive tracers in science and technology. In particular, this method has been used in hydrotechnical and melioration research for measurement of the rate and direction of flow [1-6]. In peat technology great importance attaches to the problem of drainage of peat deposits, the successful solution of which involves studies of the aqueous properties of peat. For effective utilization of drainage methods and of open drainage systems used in the peat industry it is necessary to study the motion of water in the deposit, and its relationship to the solid phase in the peat.

After the first investigations by Dumansky and his associates [7], several methods for studying free and bound water in peat have been described [8]. The use of the radioactive tracer method opens up new ways for studying the aqueous properties of peat, and in particular makes it possible to study the movement of moisture in peat, which was not feasible before. For this, it was first necessary to develop techniques for studying the aqueous properties of peat by means of radioactive isotopes.

In developing the methods, it was first necessary to solve the problem of the choice of a suitable radioactive tracer for the water whose motion was to be observed. This was fairly difficult, as there have already been unsuccessful attempts in experiments with soils [6]. After a number of preliminary experiments it was found that the most successful tracer is radioactive sulfur S^{35} (as aqueous $Na_2S^*O_4$) which, as will be shown later, is only slightly adsorbed by the peat particles. The S^{35} sulfur isotope, as is known, disintegrates with the emission of β-particles of 0.16 Mev; the half life of this isotope is 87 days.

The filtration of tagged water through specimens of peat with intact structure was studied in experiments with S^{35} under laboratory conditions. The laboratory apparatus is shown in Fig. 1. The peat specimen 1 cut from the deposit was placed in the glass tube 2 (2.4 cm in diameter) and impregnated with distilled water to constant weight. Tagged water was then poured into the tube over the peat, the level being kept constant by means of the flask 3. The specific activity of the water, tagged with the S^{35} isotope, used in the experiments was 0.005-0.01 μC per 1 ml. The filtrate was collected in the buret 4 with a stopcock and at intervals (when 2 ml had accumulated) was transferred to test tubes fixed in the rotating disk 5. Toward the end of the experiment samples 2 ml in volume alternated with 8-10 ml samples. The time for accumulation of the filtrate in the buret was also noted.

The activity of the filtrate samples was measured by the T-25-BFL window-type counter contained in the universal lead casing IFKh-2, by means of the B-2 type installation. Filtrate samples 1 ml in volume were transferred from the test tubes into brass foil cups and dried under an infrared lamp.

The results of one of the experiments with fuscum peat with degree of decomposition R = 10% are given in Fig. 2. The height of the peat specimen was 6 cm, and the pressure h, 18 cm (see Fig. 1); the relative humidity of the peat, w, was 91.1%. In Fig. 2 the values of the volume V of the filtered liquid in milliliters are taken along the abscissa axis, and the counting rates N for the filtrate in pulses per minute along the ordinate axis. Corrections for radioactive decay and background [9, 10] were introduced in calculation of the counts N. The relative error of the activity determinations, performed under strictly similar conditions, did not exceed 3% [11]. Fig. 2 also shows the variation of the volume V of the filtered liquid with the filtration time τ in minutes. The variation is almost linear, which shows that the filtration coefficient remains constant during the experiment.

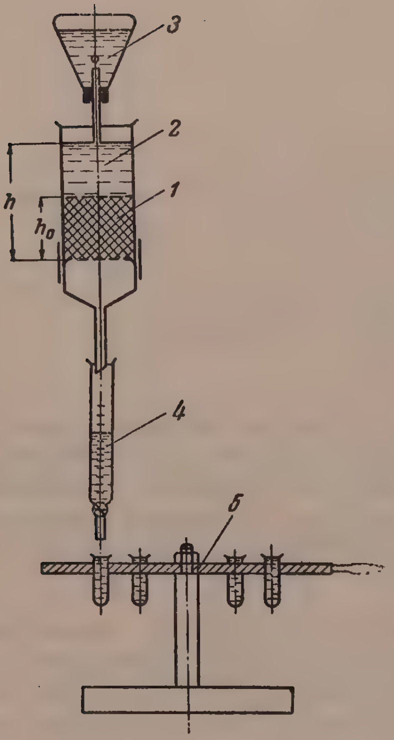

Fig. 1. Diagram of laboratory apparatus for studying the filtration of tagged water through peat.

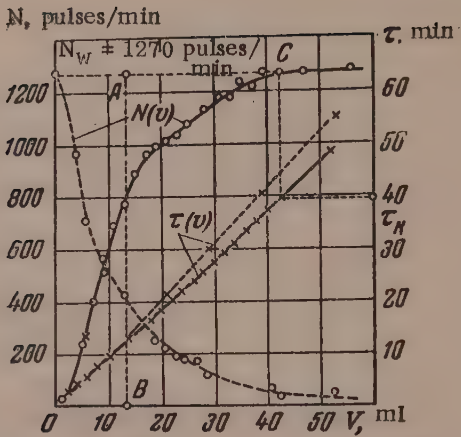

Fig. 2. Results of experiments on the filtration of tagged water through a peat specimen (continuous curves) and subsequent filtration of pure water (broken curves); fuscum peat, R = 10%.

As Fig. 2 shows, the activity of the filtrate samples gradually increases and after a certain time τ_k = 39.5 minutes reaches, at the point C, the value N_w = 1270 pulses/minute, which is the activity of the tagged water entering from above. Analysis of the N – V curve leads to the following suggested mechanism of filtration.

The tagged water moves along the pores in the peat and displaces the free (gravitational) water contained in them. Water is displaced first from the large and then from the finer pores, and finally, at time τ_k, the tagged water fills all the water conduction paths in the peat. After this the activity of the filtrate becomes equal to N_W, the activity of the tagged water. If all the pores in the peat were of the same size, then the N – V graph would be represented by the broken line OBAC in Fig. 2. The deviation of the actual N – V curve from this broken line is a measure of the heterogeneity of pore size in the peat specimen. It must be remembered that this refers only to water-conducting pores along which the filtering liquid moves.

If it is assumed that the paths for the movement of liquid in the peat specimen do not change during the experiment described above, then the N – V curve can be used to plot distribution curves for the amounts of filtering liquid by rates of filtration and dimensions of the water-conducting pores. Pore size distribution in active carbon was determined by Figurovsky [12] from the kinetics of displacement of one liquid from the pores by another.

The calculation data for an experiment with fuscum peat are given in Table 1.

In Table 1 the activity changes ΔN of the filtrate samples have been calculated for different volumes V of the filtered liquid and the time intervals $\Delta\tau$ corresponding to them on the τ – V graph. It is easily seen that in the region OC of the N – V curve (Fig. 2) the activity increment Δ N is proportional to Δ Q, the amount of tagged water, moving at rates from u_n to u_{n+1} where $u_n = h_0/\tau_n$ and h_0 is the height of the specimen, taken to be equal to the length of the liquid path. The fractions of the amount of water for each rate range are given in Table 1 as percentages of the total amount of liquid flowing across all the cross sections of the specimen.

TABLE 1

Calculation of Distribution Curves of the Amounts of Filtering Water by Filtration Rates and Equivalent Dimensions of the Water-Conducting Pores for Fuscum Peat of R = 10%

V in ml.	Time intervals Δ_{τ} in min.	ΔN in in pulses/ / min.	ΔQ in %	Rate ranges Δu in cm/min.	Pore size ranges ΔD in μ
0—2 m,	0— 2.0	25	2.0	∞— 3.0	∞—23.1
2—4	2.0— 3.8	45	3.5	3.0 —1.58	23.1—16.8
4—6	3.8— 5.5	160	12.6	1.58—1.09	16.8—13.9
6—8	5.5— 7.2	161	12.7	1.09—0.83	13.9—12.1
8—10	7.2— 9.0	129	10.2	0.83—0.67	12.1—10.9
10—14	9.0—12.5	270	21.2	0.67—0.48	10.9—9.25
14—18	12.5—16.2	160	12.6	0.48—0.37	9.25—8.1
18—32	16.2—29.2	210	16.5	0.37—0.20	8.1 —5.95
32—∞	29.2—∞	110	8.7	0.20—0	5.95—0
		1270	100.0		

By means of Poiseuille's law it is easy to pass from the flow rates to the dimensions of the water-conducting pores (the equivalent diameters D), using the formula

$$D = 4\sqrt{\frac{2\,\eta h_0 \cdot u}{p}}, \qquad (1)$$

where η is the viscosity of the liquid, h_0 is the length of the path (height of the specimen), u is the flow speed of the liquid and p is the pressure difference between the ends of the specimen.

The calculated values of the equivalent diameters are, naturally, far from the true dimensions of the pores, which have highly complex outlines. Despite this, it would be of interest, as is customary in dispersion analysis [13], to make at least an approximate evaluation of the dimensions of the water-conducting pores in peat.

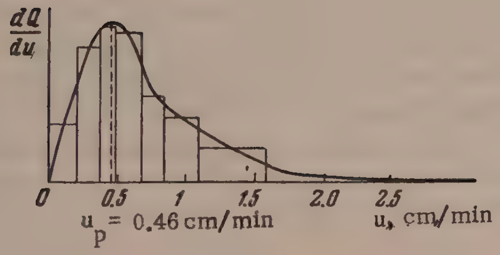

Fig. 3. Distribution of the amounts of filtering liquid by rates of flow in a fuscum peat specimen.

A curve for the distribution of the amounts of filtering liquid by its rates of motion through fuscum peat is given in Fig. 3, where the flow speeds u in cm/minute are shown along the abscissa axis, and values of the distribution function dQ/du along the ordinate axis. The flow speeds vary within wide limits; 75% of the liquid flowing through the specimen moves at speeds from u = 0 to u = 0.9 cm/minute. The mean, most probable speed is u_p = 0.46 cm/minute.

In Fig. 4, the continuous line represents the distribution of the amounts of liquid filtered by sizes of the water-conducting pores. The values of the equivalent diameters D in microns are taken along the abscissa axis. Examination of the distribution curve shows that most of the liquid flows through pores with D equal to $8 - 12\mu$. The size distribution curve of the water-conducting pores may serve to characterize the peat microstructure, which determined its water-conducting properties.

The procedure described above was tested on a simple disperse system close to ideality, namely, homogeneous fine sand with grain diameter < 0.25 mm. The size distribution curve of the water-conducting pores in sand is shown as a dotted line in Fig. 4. The experiments with sand were performed under the same conditions as with peat. Fig. 5 shows the variation of the activity of filtrate samples for sand.

As Fig. 4 shows, the calculated diameters of the water-conducting pores in sand vary in the range of 30 to 100μ. The values are in good agreement with the actual pore sizes, comparable with the sand grain size (D < 250μ).

As has already been stated, only part of the water present in the water-conducting pores in peat moves during filtration. The amount of immobile (fixed) water is evidently an important physicochemical characteristic of peat, which determines its aqueous properties. Water bound in various ways (according to Rebinder, see Korchunov [14]) with the peat particles: by adsorptive, osmotic, and microcapillary bonding, may be regarded as immobile. Immobile water includes also the part of the fixed water filling the blind and closed pores of the peat.

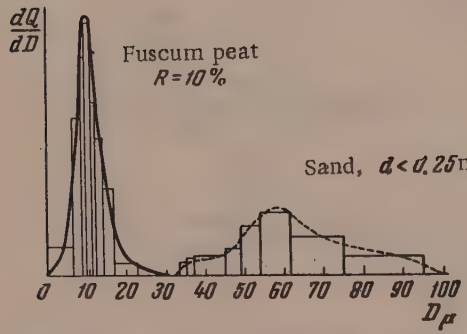

Fig. 4. Distribution of the amounts of filtering liquid by the sizes of water-conducting pores in peat and sand.

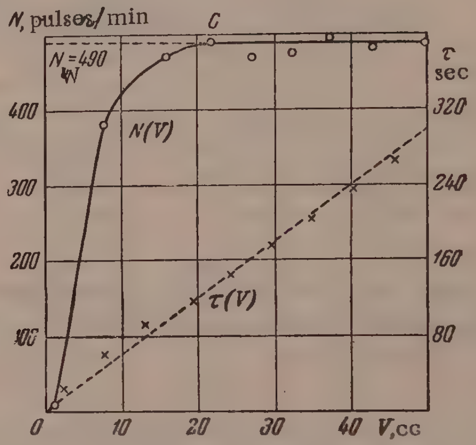

Fig. 5. Results of an experiment on the filtration of tagged water through sand.

It should be pointed out that direct methods for determination of immobile water have not yet been developed [15] . In soil science, the content of fixed water is regarded as being close to the wilting moisture content, corresponding to the limit of mobility of water in the soil [16].

The content of immobile water in peat may be determined from experiments on the filtration of tagged water. As is clear from Fig. 2, the filtrate volume V_f passing through the peat specimen in time $\tau > \tau_k$, contains a part of the tagged water V_t with specific activity N_w, and all the free (mobile) water V_m displaced from the peat during filtration. If the volume of the filtrate in Fig. 2 is represented by a rectangle of height N_w and base V_f, then the volume of mobile water will correspond to the area enclosed between the ordinate axis, the N – V curve, and the broken line (N_w). The specific activity of the filtrate N_f (average for the volume V_f) is lower than the activity of the tagged water N_w owing to dilution by mobile water from the peat. Since the volume of tagged water in the filtrate $V_t = \frac{V_f N_f}{N_w}$, then the amount of immobile water remaining in the peat can be calculated from the formula:

$$V_i = V - V_m = V - V_f + \frac{V_f \cdot N_f}{N_w}, \qquad (2)$$

where V is the total amount of water in the peat specimen.

The amount of immobile water can also calculated from the N – V graph, from the area corresponding to the amount of mobile water.

The results of determinations of immobile water in some types of peat are given in Table 2. Here w and W represent the moisture content of the peat specimen; w_I and W_I are the contents of immobile water in the peat.

TABLE 2

Contents of Immobile Water in Some Types of Peat

Type of peat	Degree of decomposition R in %	Relative moisture content, %			Absolute moisture content, %	
		w	$w_н$		W	W_I
			by filtration method	by displacement method		
Fuscum peat	10	91.1	41.1	40.8	1016	458
Medium peat	10	88.5	38.5	36.9	788	343
Bog sedge	35	90.0	30.2	30.7	892	300

The data in Table 2 show that a considerable amount of water in peat is not involved in filtration. This distinguishes peat from soils, in which the amount of fixed water, determined as water of wilting, does not exceed 10-15% [16]. The active porosity of peat, corresponding to the content of water-conducting pores, with the immobile water taken into account, for fuscum peat, is $n_0 = 51.7\%$. The porosity of the specimen with the immobile water not taken into account is $n = 94.3\%$. From this, the average speed of the water in the peat pores may be calculated:

$$u = \frac{v}{n_0} = \frac{0.246}{0.517} = 0.476 \text{ cm/minute} \tag{3}$$

where $v = 0.246$ cm/minute = the filtration rate, found from the experimental data:

$$v = \frac{Q}{F}, \tag{4}$$

where Q is the amount of filtering liquid and F is the cross section of the specimen. The value found for the average speed is close to the probable speed of the water $u_p = 0.46$ cm/minute (see Fig. 3).

Experiments with filtration of tagged water through sand ($D < 0.25$ mm), performed for comparison, showed that sand contains practically no immobile water. This is in good agreement with Rode's data [16], who estimated the wilting moisture of sand at some tenths of one per cent. This also accounts for the very great difference in the dimensions of the water-conducting pores in sand and in fuscum peat with R = 10% (see Fig. 4), although they are both coarsely disperse systems. The pore cross sections in peat are constricted by immobile water, while in sand all the pores are water-conducting.

The amount of adsorptively bound water, determined by Dumansky's method of negative adsorption of sugar [7, 8] is given by values of w of 15-20% for fuscum and medium peats with R = 10%. Consequently, up to 20-25% of the relative moisture content belongs to osmotically bound water, microcapillary water, and water in blind and closed pores. Thus, by the proposed method in conjunction with the negative adsorption method, N. S. Kurnakov's tensimetric method, and the Volarovich and Gusev method of x-ray structure analysis [17], it is possible to make a more precise evaluation of the types of water in peat according to the forms in which it is bound.

However, the results of the above experiments are valid only if the peat particles adsorb only small amounts of the radioactive tracer. To elucidate this point, after the filtration of tagged water further experiments were carried out, in which the tagged water which had filled the water-conducting pores of the peat during the first experiment was displaced by pure water. The experiments with filtration of pure water were analogous to the preceding experiments with filtration of tagged water, but in this case the mobile water in the peat was tagged water. The results of one such experiment are given in Fig. 2. The $N - V$ and $\tau - V$ curves for the filtration of pure water are represented by dotted lines. The activity of the filtrate in this case decreases from the value N_W for the tagged water, to zero. The symmetrical nature of the N — V curves shows that the experiment is reversible and that no appreciable adsorption of the tracer occurs.

The results of experiments on the displacement of tagged water can also be used to calculate the content of immobile water in peat; this is equal to

$$V_i = V - \frac{V_f \cdot N_f}{N_w}; \qquad (5)$$

in the same notation as before.

If the radioactive tracer had been adsorbed by the peat, the amounts of immobile water determined by the filtration method and the displacement of tagged water would be different. It is easily seen that the values for the content of immobile water in peat would be somewhat high in the first case and somewhat low in the second. The results of the experiments are given in Table 2.

Table 2 shows that the values found for w_i differ only slightly; therefore the amount of tracer adsorbed is not large. This is explained by the negative adsorption of Na_2SO_4 at the interphase in an aqueous medium (as in the case of sucrose), which has also been reported by Dumansky [7, 18].

After displacement of tagged water from the peat, the specimen was removed from the apparatus and cut into equal portions along its height. The pieces were dried and made into samples the activity of which was measured with the window-type counter. Self-absorption of radiation in the peat powder was taken into account in the activity measurements. From the amounts of tagged water which passed through the peat and which remained in the peat, it was calculated that not more than 3-4 % of the radioactive tracer is retained in the peat. This may be attributed both to adsorption of the tracer and to its diffusion into blind pores and immobile water.

An attempt to use the P^{32} phosphorus isotope (aqueous $Na_2HP^*O_4$ solution) as radioactive tracer for water in filtration experiments was unsuccessful. Radioactive phosphorus is almost totally taken up by the peat (90-95%).

At low filtration speeds, appreciable distortion of the N — V curves, and therefore of the results, may occur owing to diffusion of the given radioactive tracer in the liquid. To study the influence of diffusion, a peat specimen was placed in a horizontal glass tube. Tagged water was put into the left hand side of the tube, and pure distilled water in the right hand side. The ends of the tube were connected to storage vessels. The pressure was the same in both parts of the tube, and therefore the tracer could penetrate through the peat from the right to the left of the tube only by diffusion. The tube and specimen dimensions were the same as in the filtration experiments. 0.5 ml samples were regularly withdrawn from the right and left sides of the tube at the surface of the peat specimen. The samples were dried and their activities determined by means of the window-type counter. The determinations were continued for several weeks, but the tracer was not detected in the samples taken from the left of the tube. This indicates that diffusional transfer of the indicator is insignificant in the conditions of the filtration experiments. Calculations carried out in order to give an approximate estimate of the influence of diffusion of the tracer show that at filtration speeds above 0.1 m per day the influence of diffusional transfer can be neglected for practical purposes.

The results of these experiments, the main object of which was to develop methods for studying the aqueous properties of peat by means of radioactive tracers, may be applied in extensive investigations both in laboratory and in field conditions.

SUMMARY

1. A method for studying the filtration of water through peat with the use of radioactive tracers has been developed.

2. The radioactive tracer for water used in studying the aqueous properties of peat was the radioactive sulfur isotope S^{35} in the form of $Na_2S^*O_4$. The adsorption of this tracer by peat does not exceed 3-4 %. Diffusion of the tracer, at the filtration rates used in the experiments with peat, has no appreciable effect on the results.

3. The results of the experiments on the filtration of tagged water through peat specimens have been used to develop a method for determining the dimensions (equivalent diameters) of the water-conducting pores in peat and the liquid flow speeds in them. Curves for the distribution of the amount of filtering liquid by flow speeds and sizes of water-conducting pores in peat and sand have been obtained.

4. A method is described for determination of the amount of immobile water, not involved in filtration, in peat; this is based on displacement of mobile water from peat by water tagged with a radioactive tracer. In conjunction with the negative adsorption method, this method can be used for a more precise classification of water in peat according to type of bonding.

5. The results of the experiments show that peat contains considerable amounts (up to 30-40%) of water which is not involved in filtration.

The Moscow Peat Institute
Chair of Physics

Received October 25, 1956

LITERATURE CITED

[1] A. N. Glazov, Hydrotechnics and Melioration, No. 9, 19 (1956).

[2] A. Montens, GWF, H. 14, 411 (1952).

[3] S. A. Kursin and V. N. Mikhailovsky, Hydrotechnics and Melioration, No. 6, 33 (1956).

[4] A. Montens, Bautechnik, H. 9, 297, (1955).

[5] H. Seligman, Technik, No. 5, 349, (1956).

[6] V. N. Breslav, G. A. Melik-Shakhnazarova, and I. M. Taksar, Bull. Acad. Sci. Latvian SSR, No. 3 (92), 99 (1955).

[7] A. V. Dumansky, Lyophility of Disperse Systems (Voronezh State University Press, 1940).*

[8] N. N. Kulakov, Introduction to the Physics of Peat (State Power Press, 1947).*

[9] V. I. Spitsin et al., Methods of Use of Radioactive Tracers (Acad. Sci. USSR Press, 1955).*

[10] A. V. Sokolov and I. P. Serdobolsky, Use of Phosphorus Isotopes in Agrochemical Investigations (Acad. Sci. USSR Press 1954).*

[11] I. N. Verkhovskaya et al., The Tagged Atom Method in Biology (Moscow University Press, 1955).*

[12] N. A. Figurovsky, Proc. Acad. Sci. USSR, 20, No. 6,453 (1938); J. Phys. Chem., 12, No. 5-6,619 (1938).

[13] N. A. Figurovsky, Sedimentometric Analysis (Acad. Sci. USSR Press, 1948).*

[14] S. S. Korchunov, Investigation of the Physicomechanical Properties of Peat (Symposium, State Power Press, 1953).*

[15] A. I. Budagovsky, Absorption of Water by Soil (Acad. Sci. USSR Press, 1955).*

[16] A. A. Rode, Soil Moisture (Acad. Sci. USSR Press, 1952).*

[17] M. V. Volarovich and K. F. Gusev, Trans. Moscow Peat Inst., No. 2, (State Power Press, 1953) p. 97.*

[18] A. V. Dumansky, The Science of Colloids (State Chem. Press, 1948).*

---

* In Russian.

HEATS OF SWELLING AND OF SOLUTION OF ~~NITRO~~CELLULOSE

D. I. Gal'perin and L. I. Moseev

The information available in the literature on the heats of interaction of nitrocellulose with solvents is scanty and restricted to a relatively narrow range of systems, in which volatile solvents predominate. Nevertheless considerable interest attaches to heats of interaction of nitrocellulose with solvents of low volatility, "plasticizers", which are widely used in the production of cellulose ester plastics. It is particularly important to study the heats of swelling of nitrocellulose over the entire concentration range, so that it is possible to determine the molar ratio of nitrocellulose to solvent in the energy-saturated solvate layer. Integral heats of interaction in the system nitrocellulose – dibutyl phthalate have therefore been determined over the whole concentration range, and the effects of temperature, varied in the range of 0 to 80°, on the integral heats of swelling and solution of nitrocellulose in certain volatile and nonvolatile solvents have been studied.

The same sample of ground nitrocellulose, of medium viscosity lacquer type, containing 12% nitrogen, was used in all the experiments. The heats of swelling were determined with the aid of a variable temperature calorimeter of the type described previously [1]. The integral heats in the dilute solution region (from 0.5 to 3%) were determined directly, by introduction of small weighed quantities of pure nitrocellulose into 150 ml of solvent. In the concentrated solution region, the following procedure [2], based on the Hess law, was used: nitrocellulose samples previously swollen in a restricted amount of solvent, at different component ratios, were first prepared; the heats of dilution of these samples in an excess (150 ml) of the same liquid were then determined. The required integral heat of swelling was then calculated as the difference between the integral heat of solution of pure nitrocellulose in a large quantity of solvent, and the heat of dilution of the sample.

In the case of acetone, the previously swollen nitrocellulose samples were prepared by absorption of the solvent vapor in a vacuum dessicator at room temperature to a definite weight increase [2]. In swelling in dibutyl phthalate, an exact weight of nitrocellulose was treated with dibutyl phthalate diluted with five times its own volume of pure ethyl ether, which was then allowed to evaporate in air with continuous stirring of the mixture. The residual ether was quantitatively removed by heating the specimen under vacuum at 60° for 2 hours. The heats of interaction in dilute solutions at 25° were, per 1 g of nitrocellulose, 18 cal. for acetone, and 10.9 cal. for dibutyl phthalate. The results of determinations of integral heats of interaction over the whole concentration range are shown graphically in Figs. 1 and 2, the integral heats being expressed in calories per 1 g of solution ($-\Delta H$). The maxima on the curves correspond to the limiting concentration of the solvent, at which and above the heat of dilution is zero. This concentration, which corresponds to the energy-saturated solvate layer, is $\sim 34\%$ for acetone and $\sim 53\%$ for dibutyl phthalate.

The influence of temperature on the integral heats of interaction of nitrocellulose with solvents was studied in dilute solutions ($\sim 1\%$), for acetone, butyl acetate, dibutyl phthalate, and tricresyl phosphate *. The same solvents were used by Lipatov and Meerson [3] in an investigation with the same object in view. The results of the determinations, which are averages for numerous determinations, are given in the table, which shows negative temperature coefficients of the integral heat for acetone and butyl acetate, a small negative coefficient for dibutyl phthalate, and a positive coefficient for tricresyl phosphate.

---

* M. M. Iovleva and L. Ya. Muzheva participated in this section of the work.

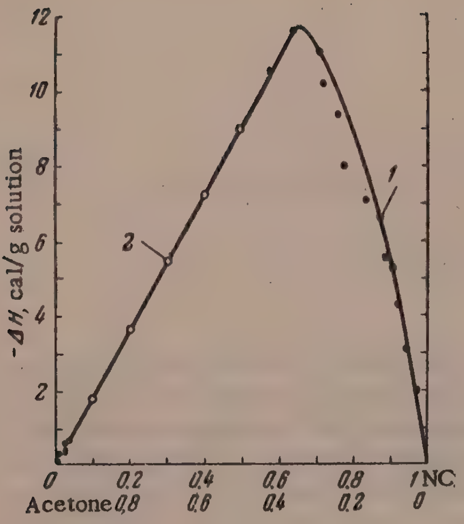

Fig. 1. Variation of integral heats of interaction with solution composition in the system nitrocellulose-acetone: 1) experimental data; 2) calculated data.

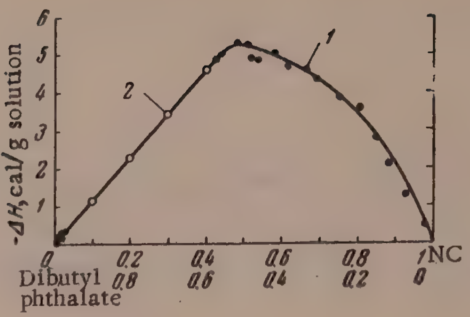

Fig. 2. Variation of integral heats of interaction with solution composition in the system nitrocellulose — dibutyl phthalate: 1) experimental data; 2) calculated data.

TABLE

Integral Heats of Interaction of Nitrocellulose with Solvents at Various Temperatures

(weight taken ~1.5 g per 150 ml of liquid)

Temperature in °C	Q in cal/g of nitrocellulose			
	acetone	butyl acetate	dibutyl phthalate	tricresyl phosphate
0	17.9	—	10.7	—
25	18.0	17.5	10.9	3.9
40	15.5	16.0	11.0	6.7
50	12.0	—	—	—
60	—	14.0	10,0	9.9
70	—	13.1	—	10.6
80	—	11.3	—	11.3

DISCUSSION OF RESULTS

Our values for the integral heats of solution of nitrocellulose in acetone for dilute solutions at 25° (18 cal./g of nitrocellulose) agree with the previously published results of Kargin and Tager [4], and also of Lipatov and Meerson [3]. The boundary concentration (34% acetone) at which the solvate layer becomes energy-saturated, corresponds to 1-1.06 mole of acetone per 1 mole of $-ONO_2$ groups, if it is assumed that there are on the average 2.2 $-ONO_2$ groups per each monomer unit in 12% nitrocellulose. This confirms analogous data for acetone, published earlier [1].

The corresponding boundary concentration for dibutyl phthalate (53% by weight) represents a ratio of 1 mole of dibutyl phthalate per 2.2 moles of $-ONO_2$ groups. Thus, in the formation of a monomolecular saturated solvate layer dibutyl phthalate exhibits bifunctional properties in relation to the number of active (ester) groups in its molecule. The above data indicate, moreover, that in the case of dibutyl phthalate only the $-ONO_2$ groups are involved in the formation of the solvate layer. It seems likely that this type of interaction is not universal, but depends on the nature of the active groups in the solvent and the degree of nitration of the nitrocellulose.

As regards the effect of temperature on the integral heats of interaction between nitrocellulose and solvents, our experiments in general (with the exception of dibutyl phthalate) confirm the results of Lipatov and Meerson [3]. However, we cannot agree with the interpretation given by Lipatov and Meerson [3, 5].

It is known that the variation of the heat effect of any process with temperature obeys Kirchhoff's law [6]

$$dQ_p / dT = -\Delta C_p = -(\Sigma C_p \text{ prod} - \Sigma C_p \text{ init.}),$$

where Q_p is the heat effect of the process; C_p prod is the heat capacity of the final products; C_p init is the heat capacity of the initial substances.

In the case of the solution process, Q_p is the heat of solution, $C_{p\ prod}$ is the heat capacity of the solution, and $C_{p\ init}$ is the heat capacity of the initial components. If, in any temperature region, the heat capacity of the solution is the sum of the heat capacities of the initial components ($\Delta C_p = 0$), then the heat effect of solution in this temperature region will not vary with temperature. If the heat capacity of the solution is greater than the sum of the heat capacities of the initial components ($\Delta C_p > 0$), then the heat effect will decrease with rise of temperature. If $\Delta C_p < 0$ the reverse is the case.

Very little information on heat capacities of polymer solutions is available in the literature. It is noted in one of Skuratov's papers [7] that, in the systems studied by him, either the heat capacities are additive ($\Delta C_p = 0$), or the heat capacity of the solution is greater than the sum of the heat capacities of the initial components ($\Delta C_p > 0$). He did not find any decreases of the heat capacities of solutions relative to the heat capacities of the initial components ($\Delta C_p < 0$). An increase of heat capacity ($\Delta C_p > 0$) was found for diacetylcellulose solutions. A similar effect is to be expected in the case of nitrocellulose.

In our opinion, the increase in the heat capacity of the system when nitrocellulose passes into solution is the cause of the decrease of the integral heats of solution of nitrocellulose in acetone and butyl acetate with temperature, which was found by Lipatov and Meerson and in our experiments.

We extend this conclusion to solvents of low volatility (dibutyl phthalate, tricresyl phosphate), for which the heats of interaction with nitrocellulose should also decrease with increasing temperature. If this effect does not occur, but even the reverse is found (for dibutyl phthalate and tricresyl phosphate in Lipatov and Meerson's experiments, and only for the second of these solvents in our experiments), this must be the result of a retarded swelling process, the duration of which at ordinary temperatures is outside the limits of the ordinary calorimetric determination, but which decreases rapidly with increase of temperature. This applies especially to tricresyl phosphate, which has particularly high viscosity and a large molecular volume; this gives grounds for attributing only a provisional significance to the heat effects found in experiments with tricresyl phosphate, at least at temperatures between 25 and 60°.

The retarded swelling factor is less prominent in the case of dibutyl phthalate, which has lower viscosity and molecular volume. Therefore, in using ground nitrocellulose, we not only did not find an increase of the heat effect in its interaction with nitrocellulose as the temperature increased from 0 to 60°, but even found some tendency to a decrease (see Table). Thus, in contrast to Lipatov and Meerson, we do not attribute the difference of the signs of the temperature coefficients of the integral heats of solution of nitrocellulose in volatile solvents and in tricresyl phosphate to differences in the type of energy interaction of volatile solvents and " plasticizers" with nitrocellulose, but regard it as the result of the influence of the diffusional kinetic factor. In conditions of a brief calorimetric experiment, the effect of this factor compensates and even exceeds the influence of the true thermodynamic factor of heat capacity increase. Confirmation of this viewpoint was provided by the data, cited above, on the heats of interaction of nitrocellulose with dibutyl phthalate over the entire concentration range, showing that dibutyl phthalate does not in any way differ in principle from acetone in the character of its energy interaction with nitrocellulose. Energy saturation is reached in both cases on interaction of 1 mole of active solvent groups with 1 mole of $-ONO_2$ groups. Any difference in the nature of the energy interaction of nitrocellulose with dibutyl phthalate and butyl acetate is still less to be expected, as both these solvents are esters, i. e., they have active groups of a similar nature.

Neither can we agree with the interpretation given by Lipatov and Meerson [3, 5] of the decrease with temperature of the heat of solution of nitrocellulose in volatile solvents. In this interpretation it is postulated that at normal temperatures the systems nitrocellulose – acetone or nitrocellulose – butyl acetate are not true solutions but gels.

It is known that such solvents are compatible with nitrocellulose in all proportions at all temperatures studied, to form one-phase systems [4, 8]. In relation to these actual systems, especially at low concentrations, one can hardly speak of any critical temperature (within the range in question) of spontaneous transition of a gel into a molecular solution and vice versa. This would be in clear contradiction to experimental results which (in absence of external influences) never show syneresis in such solutions, even if they are cooled to temperatures considerably below the "critical" values. The extensive production experience of many branches of industry in which nitrocellulose solutions are used confirms this.

SUMMARY

1. The integral heats of interaction of 12% nitrocellulose with dibutyl phthalate and acetone over the entire concentration region have been determined. It is shown that the energy-saturated solvate layer corresponds to ratios of one molecule of dibutyl phthalate or of two molecules of acetone per 2 $-ONO_2$ groups. Therefore both ester groups in dibutyl phthalate are involved in blocking the polar groups of nitrocellulose. It was found that only $-ONO_2$ groups enter into energy interaction with these solvents in the formation of monomolecular layers.

2. A negative temperature coefficient of the heat effect has been found for acetone and butyl acetate, a small negative coefficient for dibutyl phthalate, and a positive temperature coefficient for tricresyl phosphate.

In conclusion, the authors express their gratitude to A. A. Tager for participation in discussions of the results of this work.

Regional town of Molotov Received December 10, 1955

LITERATURE CITED

[1] V. A. Kargin and S. A. Papkov, J. Phys. Chem., 7,483 (1936).

[2] A. A. Tager and Zh. S. Dombek, Colloid J., 15,69 (1953).

[3] S. M. Lipatov and S. I. Meerson, Colloid J., 12,122,427 (1950).

[4] A. A. Tager and V. A. Kargin, J. Phys. Chem. 15,1029,1036 (1941).

[5] S. M. Lipatov and S. I. Meerson, Colloid J., 17,230 (1955).

[6] M. Kh. Karapetyants, Chemical Thermodynamics, (State Chem. Press, 1949). (In Russian.)

[7] S. M. Skuratov, Colloid J., 9,133 (1947).

[8] P. I. Zubov, Z. I. Zhurkina, and V. A. Kargin, Colloid J., 9,109 (1947).

INVESTIGATIONS OF THE PHYSICAL CHEMISTRY OF AGAR

1. METHOD FOR THE DETERMINATION OF THE INTRINSIC VISCOSITY OF AGAR

S. A. Glikman and I. G. Shubtsova

As is known, polyelectrolyte solutions are characterized by a sharp rise of the reduced specific viscosity in the low concentration region. This anomalous effect is diminished by additions of mineral salts. The pronounced role of the valency of the added salt led Smoluchowski and Kruyt to advance the theory of the so-called electroviscous effect. Complete suppression of the effect is not always possible because of coagulation. However, even when a linear $\eta_{sp} / c - c$ relationship is attained, extrapolation of the line to zero polyelectrolyte concentration gives different values for η which decrease with increasing salt content. Interpretation of these results presents a fairly difficult problem.

According to modern theories, if groups ionizable in a given medium are present along a polymer molecule, the bulk of the randomly kinked or globularly coiled polymer molecule increases owing to forces of repulsion. The bulk of such a molecule depends on the number of ionizable groups and on their degree of dissociation. It therefore increases with dilution of the polyelectrolyte, decreases with additions of salts, and depends on the composition of the solvent. Intramolecular forces between the polar groups (ionizable and nonionizable), which in their turn depend on the composition of the solvent and on the contents of electrolytes and nonelectrolytes in the solution [1, 2], also play a part.

The object of our work was to develop a technique for finding the true values of the intrinsic viscosity of different agar specimens and fractions with complete suppression of ionization, i. e., values of η_{∞}, corresponding to the behavior of a single randomly kinked molecule devoid of electric charge.

As is known, agar solutions exist in a state of molecular dispersion only above a certain limiting temperature. At lower temperatures they are "gel solutions" ; their viscosity greatly depends on the efflux rate, and an elastic limit may be detected in them by sensitive methods.

It was established by preliminary experiments that, of the samples studied (Japanese and domestic Far Eastern agar and their fractions), one of the fractions of the Far Eastern sample * had the highest transition temperature from a true solution to an aggregated system. The approximate value of the critical temperature, 58°, corresponds to the intersection of two straight lines (Fig. 1), expressing the efflux time – temperature relationship for the solutions in the chosen conditions. To obtain comparable results, all subsequent viscosity determinations were performed at 60° ± 0.01. The temperature was maintained constant by means of a well insulated water ultrathermostat.

The aqueous solutions of the samples were prepared as follows. A weighed portion of agar, after 10-12 hours of swelling, was heated on the water bath at 100° for 15 minutes. The hot solution was filtered through a No. 3 glass filter with suction, and then placed in a thermostat at 60° for 30 minutes. 10 ml of the solution was taken out by means of an accurate pipet (kept in an air thermostat at 60°) and transferred to an Ubbelohde viscosimeter of the hanging level type. Viscosity measurements were started after 15-20 minutes. The concentration of the original solution was found from the dry residue. The efflux time for water in this instrument at 60° was 220.8 seconds. The maximum value of the kinetic energy correction for a solution with the lowest specific viscosity $\eta_{sp} = 0.008$ was 0.052%, so that this correction could be neglected.

---

* The fractionation procedure is described in our next communication.

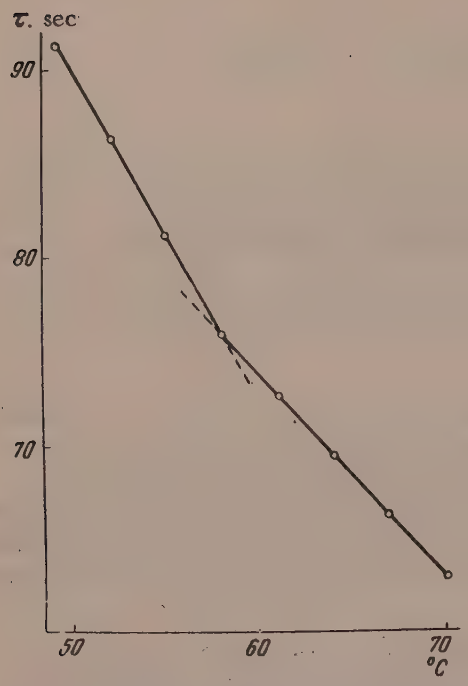

Fig. 1. Effect of temperature on the viscosity of a 0.5% solution of fraction V of Far Eastern agar.

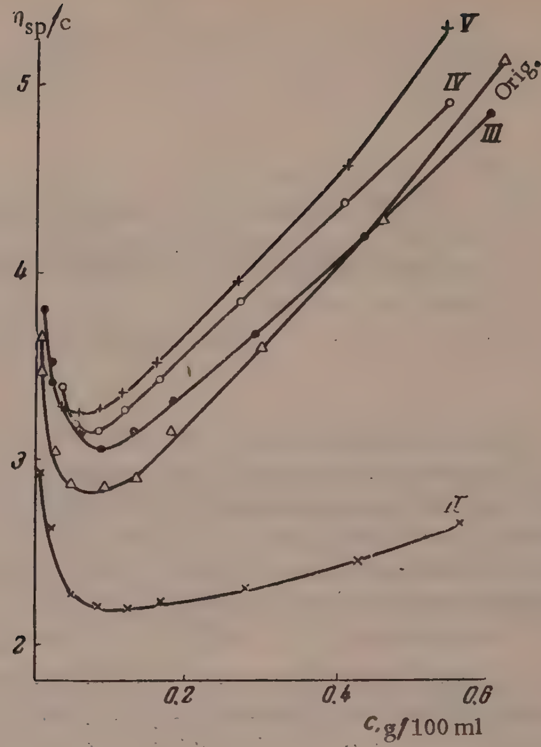

Fig. 2. Effect of concentration on the reduced specific viscosity of fractions (II, III, IV, V, original) of Far Eastern agar.

To prevent evaporation of the solvent during the determinations, the air space of the viscosimeter was closed by joining the ends of its tubes together.

The solutions were diluted in the viscosimeter by the volume method, with the solvent contained in the thermostat at the same temperature. Repeated weighing of the volume of liquid taken up by the same pipet showed that the dilution error does not exceed 0.2%. The accuracy of the specific viscosity found in our experiments depended mainly on the unavoidable error in determinations of the efflux time (within ± 0.1 second). Calculations showed that for most of the solutions studied, even the most dilute, the relative error did not exceed 1%.

Figure 2 shows the effect of concentration on the reduced specific viscosities of fractions of one of the agar samples. It is seen from Fig. 2 that a pronounced electroviscous effect is found in all cases in the low concentration region, and extrapolation to zero concentration is impossible. Minimum values of η_{sp}/c, different for different fractions, were found for agar concentrations of the order of 0.1%. Similar results were obtained for the sample of Japanese agar.

The effects of mineral salt additions on the viscosity of aqueous agar solutions were studied on 0.1% solutions of Far Eastern and Japanese agar fractions. Similar results were obtained for both (Fig. 3).

With increasing valency of the cations in the chlorides added to aqueous agar solutions, the viscosity minimum is shifted in the direction of lower salt concentration c_i ; the decrease of viscosity becomes greater as the region in which η_{sp}/c is constant becomes narrower, while the viscosity increase beyond the minimum is greater.

On the assumption that viscosity depends on the effective volume of the randomly kinked molecule, and that local or complete charge reversal of the polyelectrolyte molecule is possible, all these differences can be explained by the influence of the valency of the cation on compression of the ionic atmosphere, on the adsorbability of the cations (i. e., their attachment to the anionic groups of the polymer molecule), on the intramolecular binding of individual anionic groups, and on repulsion of groups of like charge, with charges reversed owing to adsorption of cations.

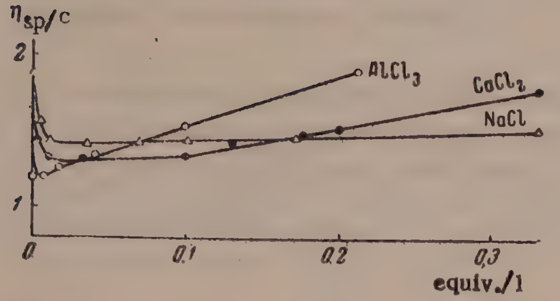

Fig. 3. Effect of electrolytes on the viscosity of 0.1% solutions of fraction II of Far Eastern agar.

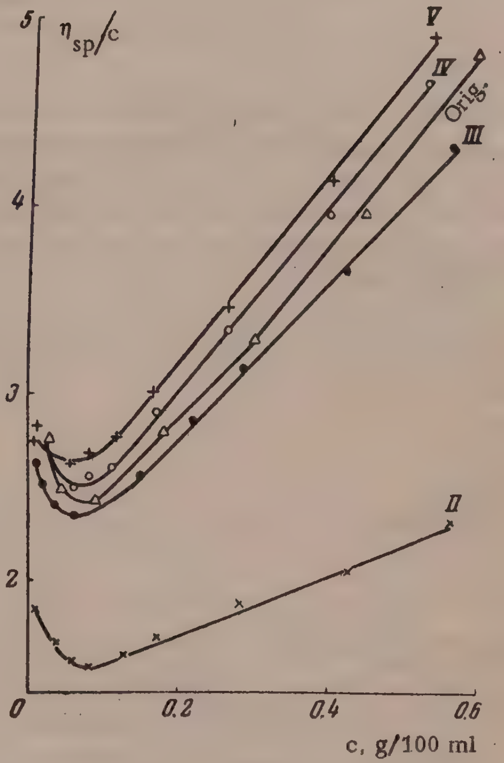

Fig. 4. Effect of concentration on the viscosities of fractions (original, II, III, IV, V) of Far Eastern agar solutions containing 0.01 g-equiv. $CaCl_2$ per liter.

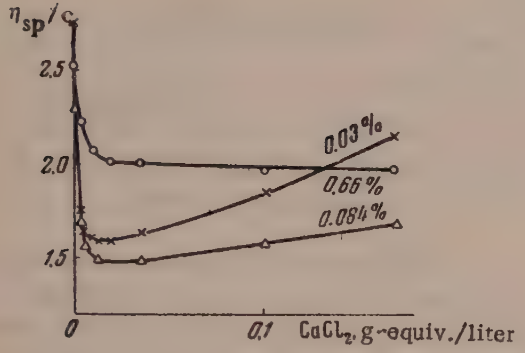

Fig. 5. Effect of $CaCl_2$ on the viscosity of Japanese agar solutions of various % concentrations.

Since agar is essentially the calcium salt of a sulfuric acid ester of a linear polygalactan, to avoid complicating effects (ion exchange), we first studied the influence of calcium chloride on the electroviscous effect. Since, as Fig. 3 shows, the viscosity of 0.1% agar solutions was at a minimum when the solutions contained 0.01 g-equiv. $CaCl_2$ per liter, the viscosities of all the agar solutions were determined at the same calcium chloride content. The data so obtained on the variation of η_{sp}/c with concentration for solutions of Far Eastern agar containing 0.01 g-equiv. $CaCl_2$ per liter are given in Fig. 4. Similar results were obtained for Japanese agar.

Comparison of Figs. 4 and 2 shows that addition of 0.01 g-equiv. $CaCl_2$ to agar solutions results in a considerable viscosity decrease, but does not eliminate the electroviscous effect. The explanation for the latter fact may be that, at low agar concentrations, adsorption of bivalent Ca^{2+} ions on the anionic groups of the agar causes reversal of the molecular charge. This is confirmed by data on the influence of calcium chloride on agar solutions of various concentrations (Fig. 5).

While in the case of 0.66% agar solution the values of η_{sp}/c, after a sharp fall, remain constant over a wide range of $CaCl_2$ concentrations, the curves for agar solutions of lower concentrations show more or less definite maxima. The ascent of the curve after the minimum is the result of partial or total charge reversal of the polymer molecules. Naturally, the role of charge reversal is greater at lower agar concentrations.

Adsorption of bivalent cations on univalent anionic groups of the agar molecules is the reason why the viscosity minimum attained at low calcium chloride concentration is not in any way a measure of the effective volume of the uncharged agar molecule. It is not possible to explain in any other way the higher value of the viscosity minimum for 0.03% agar solution in comparison with the minimum for 0.083% solution. The ionic atmosphere is apparently not yet compressed to the limit, the potential is not yet reduced to zero, the effective volume of the molecules has not yet reached the minimum value, but adsorption of calcium ions on individual $(-OSO_2O-)$ groups leads to increase of the effective volume owing to Coulomb repulsion of the $(-OSO_2OCa)^+$ groups formed.

The region of constant η_{sp}/c values at higher calcium chloride concentrations is the consequence of mutual compensation of two opposing factors: a decrease of the total negative charge of the agar molecule and formation of local positive charges. That is why the electroviscous effect cannot be suppressed by additions of salts with bivalent cations in any concentrations. There are no grounds for extrapolation of the linear portion of the curve to zero agar concentration, as the values of $(\eta_{sp}/c)_{c\to 0}$ so obtained would not have any definite physical meaning.

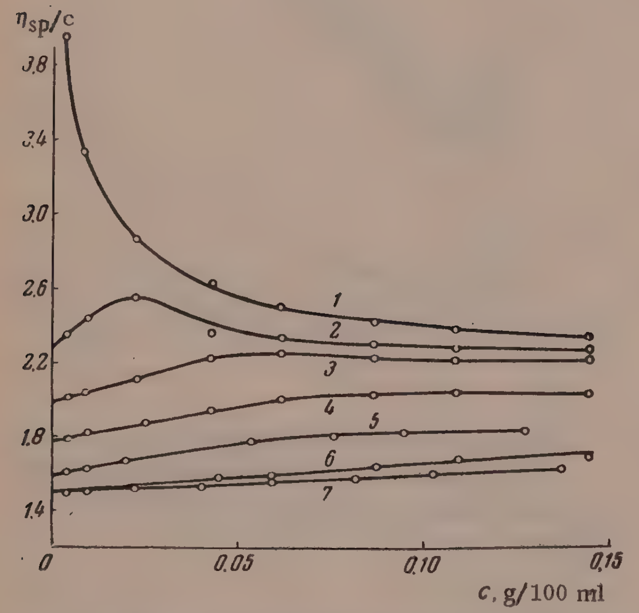

Fig. 6. Effect of concentration on the reduced specific viscosity of Japanese agar solutions containing various amounts of KCl: 1) without KCl; 2) 0.0001 N KCl; 3) 0.0002 N KCl; 4) 0.0005 N KCl; 5) 0.005N KCl; 6) 0.05 N KCl; 7) 0.25 N KCl.

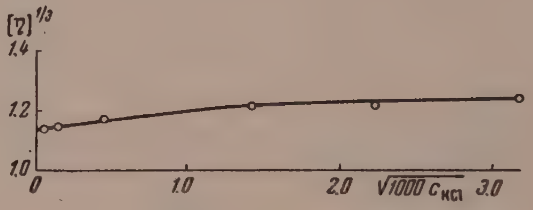

Fig. 7. Variation of intrinsic viscosity of agar with the KCl content of the solution.

A different state of affairs should be found in systems containing a salt with a univalent cation, such as potassium chloride, as the added electrolyte. Here attachment of the K^+ ion to the anionic $(-OSO_2O-)$ group cannot lead to charge reversal, but only has an effect on compression of the ionic atmosphere and decrease of the charge on the agar polyanion. The role of K^+ ion adsorption on the hydroxyl groups of the agar molecule at low potassium chloride concentrations is evidently not great. This is shown by the wide range over which η_{sp}/c is constant in presence of various amounts of KCl (Fig. 6).

We obtained a group of curves for viscosity as a function of concentration, for various potassium chloride concentrations from 0.0001 to 0.25 g-equiv./liter, analogous to the curves obtained by Fuoss and Strauss [3] for polyvinylpyridinium bromide, and by Pals and Hermans [4] for sodium pectate, with characteristic maxima which gradually level out with increasing salt contents (Fig. 6). Pals and Hermans [4] attribute the maxima to the relationship between the concentrations of the polyelectrolyte ions and the ions of the added low-molecular electrolyte. At low concentrations of the polyelectrolyte, for example of sodium pectate, the number of its ions is far smaller than the number of NaCl ions. Therefore in the initial region of the curve the ionic strength of the solution (at constant NaCl concentration) varies very little with the polyelectrolyte concentration and therefore the degree of uncoiling of its molecules (their bulk) remains almost constant, while the regions of the η_{sp}/c curve to the left of the maximum, in agreement with the Huggins equation, remain linear.

Extrapolation of the initial linear region to zero concentraion gives a value of η_{∞}, corresponding to the given degree of ionization of the polyelectrolyte. The higher the ionic strength of the solution, the less will be the effective volume of the polyelectrolyte molecule, and the lower the value of η. With excess of added salt, the minimum value of η_{∞} is reached, corresponding to the effective volume of a molecule completely devoid of charge, i. e., unionized.

We used the Fuoss method [3] to plot the relationship $\eta^{1/3} = f(c_{KCl})^{-1/2}$ for our data for agar, and obtained a straight line (Fig. 7), extrapolation of which to infinite concentration of electrolyte gives the true value for the intrinsic viscosity η_{∞} corresponding to uncharged, randomly kinked agar molecules, the effective volume of which is determined only by the micro-Brownian movement of the chain segments in the given conditions.

The value found for η_{∞} proved to be equal to the constant value of η for solutions containing from 0.05 to 0.25 g-equiv. of potassium chloride per liter. On this basis, without plotting groups of curves similar to that shown in Fig. 7 for each fraction, but by adding electrolyte to the agar solutions in sufficient quantities to stabilize the viscosity values, we can obtain quite definite data on the true values of η_{∞} for different agar samples and their fractions.

SUMMARY

1. The effect of mineral salt concentrations on the viscosity of agar solutions has been studied. The results are discussed in the light of the modern theory of polyelectrolyte solutions.

2. A method has been developed for determining the true intrinsic viscosity η_{∞} of agar solutions, corresponding to the effective volume ("bulk ") of undissociated, randomly kinked molecules, the configuration of which is determined only by the micro-Brownian movement of the chain segments.

Saratov State University

Received September 10, 1955

LITERATURE CITED

[1] H. Kruyt, Colloid Science, vol. 2, Reversible Systems (1949).

[2] A. Katchalsky, J. Polymer Sci., 12, 159 (1954).

[3] R. M. Fuoss, P. Strauss, J. Polymer Sci., 3,602 (1948).

[4] D. Pals, J. J. Hermans, J. Polymer Sci., 3,897 (1948); 5,733 (1950).

AGGREGATIVE STABILITY OF PIGMENT SUSPENSIONS IN HYDROCARBONS, ALCOHOLS, AND ESTERS OF LOW MOLECULAR WEIGHT

Ya. M. Gurevich

It was found in our investigation [1] that if pigment suspensions in gasoline are stabilized by oleic acid these pigments also form aggregatively stable suspensions in butanol. Otherwise, the latter are unstable. It was therefore suggested that the factors which determine stability have the same mechanism in both cases. This mechanism consists of adsorption of stabilizer molecules (oleic acid) on the pigment surface in the one case, and of molecules of the dispersion medium (butanol) in the other.

The validity of this view in relation to other organic media has been tested in the present investigation. The following dispersion media were used: lacquer gasoline, xylene, butanol, ethylene glycol, butyl acetate, dibutyl phthalate, tricresyl phosphate, and mixtures of esters with xylene. Twelve pigments were studied, namely: iron blue, ultramarine, cobalt blue, emerald green, Mars brown, yellow ocher, titanium dioxide, zinc sulfide, red ocher, chrome yellow, cadmium yellow, and vine black (suspensions in 2% concentration by volume).

The stability of the suspensions was evaluated by their sedimentation time until clear. All the pigments used contain a certain proportion of particles of fractions of one micron in size. In the unaggregated state such particles remain in suspension and color the suspension throughout the layer for several days, even in media of low viscosity.

In suspensions with low aggregative stability and fairly high pigment concentrations, all the pigment particles are distributed simultaneously among the aggregates formed, and in consequence the aggregates are of the same size and density and settle at the same rate. When they come into contact at the bottom of the vessel, the aggregates cohere and form a loose continuous structure, which gradually becomes more compact under the force of gravity. In such suspensions, a measure of the aggregative stability can be taken to be the time which elapses from the end of agitation of the suspensions to the start of settling of the aggregates formed, which is indicated by the appearance of a layer of pure dispersionsmedium in the upper part of the vessel.

In suspensions in which aggregates of different sizes, settling consecutively at the bottom of the vessel, are formed, a measure of the aggregative stability is provided by the time for the complete settling of all the pigment particles and clarification of the suspension over the entire layer.

In suspensions of the intermediate type, in which part of the pigment particles forms aggregates of the same size forming a continuous structure at the bottom of the vessel, and part forms smaller aggregates of various sizes remaining in the suspended state, a measure of the aggregative stability can be taken to be the time for complete settling of the pigment and clarification of the suspension in the layer from the top to the boundary of the continuous structure.

A similar method for qualitative evaluation of the aggregative stability of suspensions was used by Rebinder, Serb-Serbina, and Kordyukov [2] in studying the wetting action of surface-active agents.

The results of visual observations on the settling of pigment suspensions are given in schematic form in Tables 1 and 2. Table 1 gives results for pigment suspensions in alcohols and hydrocarbons. Table 2 compares results for suspensions in esters and their mixtures with xylene. Table 1 shows that the aggregative stability of suspensions of all pigments in hydrocarbons is low, and that there is a similarity between the degree of stability in alcohol suspensions and in suspensions in lacquer gasoline stabilized with oleic acid.

The explanation for the low aggregative stability of suspensions in hydrocarbons is that the hydrocarbon molecules, devoid of polar groups, do not saturate the secondary valencies of the polar active centers in the pigment surface when adsorbed on it. Secondary valency forces appear in these centers; under the action of these the pigment particles cohere on collision, and the suspension passes into an aggregated state.

The reason for the similarity between alcohol suspensions and suspensions in gasoline stabilized with oleic acid in the degree of aggregative stability lies in the fact that the polar active centers of the pigment surface, which have an affinity for carboxyl groups, have a similar affinity for hydroxyl groups. Therefore pigments rich in active centers, capable of firmly adsorbing oleic acid molecules, have the same property with regard to alcohol molecules.

Both in the adsorption of oleic acid molecules and in the adsorption of alcohol molecules two effects occur: the secondary valencies of the active centers become saturated and other active centers, situated in the areas occupied by the firmly adsorbed acid or alcohol molecules, become blocked.

TABLE 1

Sedimentation Times of Pigment Suspensions in Hydrocarbons and Alcohols

Pigment	Dispersion medium			
	Hydrocarbons		Alcohols	
	lacquer gasoline, xylene	lacquer gasoline with 3-5% of oleic acid	Butanol	Ethylene glycol
Iron blue	—	+++	+++	+++
Ultramarine	—	+++	++	+++
Cobalt blue	—	+++	++	+++
Mars brown	—	+++	++	+++
Emerald green	—	+++	++	++
Red ocher	—	+++	++	++
Titanium dioxide	—	—	—	—
Zinc sulfide	—	—	—	—
Yellow ocher	—	—	—	—
Chrome yellow	—	—	—	—
Cadmium yellow	—	—	—	—
Vine black	—	—	—	—

Symbols: +++ suspension colored throughout the layer for more than 5 days; ++ pigment settles between 3 hours and 5 days; — — pigment settles or upper zone clarifies in less than 3 hours.

It is seen from Table 2 that as the number of polar groups in the ester molecule increases, the number of pigments forming suspensions of a high degree of stability in these media increases also. Dilution of suspensions of pigments in esters with xylene decreases their stability. The dilution effect depends not only on the amount of xylene added, but also on the properties of the pigment and the ester: it increases in the order of the pigments as given in Table 2, and decreases with increasing number of polar groups in the ester molecule.

This behavior is in agreement with the view that the degree of aggregative stability is determined by the stability of the bonds between the pigment surface and the molecules adsorbed on it.

As the number of ester groups in the molecule increases, there is an increase in the number of polar contacts by which it is attached to the pigment surface, and the degree of saturation and shielding of the pigment particle surface increases accordingly.

Dilution of pigment suspensions in esters by xylene reduces their aggregative stability owing to increased desorption of the ester molecules. The effect of dilution should increase with decreasing stability of the bonds between the adsorbed ester molecules and the pigment surface, and with decreasing number of contacts between them. This is illustrated by Table 2.

To sum up the interpretation of Tables 1 and 2, we may conclude that in all the suspensions studied the degree of aggregative stability is determined by the ratio of the saturated and blocked active centers of the pigment surface to the active centers in this surface in which secondary valency forces are free to develop. This is analogous to P. A. Rebinder's theory [3] of the conditions which determine the formation of thixotropic structurized suspensions.

It must be pointed out that the above considerations are only valid for suspensions in media of low molecular weight. As has been shown in our studies [1, 4], aggregative stability in suspensions containing substances of high molecular weight depends not only on the degree of saturation or blocking of secondary valencies in the pigment surface, but also on the degree of saturation of those secondary valencies of the adsorbed molecules which do not interact with the pigment surface.

TABLE 2

Sedimentation Times of Pigment Suspensions in Esters and Their Mixtures with Xylene

Pigment	Dispersion medium								
	butyl acetate–xylene			dibutyl phthalate–xylene			tricresyl phosphate – xylene		
	100–0	60–40	20–80	100–0	60–40	20–80	100–0	60–40	20–80
Vine black	+++	++	—	+++	+++	+	+++	+++	++
Iron blue	+++	++	—	+++	+++	+	+++	+++	++
Red iron ocher	—	—	—	+++	++	—	+++	+++	+
Chrome yellow	—	—	—	+++	++	—	+++	+++	+
Cadmium yellow	—	—	—	+++	++	—	+++	+++	—
Cobalt blue	—	—	—	+++	++	—	+++	++	—
Emerald green	—	—	—	+++	++	—	+++	++	—
Ultramarine	—	—	—	+++	++	—	+++	++	—
Mars brown	—	—	—	—	—	—	+++	++	—
Yellow ocher	—	—	—	—	—	—	+++	++	—
Titanium dioxide	—	—	—	—	—	—	+++	++	—
Zinc sulfide	—	—	—	—	—	—	+++	++	—

Symbols: +++ suspension remains colored throughout the layer for more than 5 days; ++ pigment settles in 1-5 days; + pigment settles in 3-24 hours; — — pigment settles or upper zone of the suspension clarifies in less than 3 hours.

Some specific conclusions concerning the properties of individual pigments may be drawn from the data in Tables 1 and 2.

Iron blue, ultramarine, cobalt blue, and emerald green have high affinity for carboxyl, hydroxyl, and ester groups. Vine black, red iron ocher, chrome yellow, and cadmium yellow have strong affinity for ester groups and weak affinity for carboxyl and hydroxyl groups.

Mars brown and yellow ocher have strong affinity for carboxyl and hydroxyl groups, and weak affinity for ester groups.

Titanium dioxide and zinc sulfide have weak affinity for carboxyl, hydroxyl, and ester groups.

From the rule that polar regions of the molecules interact with polar groups and nonpolar with nonpolar, it may be assumed that the different affinities of various polar groups of the adsorbed molecules for the active centers of the pigment surface are determined by correspondence of their polarities.

It follows from the experimental results that hydroxyl and carboxyl groups are similar to each other, and differ significantly in polarity from ester groups, and that on the pigment particle surfaces there are active centers of different degrees of polarity, which interact with groups differing in polarity in the adsorbed molecules.

SUMMARY

1. Investigations of the aggregative stability of pigment suspensions in hydrocarbons, alcohols, and esters of low molecular weight show that the degree of aggregative stability of suspensions in these media depends on the stability of the bonds between the pigment surface and the molecules of the medium adsorbed on it.

2. The stability of the bonds between pigment surfaces and adsorbed molecules increases with increasing number of polar groups in the latter.

3. Pigments differ in their affinities for hydroxyl, carboxyl, and ester groups in the adsorbed molecules; this is determined by correspondence between the polarities of the active centers in the pigment surface and of the groups of the adsorbed molecules interacting with them.

State Research and Project Institute
Moscow

Received April 16, 1956

LITERATURE CITED

[1] Ya. M. Gurevich, Colloid J., 18,158 (1956).

[2] P. A. Rebinder, N. N. Serb-Serbina, S. A. Kordyukov, Symposium, The Struggle against Silicosis, vol. 1 (Acad. Sci. USSR Press, 1953).

[3] P. A. Rebinder, Discussions Faraday Soc., No. 18 (1954); A. A. Abduragimova, P. A. Rebinder, and N. N. Serb-Serbina, Colloid J., 7, 184 (1955).

[4] Ya. M. Gurevich, Colloid J., 14,93 (1952).

DEPENDENCE OF THE EXCHANGE ADSORPTION OF IONS ON THEIR STRUCTURE

2. ADSORPTION OF BIVALENT AMINES

A. T. Davydov and R. F. Skoblionok

The numerous investigations on the exchange of mineral ions do not exhaust the whole range of phenomena which determine the nature of their adsorption. Investigations of exchange adsorption of organic ions are of especial theoretical and practical interest because the information available in this field is very restricted. It is known that the relationships established for exchange adsorption of mineral ions are not fully applicable to the exchange of organic ions on modern ion exchange resins. An important difference of the exchange adsorption of organic ions, as compared with mineral ions, is the simultaneous operation of electrostatic and van der Waals forces [1-5]; the significance of the latter increases with increasing size of the organic ions and their concentration in the solution. In studies of the exchange adsorption of organic ions it is natural to assume that their structure should have a greater influence than that of mineral ions. The question of the influence of the structure of organic ions on the extent and nature of their adsorption is of undoubted interest.

The present paper describes a study of the extent and nature of the adsorption of bivalent organic ions in relation to their structure. The substances chosen for the study were the hydrochlorides of ortho-, meta- and para-phenylenediamines, which are readily soluble in water and dissociate in aqueous solution. In earlier investigations we studied the adsorption of univalent amines [5]; the reason for choosing phenylenediamines was that by comparing their adsorption (of ions of different phenylenediamines) with the adsorption of univalent amines from solutions of their hydrochlorides it is possible to estimate the influence of the valency of the ion. Ca-sulfocarbon and Ca-Espatite were used for the investigations. Solutions of ortho-, meta-, and paraphenylenediamine hydrochlorides of various concentrations from 0.05 to 1.00 N were prepared. Five gram samples of the adsorbents were covered with 50 ml each of a solution of the given phenylenediamine of the appropriate concentration. The experimental procedure used is described in the preceding paper [5].

In the study of the adsorption of univalent amines [5] it was found that equivalence between the amount of Ca^{2+} desorbed and the amount of amine adsorbed from the solution was not maintained. Nonequivalence of the exchange began to appear in the region of moderate concentrations, and increased with increasing concentration. To determine whether the number of equivalents of Ca^{2+} desorbed corresponds to the number of equivalents of phenylenediamine adsorbed, the concentrations of the phenylenediamine ions in the original and equilibrium solutions were determined, in addition to the Ca^{2+} concentration in the equilibrium solution. The Ca^{2+} concentration was determined gravimetrically (the volumetric method for Ca^{2+} determination could not be used in presence of colored solutions), and the concentrations of the phenylenediamine ions were determined by potentiometric titration by sodium nitrite in a hydrochloric acid medium [6].

To test for molecular adsorption when the adsorbents were treated with salts or organic ions, the chloride ion concentrations in the original and equilibrium solutions were determined by potentiometric titration with $AgNO_3$ solution. The results are given in Table 1.

The difference between the Cl^- ion concentrations in the original and equilibrium solutions, as was to be expected, was within the limits of experimental error; this shows that molecular adsorption of phenylenediamine hydrochlorides does not take place.

TABLE 1

Desorption of Ca^{2+} Ions by Bivalent o-, m-, and p-Phenylenediamine Ions on Sulfocarbon and Espatite

System	Ion exchange on sulfocarbon				Ion exchange on Espatite			
	amine concentration in solution, normality		amount of amine in mg-equiv. adsorbed by 10 g	amount of Ca^{2+} in mg-equiv. displaced from 10 g	amine concentration in solution, normality		amount of amine in mg-equiv. adsorbed by 10 g	amount of Ca^{2+} in mg-equiv. displaced from 10 g
	initial	equilibrium			initial	equilibrium		
[Ca] + o-phenylenediamine hydrochloride	0,025	0,001	4,8	4,99	0,025	0,0005	4,9	3.57
	0,055	0.002	10.6	7,42	0,055	0,002	10,6	6.99
	0.132	0,027	21,0	11.98	0.132	0.022	22,0	15.26
	0.255	0,125	26,0	13.27	0.255	0.118	27.4	18.69
	0,382	0.245	27.4	13.55	0,382	0.225	31.4	19.26
	0.519	0.367	30,4	13.84	0.519	0.353	33.2	19.54
[Ca] + m-phenylenediamine hydrochloride	0,054	0.001	5.3	4.78	0,054	0.002	5,2	4.07
	0.102	0,007	9.5	7,99	0,102	0,006	9.6	8.13
	0.265	0.092	17.3	12.62	0,265	0.075	19,0	15.30
	0,538	0.345	19.3	12.98	0.538	0.326	21,2	17,19
	0.768	0.550	21.8	13.12	0.768	0,544	22.4	17.69
	1,133	0.811	32.2	13,27	1.133	0.806	32.7	17,97
[Ca] + p-phenylenediamine hydrochloride	0.023	0.001	4,4	5.42	0,023	0,001	4.4	4,57
	0.051	0.005	9,2	8.56	0.051	0.005	9.2	7,70
	0.121	0.051	14,0	12.41	0.121	0.037	16.8	13.55
	0.280	0.187	18.6	14.84	0.280	0.164	23.2	16.69
	0,444	0.350	18.8	15.26	0.444	0.304	28.0	17.83
	0.514	0.420	18.8	15.55	0,514	0.368	29.2	—

As the solution concentrations varied from 0.05 to 1.00 N, the pH decreased from 2.2 to 1.0. The pH values of the original and equilibrium solutions were equal, eliminating the possibility of participation of H^+ ions in ion exchange reactions.

As in the titration of o- and p-phenylenediamines by sodium nitrite, probably only one amino group is diazotized [7] (this can be confirmed by comparing the results of amine and chloride determinations in the original solutions); the values found for the normalities of their solutions are halved. This was taken into account in calculations of the amounts of the amines in milligram equivalents adsorbed by 10 g of the adsorbents (the differences between the number of equivalents in the original and equilibrium solutions of o- and p-phenylenediamines were doubled).

Table 1 shows that the number of equivalents of the amine adsorbed is greater than the number of equivalents of Ca^{2+} desorbed, and this difference is especially great in the region of high concentrations. With a constant concentration of Cl^- in the solution this may be attributed to adsorption of a nonpolar form of the amine. Comparison of the number of equivalents of Ca^{2+} desorbed by various organic cations (aniline, and o-, m-, and p-toluidines, with one amino group [5]) with desorption of Ca^{2+} by bivalent ions (o-, m-, and p-phenylenediamines) from sulfocarbon (Table 1) gave the same results. This behavior of phenylenediamines suggests that, despite the presence of two amino groups, they are present in the form of univalent ions in aqueous solutions. This is confirmed by the difference between the first and second ionization constants of p-phenylenediamine [8]: $K_1 = 1.1 \cdot 10^{-8}$; $K_2 = 3.5 \cdot 10^{-12}$.

The identical behavior of all three phenylenediamine derivatives in adsorption indicates that the difference between the first and second ionization constants is of about the same order, 10^4, for the ortho and meta derivatives. Since the value of the acidity constant of one of the ions is very high, of the order of 10^{-2}, its dissociation is so great that the H^+ ions are not in fact held by the amino group. Our hypothesis is also confirmed by the fact that phenylenediamine sulfates $[C_6H_4(NH_2)_2]_2\ H_2O_2SO_2$ contain univalent phenylenediamine ions [9].

If we are to assume that adsorption of phenylenediamine ions in univalent form occurs owing to hydrolysis of one of the ions, we must also assume that the hydrolysis is complete at all the equilibrium phenylenediamine concentrations studied, in the pH region 1.0-2.2, which is highly improbable. The assumption concerning the influence of hydrolysis is also contradicted by literature data [10] which show that phenylenediamine is hydrolyzed as a univalent ion in aqueous solution.

We have therefore considered, on the basis of our experimental data and information available in the literature, the exchange adsorption of phenylenediamines as the adsorption of univalent ions.

TABLE 2

Calculation of the Gapon Equation Isotherms

Systems	a	$x = \frac{\sqrt{a/2}}{100\ c}$	$y = \frac{1}{a}$	y_{calc}	a_m	K	σ_y
Sulfocarbon-Ca + o-phenylenediamine hydrochloride	4.99	5.2650	0.200	0.194	14,0 ± 0.5	0.33 ± 0,08	0.005
	7.42	3,2102	0,135	0.146			
	11.98	0.4450	0.084	0.082			
	13.27	0,1026	0,075	0.074			
	13.55	0.0531	0,074	0,073			
	13,84	0.0358	0.072	0,072			
Sulfocarbon-Ca + m-phenylenediamine hydrochloride	4,78	5,1533	0.209	0.200	13,8 ± 1.1	0.34 ± 0.07	0.009
	7.99	2,8553	0.125	0,143			
	12,62	0,2730	0,079	0,079			
	12,98	0,0738	0,077	0,074			
	13,12	0,0466	0,076	0,073			
	13.27	0,0318	0,075	0.073			
Sulfocarbon-Ca + p-phenylenediamine hydrochloride	5.42	5.4873	0,185	0.185	14.7 ± 0.4	0.32 ± 0.14	0.005
	8.56	2,0687	0,117	0.116			
	12.41	0.2442	0.081	0.076			
	14.84	0,0728	0.067	0,068			
	15.26	0.0394	0.065	0.067			
	15.55	0.0332	0.064	0.066			
Espatite-Ca + o-phenylenediamine hydrochloride	3.57	13.3600	0.280	0.283	18,8 ± 0.5	0,32 ± 0.03	0,004
	6.99	4,6738	0,143	0.134			
	15,26	0,6424	0.065	0.064			
	18.69	0.1301	0.054	0.055			
	19,26	0.0688	0,052	0.054			
	19.54	0.0433	0.051	0.053			
Espatite-Ca + m-phenylenediamine hydrochloride	4,07	7,1325	0,246	0,238	18,9 ± 1.0	0,49 ± 0.08	0,005
	8.13	3,3602	0.123	0.140			
	15.30	0.3688	0,065	0,063			
	17,19	0,0900	0.058	0,056			
	17,69	0,0551	0,056	0,055			
	17,97	0.0372	0,055	0,054			
Espatite-Ca + p-phenylenediamine hydrochloride	4.57	5.0390	0,219	0,220	17,2 ± 0.6	0.55 ± 0.16	0,003
	7,70	2.1801	0.130	0,128			
	13.55	0.3471	0.074	0.069			
	16,69	0.0883	0.060	0.061			
	17,83	0.0492	0.056	0.059			

For the exchange of bivalent with univalent ions, the Gapon isotherm equation [11] has the form:

$$\frac{1}{a} = \frac{1}{a_m} + \frac{K}{a_m}\sqrt{\frac{a/2}{100c}},$$

where a is the number of mg-equivalents of desorbed cation per 10 g of adsorbent, equal to the number of mg-equivalents of the adsorbed univalent cation: a_m is the maximum adsorption in mg-equivalents per 10 g of adsorbent; c is the equilibrium concentration of the univalent cation in millimoles per 1 ml (in calculations of c the concentration of hydrolyzed ions was not taken into account, as it is very low, of the order of 10^{-5} - 10^{-6} millimole/ml); K is the exchange constant.

TABLE 3

Constants for the Exchange Adsorption Isotherms for Univalent Amines

Systems	a_m	K
Sulfocarbon - Ca + aniline hydrochloride	15.3 ± 0.9	0.64 ± 0.23
" + o-toluidine hydrochloride	14.7 ± 2.1	0.52 ± 0.04
" + m-toluidine hydrochloride	15.9 ± 0.6	0.66 ± 0.09
" + p-toluidine hydrochloride	13.9 ± 2.8	0.55 ± 0.06
" + o-phenylenediamine hydrochloride	14.0 ± 0.5	0.33 ± 0.08
" + m-phenylenediamine hydrochloride	13.8 ± 1.1	0.34 ± 0.07
" + p-phenylenediamine hydrochloride	14.7 ± 0.4	0.32 ± 0.14

The calculated data for this equation, based on our experimental results, are given in Table 2. The small root mean square errors of the average values of the constants and of individual determinations of $y = 1/a$ show that the Gapon equation applies satisfactorily to the systems studied. The values found for y and the calculated constants for the isotherms in the exchange adsorption of o-, m-, and p-phenylenediamine on sulfocarbon and Espatite agree within the limits of experimental error. Con equently, the structure of the ions (the relative positions of the amino groups) has no influence on the extent and nature of the adsorption.

A comparison of the constants for the exchange adsorption isotherms for phenylenediamines with the corresponding constants for univalent amines [5] (Table 3) on sulfocarbon-Ca shows that the differences between them also lie within the limits of experimental error. This confirms the view that o-, m-, and p-phenylenediamines behave as univalent ions in aqueous solution. The somewhat lower values of K for the exchange of phenylenediamine ions are probably the result of somewhat greater effects of van der Waals forces.

SUMMARY

1. The exchange adsorption of o-, m-, and p-phenylenediamines on sulfocarbon-Ca and Espatite-Ca has been studied.

2. Equal exchange adsorption isotherms have been found for all the systems studied on sulfocarbon and Espatite, showing that structure of the phenylenediamines has no effect on ion exchange adsorption.

3. The adsorbents studied do not adsorb phenylenediamine hydrochlorides in molecular form from solution; this is shown by the same concentrations of Cl^- in the original and equilibrium solutions.

4. The amounts of Ca^{2+} desorbed are not equivalent to the amounts of phenylenediamine ions

adsorbed. The number of equivalents of phenylenediamine adsorbed was greater than the number of equivalents of Ca^{2+} liberated in all systems.

5. The exchange adsorption of phenylenediamine ions is of the same magnitude as that of univalent amine ions. The Gapon equation for the exchange of bivalent with univalent ions is applicable to the results obtained.

The A. M. Gorky State University
Kharkov
Chair of General Chemistry

Received May 29, 1956

LITERATURE CITED

[1] T. R. E. Kressman, J. A. Kitchener, J. Chem. Soc. No. 5, 1208, (1949).

[2] T. R. E. Kressman, J. Phys. Chem. 56, No. 1, 118, 1952.

[3] W. H. Slabaugh, J. Phys. Chem. 58, No. 2, 162, 1954.

[4] N. A. Izmailov and S. Kh. Mushinskaya, Proc. Acad. Sci. USSR, No. 1, 101 (1955).

[5] A. T. Davydov and R. F. Skoblionok, Colloid J., 18, No. 1,31 (1956).

[6] L. M. Litvinenko and A. P. Grekov, J. Anal. Chem., 10, No. 3,164 (1955).

[7] M. D. Zhorina, Factory Labs., 7, 10, 1180 (1947).

[8] Yu. Yu. Lurye, Calculation and Reference Tables for Chemists (Moscow, 1947) 193.

[9] H. Hübner, Ann. Chem. 209, 339, 1881.

[10] Victor Herbert, Veley, J. Chem. Soc. 93, 2122, (1908).

[11] E. N. Gapon, J. Gen. Chem., 3,145 (1933); 7,1438 (1937).

THE INFLUENCE OF STRUCTURE ON THE CHEMICAL ACTIVITY AND VULCANIZABILITY OF BUTADIENE POLYMERS

B. A. Dogadkin, A. V. Dobromyslova, F. S. Tolstukhina, and N. G. Samsonova

In polymerization of butadiene and its derivatives, the monomer groups join in various positions. The 4-1 and 2-1 structures are the most common:

$$\sim CH_2 - CH = CH - CH_2 - CH_2 - CH = CH - CH_2 \sim;$$

(4 – 1)

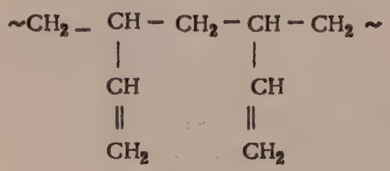

$$\sim CH_2 - \underset{\substack{|\\ CH\\ \|\\ CH_2}}{CH} - CH_2 - \underset{\substack{|\\ CH\\ \|\\ CH_2}}{CH} - CH_2 \sim$$

(2 – 1)

The relative contents of these structures have a significant influence on the physical properties of the polymer (glass transition temperature, degree of orientation, strength, etc). It is also evident that differences in the position and nature of substitution of the double bond cause differences in the chemical activity of the polymers. These differences in chemical activity are also determined by the fact that the 4-1 structure contains methylene groups in the α-position to the double bonds, which therefore have hydrogen atoms with weakened bonds with carbon. In the 2-1 structure there is a hydrogen atom attached to a tertiary carbon atom. The differences in the chemical activities of butadiene polymers were studied in their interaction with perbenzoic acid, iodine chloride, and elementary sulfur.

The materials studied were synthetic butadiene rubbers with various relative contents of 4-1 and 2-1 structures in their molecular chains. The contents of vinyl side chains in the 2-1 structure were determined by the ozonation method, from the amounts of formic acid and formaldehyde split off [1]; the double bond contents of the 4-1 structure were determined from the difference between total unsaturation and the contents of vinyl side chains.

For some of the rubbers the results were confirmed by spectrographic data from the characteristic frequencies of 965 cm^{-1} for double bonds of the 4-1 structure and 909 cm^{-1} for monosubstituted double bonds of the 2-1 structure.

Interaction with perbenzoic acid. The reaction of unsaturated compounds with perbenzoic acid was studied in detail by Prilezhaev [2]. He established that the rate of the perbenzoic acid reaction depends on the positions and nature of the substituents at the double bonds. The chief direction of the reaction is the formation of epoxide groups in the polymer, in amounts equivalent to the benzoic acid formed. Meyer* has proposed the use of the Prilezhaev reaction for determination of the structure of butadiene polymers by calculating the content of 4-1 structural units with the aid of a special diagram, based on the results of titration of model low-molecular hydrocarbons under the same conditions. Our kinetic investigations showed that, in chlorobenzene medium with 0.1 N concentration of the rubber at 20°, both types of double bonds react with perbenzoic acid, but at very different rates. Figure 1 shows the kinetics of the reactions of benzoic acid with solutions of natural rubber, one of the butadiene polymers, and vinylcyclohexene as a model substance containing a disubstituted double bond in the ring and a monosubstituted double bond in the vinyl side chain. The amount of perbenzoic acid consumed was determined by titration with 0.1 N thiosulfate solution. Natural rubber, which contains only the 4-1 structure in its molecules, reacts rapidly, and the total amount of perbenzoic acid decomposed corresponds (to within 2%) to α, the total unsaturation of this compound (Curve 1). The kinetic curve for the oxidation of vinylcyclohexene contains two distinct regions — an initial region of steep ascent, and a final linear region which represents the reaction proceeding at a low constant rate. If the linear region is extrapolated to the ordinate axis, it cuts off an intercept corresponding to 50% of the total number of double bonds in vinylcyclohexene. From this it may be concluded that the linear region represents the oxidation kinetics of the less active vinyl groups, while the steeply ascending region corresponds to rapid oxidation of disubstituted double bonds in the ring. By drawing a horizontal straight line from the point of intersection of the linear region with the ordinate axis, it is possible to find ordinates corresponding to slow oxidation of vinyl groups, for each time instant on the experimental curve, and to plot a theoretical curve representing oxidation of the double bonds in the ring only (Curve 4).

---

* Meyer's work, carried out in the laboratory of the Schkopau works, has not been published; it is mentioned by Weindlein [3].

The kinetic method for the determination of the structure of butadiene rubbers by the perbenzoic acid reaction was developed by Dogadkin and Dobromyslova [4]. Salfer and Johnson [5] consider that this method is applicable only to polymers containing more than 70% of internal double bonds.

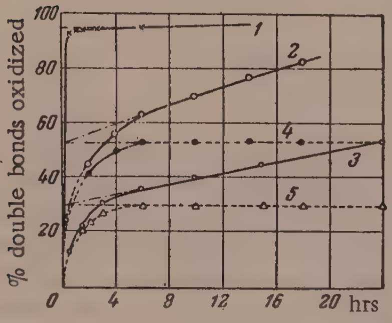

Fig. 1. Kinetics of oxidation of vinylcyclohexene and different rubbers by perbenzoic acid: 1) natural rubber; 2) vinylcyclohexene; 3) butadiene polymer SR-1; 4, 5) kinetics of double bond oxidation in the 4-1 structure of vinylcyclohexene and butadiene polymer SR-1.

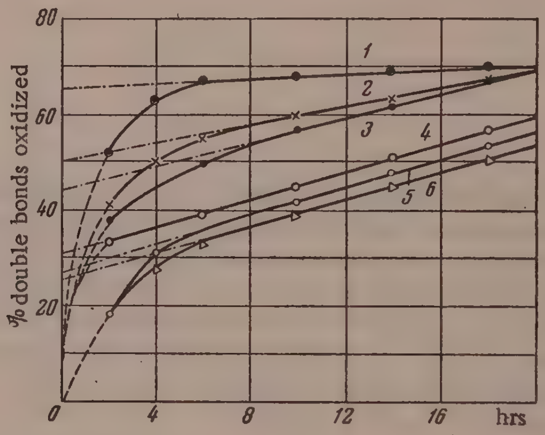

Fig. 2. Kinetics of oxidation of various butadiene rubbers by perbenzoic acid: 1) SR-6; 2) SR-5; 3) SR-7; 4) SR-4; 5) SR-8; 6) SR-9.

The kinetic curves for the reaction of perbenzoic acid with butadiene polymers are of similar form, since the latter contain two kinds of double bonds in their chains (Fig. 2). The double bonds in the vinyl side chains are oxidized very slowly, and therefore at a constant rate, because their concentration does not change significantly during the time of observation. By extrapolating the linear regions of the kinetic curves to the ordinate axis, it is possible to determine the initial contents of double bonds of the 4-1 structure, and to plot the kinetic curve for the oxidation of the 4-1 structure (Fig. 2, Curve 5) as described above.

The validity of this method of segregating the oxidation processes of different types of double bonds, and of their quantitative determination, is confirmed by data on ozonation of the same polymers (Fig. 2 and Table).* The values for the double bonds of different structures in seven grades of synthetic rubber, determined from kinetic data with perbenzoic acid, are in good agreement with the values obtained from ozonation data and data on the reaction with iodine chloride.

Interaction with iodine chloride. Reactions of rubbers with halogens have been frequently studied. The reactions are complex in character, and vary according to conditions, both in their mechanism and in the intermediate steps and final results. In many cases, addition of halogens at the double bonds is accompanied by substitution of hydrogen at the α-methylene groups and formation of intramolecular rings [6].

---

* This table appears at the end of the article.

The structure of the polymer has a significant effect on the course of the reaction. We studied the reaction between iodine chloride and butadiene polymers with various contents of 4-1 and 2-1 structures. The reaction was carried out by mixing 0.05 M (calculated on the unit molecular weight) of the rubber solution in dichloroethane with 0.2 N solution of iodine chloride in the same solvent. The halogen was in 100% excess above the theoretical amount. The course of the reaction was followed by the consumption of iodine chloride (by titration of samples with thiosulfate) and by formation of iodine (titration of samples with potassium iodate).

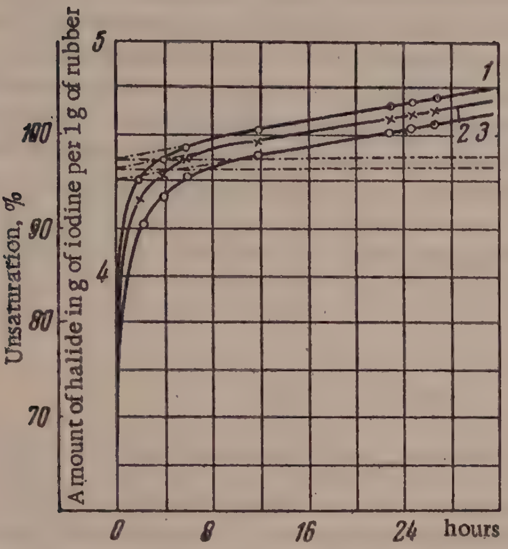

Fig. 3. Kinetics of iodine chloride absorption in the reaction with butadiene polymers: 1) SR-4; 2) SR-5; 3) SR-6.

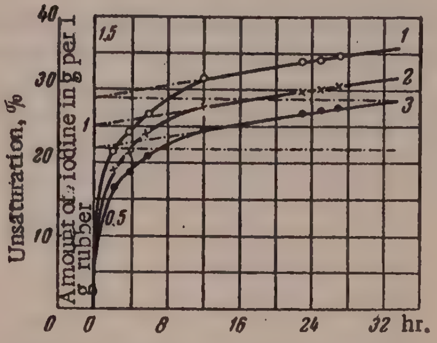

Fig. 4. Kinetics of iodine formation in the reaction of iodine chloride with butadiene polymers: 1) SR-4; 2) SR-5; 3) SR-6.

As Fig. 3 shows, absorption of iodine chloride by the polymer at 20° proceeds at a high rate during the first 6-8 hours; subsequently the reaction slows down and continues for a long time at a low constant rate (linear region of the kinetic curve). The initial region mainly represents the addition of iodine chloride at the double bonds [6] according to the schemes:

$$\sim CH_2-CH=CH-CH_2\sim \xrightarrow{ClI} \sim CH_2-CHI-CHCl-CH_2\sim \qquad (1)$$

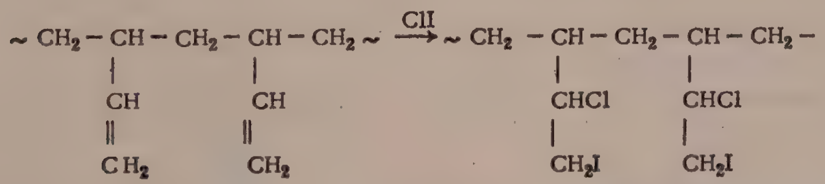

$$\sim CH_2-\underset{\substack{|\\ CH\\ \parallel\\ CH_2}}{CH}-CH_2-\underset{\substack{|\\ CH\\ \parallel\\ CH_2}}{CH}-CH_2\sim \xrightarrow{ClI} \sim CH_2-\underset{\substack{|\\ CHCl\\ |\\ CH_2I}}{CH}-CH_2-\underset{\substack{|\\ CHCl\\ |\\ CH_2I}}{CH}-CH_2- \qquad (2)$$

The linear region represents the slow reaction of hydrogen substitution, which probably occurs according to the scheme:

$$\sim CH_2-CHI-CHCl-CH_2\sim \xrightarrow{ClI} \sim CHCl-CHI-CHCl-CH_2\sim + HI \qquad (3)$$

As the result of the last reaction, an equivalent amount of iodine is liberated:

$$HI + ClI \rightarrow HCl + I_2 \qquad (4)$$

Since I_2 is titrated by thiosulfate in the same way as ClI, Reaction (4) is not reflected in the kinetic curve for the absorption of iodine chloride. If the linear region of the kinetic curve for the absorption of iodine chloride is extrapolated to the ordinate axis, it will evidently cut off an intercept corresponding to maximum absorption of ClI in the addition reaction, which in its turn corresponds to the content of double bonds in the rubber molecules.

In fact, the unsaturation determined by this method coincides with the unsaturation found as the sum of double bonds of 4-1 structure (by the reaction with perbenzoic acid) and double bonds of 2-1 structure (from the amounts of formic acid and formaldehyde in the ozonation reaction).

The liberation of iodine in the reaction medium is represented by kinetic curves analogous to the kinetic curves for the addition of iodine chloride (Fig. 4). The linear regions of the curves in Fig. 3 and Fig. 4 have the same slope. This proves convincingly that in the last stage of the process iodine is liberated according to Equation (4), and the amount formed corresponds to the HI split off in the substitution reaction represented by Equation (3). The initial rapid liberation of iodine is probably associated with a cyclization reaction [6]. If the linear region of the kinetic curve for iodine liberation is extrapolated to the ordinate axis, the intercept cut off is a measure of the maximum amount of iodine liberated in cyclization. As Fig. 5 shows, this amount increases linearly with increase of the content of the 2-1 structure in the molecules of the different rubbers. This suggests that cyclization occurs predominantly in the 2-1 structure according to the following scheme:

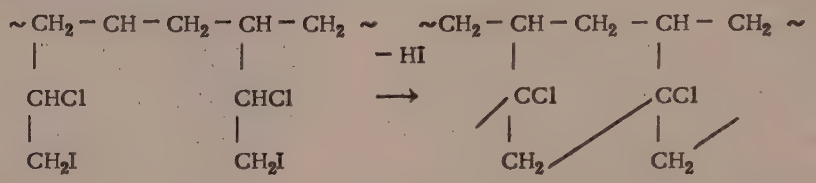

(5)

The liberated hydrogen iodide then reacts with iodine chloride to form iodine according to Equation (4).

Thus, different rubbers show the same behavior in the addition reaction at the double bonds, in the reaction with iodine chloride under the conditions studied. The cyclization process, in the other hand, develops mainly in the structure with vinyl side chains; this may be attributed to steric conditions favorable for six membered ring formation in such structures. The fact that the straight line in Fig. 5 does not pass through the coordinate origin suggests that a similar process may occur also in the 4-1 structure.

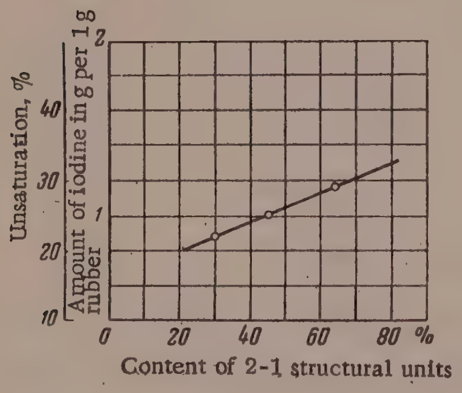

Fig. 5. Variation of the amount of iodine formed in the cyclization reaction with the contents of 2-1 structural units in various polymers.

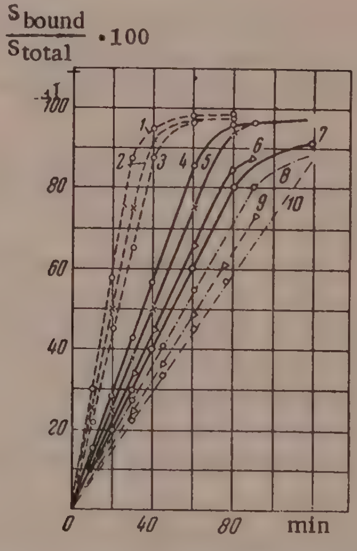

Fig. 6. Kinetics of sulfur addition to rubbers of 4-1 structure in solution in a nitrogen atmosphere at various temperatures: 1,2,3—155° 4,5,6,7,—142°; 8, 9, 10—135°; 1,4,8—SR-6—65%; 2,5—SR-5—50%; 6,9—SR-7—43%; 3,7,10—SR-4—30% of 4-1 structure.

Interaction with sulfur and vulcanization. The interaction of rubber with sulfur is the main reaction in the vulcanization process. The reaction of butadiene polymers with sulfur was studied by heating solutions in toluene in ampoules, with strict exclusion of atmospheric oxygen. The solutions contained ~ 4 g of rubber per 100 ml of solvent; the sulfur content was 2 g per 100 g of rubber. The accelerator was a condensation product of aniline with acetaldehyde and butyraldehyde (Accelerator A-100), and triethanolamine was used as activator. In the conditions described, addition of sulfur to rubber proceeds at a constant rate for nearly the total duration of the reaction (Fig. 6), which may be explained by the large excess of active centers (double bonds and α-methylene groups) in rubber, in relation to the sulfur, and the narrow variation range of the volume concentration of sulfur in the solution during the entire observation time. As Fig. 7 shows, the rate of addition of sulfur to rubber increases linearly with increasing content of the 4-1 structure in the rubber molecules. In the temperature range from 135 to 155° this reaction obeys the Arrhenius equation (Fig. 8). The apparent activation energy of the reaction of addition of rubber to sulfur depends on the structure of the polymer, decreasing with increasing content of the 4-1 structure or, which is the same thing, increasing with increasing content of the 2-1 structure (Fig. 9). Since this relationship is linear, it is possible by extrapolation to determine the activation energy for a polymer of one particular structure, i. e., to determine the activity of sulfur toward disubstituted double bonds of 4-1 structure and to monosubstituted double bonds of the vinyl side chains of 2-1 structure. Its value in the first case is 14 kcal./mole, and in the second, 19 kcal./mole, and the difference between these agrees with the corresponding value determined from the kinetics of thermal oxidation of rubbers [7].

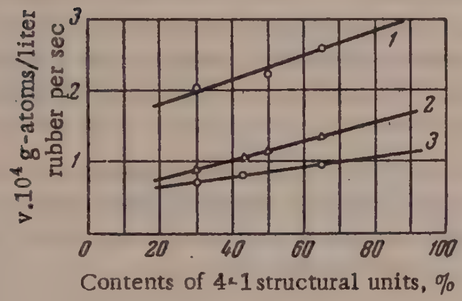

Fig. 7. Rate of sulfur addition as a function of the rubber structure: 1 — 155°; 2 — 142°; 3 — 135°

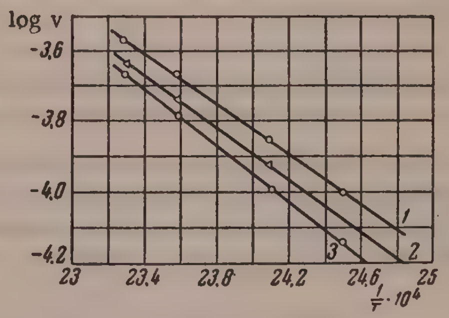

Fig. 8. Rate of sulfur addition to rubbers of 4-1 structure, as a function of the temperature: 1) SR-6, 65%; 2) SR-5, 50%; 3) SR-4, 30%.

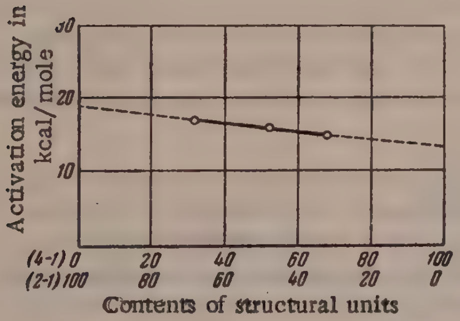

Fig. 9. Activation energy for the addition of sulfur to rubber as a function of the rubber structure.

The different chemical reactivities of double bonds of 4-1 and 2-1 structure toward sulfur were established by direct observation of variations of the intensity of the absorption bands in the infrared region of the spectrum during vulcanization. The technique developed for this was reported by Dogadkin and Klausen at the 10th All-Union Conference on Spectroscopy. Rubbers containing 65 and 50% of double bonds of 4-1 structure were studied. The absorption intensity for the 4-1 structure was measured at a frequency of 965 cm^{-1}, and for the 2-1 structure at 909 cm^{-1}. The vulcanization was carried out in films applied to rock salt plates, and in solution. In the latter case the spectroscopic determinations were made after evaporation of a sample of the solution placed on a rock salt plate. In the vulcanization experiments in solution, changes of unsaturation were also determined by the reaction with iodine chloride; the results so obtained were in good agreement with the spectroscopic data.

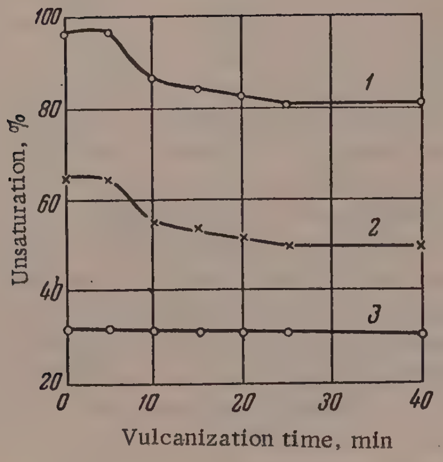

Fig. 10. Variation of the unsaturation of rubber with 65% of 4-1 structural units during vulcanization in film form in a nitrogen atmosphere at 142°; 1) total unsaturation; 2) unsaturation of 4-1 structure; 3) unsaturation of 2-1 structure.

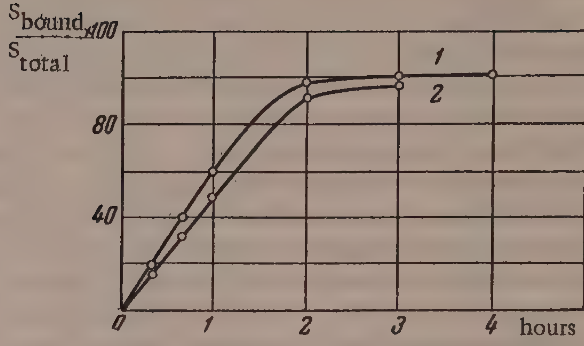

Fig. 11. Kinetics of sulfur addition to technical rubbers of different structure of the same degree of alkalinity in vulcanization without accelerators in a press at 142°; 1) SR-6, 65% of 4-1 structure; 2) SR-4, 30% of 4-1 structure.

As Fig. 10 shows, the double bonds of the 4-1 structure disappear as the result of vulcanization at about 15 times the rate for the double bonds of the vinyl side chains of 2-1 structure. It must be pointed out, however, that this evaluation does not agree with the evaluation based on kinetic data which takes into account the activation energies determined above for the addition of sulfur to 4-1 and 2-1 structures.

If the vulcanization is carried out under technical conditions in a press, the difference between the rates of sulfur addition to rubbers of different structure tends to disappear (Fig. 11). The probable explanation for this is the sharp increase of the volume concentration of double bonds, and the consequent increase of the absolute reaction rate, under these conditions in comparison with vulcanization in solution.

It is also significant that, according to spectroscopic data, there is no decrease in the double bond content at the start of vulcanization (horizontal regions in Curves 1 and 2, Fig. 10). This means that reactions involving α-methylene groups of the 4-1 structure predominate at this stage of vulcanization. The reactions involving the α-methylene groups have different mechanisms. Direct interaction with sulfur leads to formation of thiol groups and displacement of the double bonds into a new position, indicated in the case of natural rubber by the appearance of absorption bands at a characteristic frequency of 965 cm^{-1}[8]. Interaction with molecules of the accelerator (or with radicals formed by their decomposition) leads to removal of hydrogen and formation of polymeric radicals which react with each other or with the molecular rubber chains to form chemical cross bonds of the vulcanization network. The mechanism of this process has been discussed by one of the present authors elsewhere [9].

During the steady state period of vulcanization the total decrease of unsaturation is a linear function of the amount of sulfur added (Fig. 12). It is found that the loss of unsaturation (in contrast to the results described in the literature for natural rubber) is 4-6 times as great as the value calculated for the addition of one sulfur atom per double bond. The loss of unsaturation increases with vulcanization temperature between 135 and 155°. This increase in the loss of double bonds above the value calculated from maximum substitution with sulfur can be attributed either to polymerization processes involving joining of the molecular chains at the double bonds, or thermal formation of intramolecular rings. The latter hypothesis is refuted by the fact that unsaturation is not changed as the result of prolonged heating (for 12 hours) of rubber and its solutions in an inert gas at vulcanization temperatures, as shown both by spectroscopic data and by the iodine chloride reaction. As regards the hypothesis that in these conditions interaction occurs between the sulfur, accelerator, and rubber, inducing polymerization processes analogous to those which occur in the reaction between rubber and benzothiazolyl disulfide [9], this does not agree with the fact that the number of cross links in a vulcanizate (determined from the modulus) is considerably less than the number of atoms of bound sulfur. Further experimental study of this effect is therefore needed.

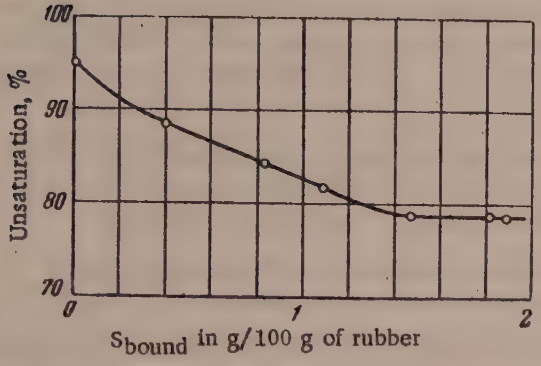

Fig. 12. Variation of the total unsaturation of SR-5 rubber with addition of sulfur during vulcanization in solution, in a nitrogen atmosphere at 142°.

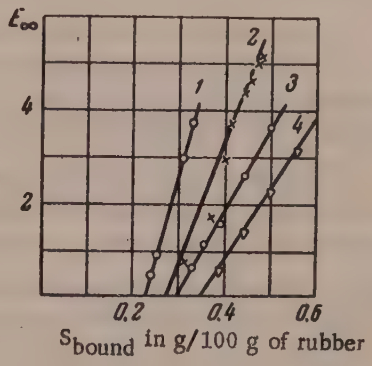

Fig. 13. Equilibrium modulus as a function of the amount of bound sulfur for rubbers with different contents of 4-1 structural units: 1) SR-6, 65%; 2) SR-5, 50%; 3) SR-7, 43%; 4) SR-4, 30% of 4-1 structure.

The number of chemical cross links formed between the molecular rubber chains was determined from the equilibrium modulus of elasticity E which, as is known, is a linear function of the number of cross links. As Fig. 13 shows, the number of intermolecular chemical bonds formed for a given amount of added sulfur increases with increasing relative content of the 4-1 structure in the molecular rubber chains.

The degree of cross linking $\Delta E/\Delta S$ is a linear function of the number of double bonds of 4-1 structure (Fig. 14). The straight line representing this relationship passes through the coordinate origin. This shows that, under certain conditions *, the formation of sulfur bonds in the spatial vulcanization network occurs only in the regions of the chains with 4-1 structure. Since the formation of chemical cross links is the main factor in the vulcanization process, this conclusion is of considerable technical significance.

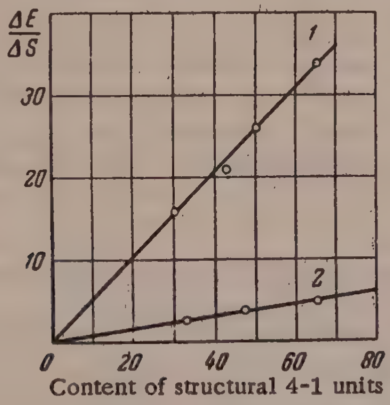

Fig. 14. Effect of rubber structure on degree of cross linking: 1) Mixture with thiuram; 2) mixture with mercaptobenzothiazole and sulfur.

SUMMARY

1. Differences between the chemical reactivities of 4-1 and 2-1 structures of butadiene are found in the reactions with perbenzoic acid, iodine chloride, and sulfur.

---

* These conditions are determined by an average molecular weight of the rubber at which E reaches its final value during the first instants of vulcanization.

2. The interaction of perbenzoic acid with solutions of butadiene polymers is represented by kinetic curves with an initial region of a high rate, mainly corresponding to the reaction of the double bonds of 4-1 structure, and a final linear region of a low rate, characterizing the reaction of the double bonds in the vinyl side chains of 2-1 structure. By extrapolation of the linear region to the ordinate axis it is possible to determine the relative contents of the 4-1 (and hence of the 2-1) structure in the polymer.

3. The kinetic curves for the interaction of the polymer solutions with iodine chloride are of analogous form. The initial region of the kinetic curve represents addition at the double bonds, while the linear region corresponds to the substitution reaction. By extrapolation of the linear region to the ordinate axis it is possible to determine the actual double bond content of the polymer.

4. The kinetic curves for iodine liberation are also of similar form; here the linear region corresponds to the substitution reaction, and the initial region corresponds to the cyclization reaction [6]. The amount of iodine liberated in this reaction is a linear function of the content of the 2-1 structure in the polymer.

5. Mainly the double bonds of the 4-1 structure react when sulfur interacts with the polymer solutions. The total rate of sulfur addition is a linear function of the content of the 4-1 structure.

6. The activation energy for sulfur addition increases with increasing relative content of the 2-1 structure in the polymer.

7. Formation of sulfur cross links in vulcanizates occurs mainly as the result of reactions in the 4-1 polymer structure. In consequence, the degree of cross linking $\Delta E/\Delta S$ is a linear function of the relative content of 4-1 structure in the polymer.

Characteristics of Butadiene polymer double bonds

Type of rubber	Total unsaturation in %, by the ClI reaction	% content of structures			Sum of double bond contents of 4-1 and 2-1 structure by oxidation with perbenzoic acid and ozonation
		4–1	2–1		
		by oxidation with perbenzoic acid	by ozonation	by difference between total unsaturation and contents of 4-1 structure	
SR - 1	87	30	57	57	87
SR - 2	92	49	40	43	89
SR - 3	94	65	31	29	96
SR - 4	94	30	—	64	—
SR - 7	96	43	—	53	—
SR - 5	95	50	—	45	—
SR - 6	96	65	—	31	—

The Moscow Institute of Fine Chemical Technology

Received November 28, 1956

LITERATURE CITED

[1] A. I. Yakubchik, A. A. Vasilyeva, V. M. Zhabina, J. Appl. Chem., 17,107 (1944).

[2] N. Prilezhaev, J. Russ. Phys. Chem. Soc., 42,1387 (1910); 43,609 (1911); 44,613 (1912).

[3] E.R. Weindlein, J. Chem. Eng. News 24, 771, (1946).

[4] B. A. Dogadkin and A. V. Dobromyslova, Trans. Moscow Inst. Fine Chem. Technol., No. 6 (1946).

[5] A. Salfer, B. Johnson, Ind. Eng. Chem. 40, 3, 538, (1948).

[6] T. S. Lee, I. M. Kolthoff, Mary Anne Mairs, J. Polym. Sci. 3, 66 (1948).

[7] A. S. Kuzminsky and N. N. Lezhnev, Proc. Acad. Sci. USSR, 70, 6,1021 (1950).

[8] N. Sheppard, C. B. Sutterland, Rub. Chem. Techn. 21, 799, (1948).

[9] B. A. Dogadkin et al., Colloid J., 17,215 (1955).

THE USE OF HIGH-FREQUENCY ANALYSIS IN COLLOIDOCHEMICAL INVESTIGATIONS

V. I. Ermakov, V. N. Maslov, and O. G. Stolyarov

The high frequency (H. F.) analysis method is already used fairly extensively in chemical research for H. F. titrations, determination of unknown concentrations, and measurements of electric constants of solutions [1-4]. The instruments used for these purposes: F-meters, Z-meters, and Q-meters, are usually fairly complicated.

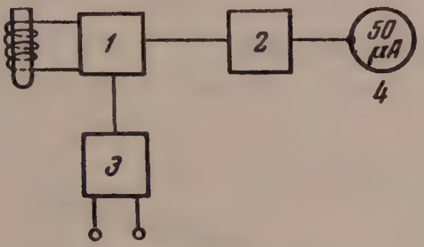

Fig. 1. Block diagram of the installation: 1) measuring generator and alternating current tube voltmeter; 2) universal shunt; 3) stabilized rectifier; 4) microammeter.

We have tested a simple measurement circuit which gives results of good reproducibility. A block diagram of the installation is shown in Fig. 1, and the circuit of the measuring generator and alternating current tube voltmeter in Fig. 2. The measuring generator (tube T_1) is of the three-point circuit type with autotransformer coupling and a high frequency grounded anode. The oscillator circuit formed by the measurement cell L and the capacity C_M is directly connected to the left half of the tube T_2, the grid circuit of which contains a grid leak Cg_2 and Rg_2 so that it acts as a grid detector. If the solution under investigation is placed in the measuring cell L, as the result of absorption of the energy of the magnetic field of the coil L by the solution the amplitude of the generator oscillations will decrease. This will be recorded by the microammeter connected in the diagonal of the measuring bridge: R_4, R_5, and R_i (the internal resistances of the right and left halves of the tube T_2). Changes in the oscillation amplitude of the circuit LC_M displace the position of the working point on the anode grid characteristic of the left half of T_2, which in turn affects its internal resistance R_i , causing unbalance of the bridge . It is important to note that for maximum sensitivity the position of the middle point a on the coil should be determined experimentally.

Eristavi and Barnashvili [5], who studied the action of ultra high frequency fields on hydrophobic sols of heavy metal ferrocyanides, advanced the view that the structure of the diffuse layer of the micelles is changed by the action of a high frequency electromagnetic field. On the other hand, changes of the electric double layer in colloidochemical processes must inevitably lead to changes in the nature of the dispersion of conductivity. This, in its turn, will change the performance of the measuring generator circuit and the oscillation amplitude, and therefore also the readings of the tube voltmeter. Satisfactory confirmation of these views is provided by studies of the coagulation of ferric hydroxide sols by the action of electrolytes.

The colloidal ferric hydroxide sol was prepared by the usual hydrolytic method. Coagulation was effected by gradual addition of electrolyte solutions. At relatively high ferric hydroxide concentrations the maximum deflection of the microammeter needle exactly corresponds to the first appearance of turbidity in the solution, while at high dilutions there is a certain lag before the turbidity is detected. This is easily explained if it is remembered that the latent coagulation period increases with dilution. Figure 3 shows variations of the $(NH_4)_2SO_4$, concentration corresponding to maximum deflection of the instrument needle, with the concentration of a ferric hydroxide sol made in redistilled water and not dialyzed. The reproducibility of the curve proved quite adequate for quantitative determination of ferric hydroxide from the concentration of the electrolyte required for coagulation. Special experiments showed that presence of variable amounts of hydrochloric acid does not appreciably influence the results. The same applies to additions of unhydrolyzed $FeCl_3$.

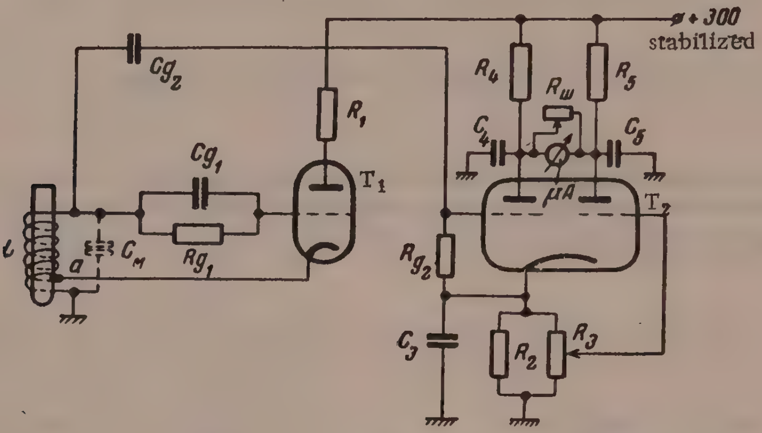

Fig. 2. Circuit diagram of the measuring generator and alternating current tube voltmeter.

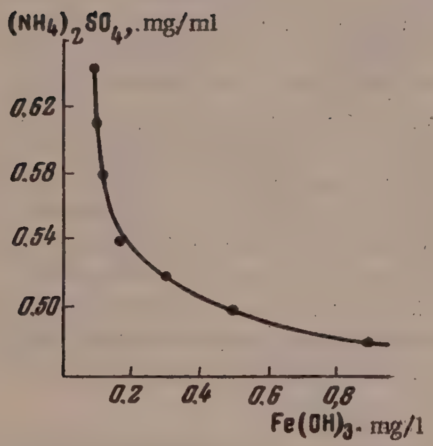

Fig. 3. Effect of dilution of ferric hydroxide sol on its coagulation by the action of ammonium sulfate.

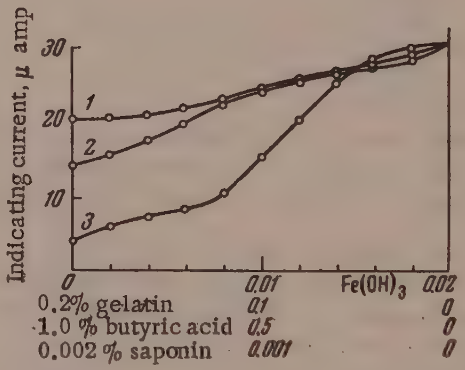

Fig. 4. Diagram of composition vs. indicating current for the following systems: 1) ferric hydroxide-gelatin; 2) ferric hydroxide-butyric acid; 3) ferric hydroxide-gladiolus saponin.

The H. F. analysis method was also used to study adsorptive interaction between colloidal particles of ferric hydroxide and gelatin molecules. Formation of adsorption complexes by the mechanism described by Ermolenko and Plenina [6]

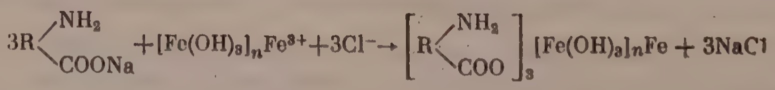

$$3R\left\langle\begin{matrix}NH_2\\COONa\end{matrix}\right. + [Fe(OH)_3]_nFe^{3+} + 3Cl^- \rightarrow \left[R\left\langle\begin{matrix}NH_2\\COO\end{matrix}\right.\right]_3[Fe(OH)_3]_nFe + 3NaCl$$

implies deep changes in the electric double layer of the particles, which should be reflected in the nature of dispersion of the conductivity . However, the composition – current diagram shown in Fig. 4, where the deflection of the instrument needle is plotted against the composition, shows almost complete additivity of the properties of the solutions studied. However, curves for the systems ferric hydroxide sol – gladiolus saponin and ferric hydroxide sol – butyric acid showed much greater deviations from additivity, which casts doubt on the mechanism, mentioned above, of the interaction of gelatin with colloidal ferric hydroxide.

SUMMARY

1) An instrument was designed for high frequency analysis in which the oscillating circuit of the generator served directly as the measuring cell.

2) With a number of coagulation and adsorption processes as example, it has been shown that high frequency analysis may be used for studying colloid-chemical phenomena associated with changes in the electrical double layer.

The D. I. Mendeleev Institute of Chemical Technology
Moscow

Received May 21, 1956

LITERATURE CITED

[1] O. L. Kaptzan and V. A. Teplyakov, J. Anal. Chem., 8, No. 3,131 (1953).

[2] V. A. Zarinsky and D. I. Koshkin, J. Anal. Chem., 10, No. 2,111 (1955).

[3] G. G. Blake, Analyst 79, No. 935, 108 (1954).

[4] J. Hall, J. Gibson, Anal. Chem. 26, 1539, (1954).

[5] D. M. Eristavi and D. Barnashvili, Proc. Acad. Sci. USSR 25, No. 7,606 (1939).

[6] N. E. Ermolenko and G. N. Plenina, Colloid J., 5, No. 3, 194 (1939).

THE STRUCTURE OF GELS

9. EFFECT OF THE NATURE OF THE PLASTICIZER ON THE PHYSICOMECHANICAL PROPERTIES OF DIVINYL–STYRENE RUBBER

M. P. Zverev and P. I. Zubov

It was shown in the previous communication [1] that plasticization of high polymers, like the swelling process, involves not only weakening of the forces between the macromolecules, but also changes in their form. The greatest plasticization effect in divinyl–styrene rubber was produced by nonpolar plasticizers. The present paper contains experimental data on the influence of the plasticizer structure (polarity) on the physicomechanical properties of SKS-30 A divinyl–styrene rubber and its vulcanizate. The composition of the mix, vulcanization conditions, and plasticizers were the same as before [1]. The effect of the nature of the plasticizer on the temperatures of transition of the polymer from one physical state into another was studied with the aid of Kargin's dynamometric balance [2]. The mechanical strength of unfilled vulcanizates, calculated on the initial cross section, was determined by means of a dynamometer of the Polanyi type. The maximum error was ±5%. The vulcanization optimum was established from the equilibrium modulus [3].

Kargin and Malinsky [4] showed that the magnitude of the plasticizing effect for nonpolar polymers is a linear function of the volume fraction of the plasticizer in the polymer. It was of interest to determine to what extent the volume fraction rule applies to divinyl–styrene rubber.

Table 1 shows the variations of the glass transition temperature of rubber with the volume fraction of the plasticizer.

TABLE 1

Variations of the Glass and Flow Temperatures of Rubber with the Volume Fraction of the Plasticizer

Plasticizer	Amount of plasticizer in volume %							
	5	10	20	30	50	5	10	20
	Glass transition temperature of rubber in °C					Flow temperature of rubber in °C		
Tetralin	—53	—56	—63	—70	—77	146	127	99
Green oil	—53	—57	—65	—72	—78	140	122	92
Ditolylmethane	—55	—58	—66	—76	—85	135	117	84
Dicumylmethane	—54	—58	—68	—77	—85	137	118	85
Dibutyl sebacate	—58	—63	—70	—81	—89	133	110	80
Dibutyl phthalate	—55	—60	—69	—82	—90	134	108	78
Diethyl phthalate*	—55	—60	—68	—	—	130	108	80
	—55	—58	—70	—	—	130	108	78

---

* Only up to 20% of diethyl phthalate and tricresyl phthalate was added to the rubber, as larger amounts of these plasticizers were not compatible with the polymer.

Table 1 shows that at low plasticizer concentrations in the rubber the volume fraction rule is obeyed fairly satisfactorily; the decrease of the glass transition temperature does not depend on the nature of the plasticizer. Deviations from this rule are found at higher concentrations. In such conditions the glass transition temperature is lower in presence of nonpolar than of polar plasticizers.

Table 1 also gives data on the influence of the nature of the plasticizer on the temperature of transition of divinyl – styrene rubber into the viscofluid state; these results show that considerable increases of the flow temperature of rubber are also produced by nonpolar plasticizers. We also investigated the effects of plasticizer structure on the mechanical strength and relative extension of the unfilled vulcanizate. The results are given in Table 2.

TABLE 2

Effect of Plasticizer Structure on the Tensile Strength and Relative Extension of Unfilled Vulcanizate

Plasticizer	Amount of plasticizer in volume %				
	5	10	20	30	50
	Tensile strength in kg/cm²				
Tetralin	16.1	14.3	12.0	9.8	7.8
Green oil	15.8	14.6	11.6	9.2	7.3
Ditolylmethane	15.7	13.9	10.7	8.8	6.5
Dicumylmethane	16.0	14.3	11.4	9.0	6.4
Dibutyl sebacate	15.7	13.6	10.6	8.6	5.8
Dibutyl phthalate	15.6	13.8	10.9	8.4	5.8
Diethyl phthalate	16.1	14.0	10.6	—	—
Tricresyl phosphate	15.8	14.3	10.5	—	—
	Relative extension in %				
Tetralin	570	580	540	530	490
Green oil	600	570	550	520	480
Ditolylmethane	590	570	540	520	450
Dicumylmethane	570	560	540	510	450
Dibutyl sebacate	570	560	550	500	420
Diethyl phthalate	570	580	540	—	—
Tricresyl phosphate	570	570	540	—	—

Table 2 shows that in presence of small amounts of plasticizer in the vulcanizate the decrease of tensile strength and the change of relative extension are practically independent of the plasticizer structure. The effects of molecular structure of the plasticizer become noticeable above 20%. With 50% plasticizer the mechanical strength and the relative extension of specimens plasticized with tetralin or green oil are approximately 25-30%, and the relative extension is 50-60%, higher than the strength and the relative extension of specimens plasticized with phthalate or sebacate esters.

SUMMARY

1. The glass and flow temperatures and the strength and relative extension of rubber depend not only on the concentration of the plasticizer but also on its molecular structure.

2. Divinyl – styrene rubber plasticized with nonpolar plasticizers has higher glass and flow transition temperatures than rubber plasticized with polar substances. The same relationships are found for the strength and relative extension of vulcanizates of this rubber.

3. Nonpolar plasticizers also weaken intramolecular interaction to a greater extent than polar plasticizers.

The L. Ya. Karpov Physicochemical Institute

Received June 13, 1956

LITERATURE CITED

[1] P. I. Zubov and M. P. Zverev, Colloid J., 18,679 (1956).

[2] V. A. Kargin and T. I. Sogolova, J. Phys. Chem., 23,530 (1949).

[3] G. M. Bartenev, Investigations of High Molecular Compounds (Acad. Sci. USSR Press, Moscow-Leningrad, 1943) 306.

[4] V. A. Kargin and Yu. M. Malinsky, Chemistry and Physical Chemistry of High Polymers (Acad. Sci. USSR Press, Moscow-Leningrad, 1952) 255.

THE HARDENING MECHANISM OF THERMOSETTING PLASTICS (MOLDING POWDERS)

I. F. Kanavets, L. G. Batalova, and A. G. Romashova

The first place among plastics, in volume of production and diversity of applications, is occupied by thermosetting plastics, and among these, by plastics based on phenol – formaldehyde resins. The conversion of thermosetting resins into the infusible and insoluble state, in the course of which thermosetting plastics acquire all the physicochemical properties necessary for processing into articles and for stability of the products in use, has so far not been sufficiently well investigated.

Thermosetting molding powders, used for the production of plastic articles, are complex compositions consisting of resins, fillers, and other components which influence their technological properties and the mechanical properties of the material in the finished articles. A clear understanding of the nature of this influence is necessary for production of molding powders with the required technological properties.

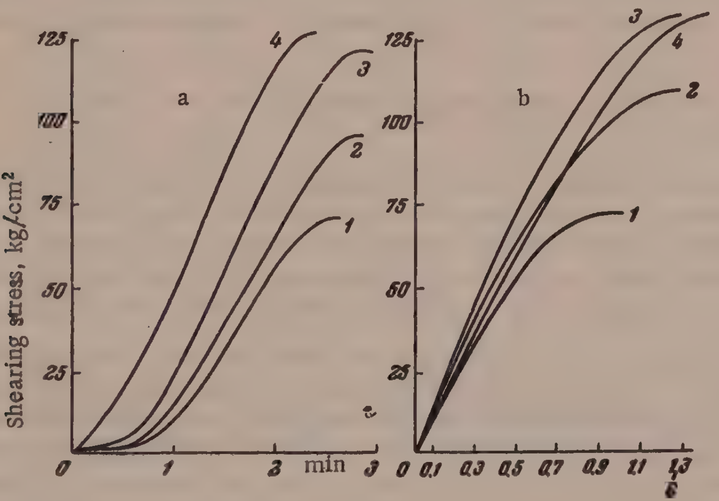

Fig. 1. Kinetics of the hardening at 170° of a molding composition of the Novolak type grade K-18-2 with different rolling times (a), and the mechanical properties for the hardening time corresponding to a stress of 25 kg/cm^2 (b): 1) rolling for 30 seconds, 2) 2 minutes, 3) 3.5 minutes, 4) 3 minutes 50 seconds.

The study of chemical reactions occurring in resins, and especially in molding powders, is a very difficult problem. A plastometer designed by one of the authors has proved very convenient for this purpose [3, 4]. Determinations of the kinetics of the hardening process by means of this plastometer are based on variations of the shearing stress with time at constant temperature, pressure, and rate of shear. The results are automatically recorded by the instrument in stress – time coordinates (in determinations of the hardening rate), and in stress – relative deformation coordinates for determination of the mechanical properties. The hardening rate is found from the time required to reach a viscosity of $2 \cdot 10^9$ poises or a shearing stress of 25 kg/cm^2. The duration of the viscofluid state is read off along the time axis up to the steep ascent of the curve (Fig. 1, a), and the mechanical properties of the molded material at the given hardening stage are read off the maximum shearing stress and relative deformation at the point at which the curve takes a horizontal course (Fig. 1, b). These are the most characteristic values for evaluation of the quality of thermosetting molding powders, as they are closely associated with the structure of the resins and of the material in the molded article.

The study was carried out with molding powders of the Novolak and resole types, made by the dry rolling method in laboratory and factory conditions from resins differing in chemical nature and degree of condensation. Molding powders made by the dry rolling method were rolled for different periods or treated in a mixer, with samples taken during the rolling, while resole powders made by the emulsion process were heated for different times during drying, also with periodic sampling. In addition, molding powders containing various amounts of additives, both reacting and not reacting with the resins, etc., were studied.

Physicochemical processes occurring during the production of molding powders.

The effects of the degree of condensation of the resins (resins of different viscosities in solution) on the technological properties of the molding powders and the mechanical properties of the molded articles were studied for molding powders based on phenol–, cresol–, and xylenol–formaldehyde resins. These resins varied in viscosity coefficients in the range of 50 to 155 centipoises for Novolaks and from 345 to 776 centipoises for resoles. The investigations showed that increase of the degree of condensation of the resins shortens the time of existence of the viscofluid state, and increases the rate of hardening, the maximum shearing stress, and the relative deformation of the material in the finished articles. This is confirmed by the test results for a large number of production batches, the average values for which are given in Table 1. More than 50 of the batches were classified into three groups by resin viscosity. The first group contains resins with viscosity coefficients from 60 to 90 centipoises (for K-18-2 resin, from 90 to 99 centipoises), the second, from 91 to 120, and the third from 121 to 160 centipoises. The results of laboratory experiments are given in Table 2.

Exceptions to the above rule are found only for molding powders K-17-2 and K-20-2, made from xylenol and cresol resins (see Table 1).

The general law that the hardening rate of molding powders increases with increasing resin viscosity may be disturbed to some extent on account of variations in the percentage compositions of isomeric phenols in the raw materials from which the resins are made. The different reaction rates of the isomeric phenols lead to different contents of the low-molecular products in the resins, to a loose resin structure, and to steric hindrances, and in consequence the hardening rate of molding powders based on these resins decreases.

The effect of rolling time was studied on samples of molding powders taken from the rolls at intervals during rolling (Fig. 1), and the effect of drying time, on samples taken after various times of drying (Fig. 2). Tests of these samples showed that, with increasing rolling or heating time (during drying), polymer chain growth and structurization of the resin take place, the duration of the viscofluid state of the molding powders decreases, the hardening time decreases (or the hardening rate increases), and the maximum shearing stress and relative deformation of the hardened material in the articles increase. Data for molding powders made from resins differing in viscosity and taken at various stages of rolling are given in Table 2.

The mixer method. The following experiment was performed to compare the properties of molding powders made by the rolling and the more up-to-date internal mixer methods: molding powder compositions of grade K-17-2, made from three resin batches ranging in viscosity from 80 to 129 centipoises, were each divided into two portions for processing on rolls and in mixers. The rolling was performed by the factory procedure established for this grade of powder, and the mixing by the factory procedure (I), and by a procedure in which the feed rate into the mixer was halved (II). The results of these trials, including one with the composition without rolling, are given in Fig. 3. Fig. 3, a shows that the technological characteristics of a molding powder rolled for one minute are similar to those of a powder made by the mixer method. As regards the mechanical properties of the mixer material, the maximum shearing stress and relative deformation are lower than in material rolled for one minute. The nonrolled molding composition (Fig. 3,c) has quite low values for maximum shearing stress and relative deformation. Nonrolled molding powders made by the solvent method (solutions of resin and urotropine in alcohol) have the same high values as the rolled. Production batches of molding powders made by the roll and mixer methods are similar in duration of the viscofluid state and hardening rate. The average results are given in Table 3 .

TABLE 1

Technological Properties of Molding Powders Made from Resins of Different Viscosities

Molding power grade	Viscosity coefficient in centipoises	Plastometer data at 170°		Shearing stress at the final hardening stage in kg/cm²	Mechanical properties	
		duration of viscofluid state in sec.	hardening time in sec.		relative deformation ϵ	Shearing stress in kg/cm²
K-18-2	96	35	89	61.2	0.95	65.5
	108	34	90	72.2	1.0	77.7
	127	32	80	82.5	1.1	90.0
K-17-2	86	39	100	78	1.4	78.5
	105	42	107	70	1.2	76.0
	128	58	131	66.5	1.1	75.7
K-15-2	84	39	101	73.5	1.1	73.0
	105	39	97	60.4	1.0	66.2
K-20-2	86	39	106	63.5	1.2	68.0
	108	40	103	65.8	1.1	67.5
	123	44	111	66.8	1.1	71.0
K-21-22	345	48	238	73.1	1.3	56.5
	535	30	188	82.0	1.7	72.4
	776	26	178	85.2	2.0	73.6
"Voloknit"	699	28	62	115.3	0.9	121.5
	900	26	58	113.9	1.05	116.6
	1059	24	54	126.8	0.8	135.5
	1457	28	66	119.2	0.86	129.5

The maximum shearing stress and relative deformation are a little higher for molding powders made by rolling than for molding powders made in mixers . The mechanical properties determined according to the technical specifications for molding powder are the same for both types.

Changes in the properties of Novolak resins on rolling with hexamethylenetetramine. Novolak resins were rolled with additions of 15% hexamethylenetetramine at the same temperature as the molding powders, to convert them into hardening resins. It was found (see Fig. 4) that such resins have considerably lower hardening rates than molding powders made from the same batches: they reach the same value of maximum shearing stress as is found for molding powders after 2 minutes rolling, only after 10-15 minutes. At the initial hardening stage, Novolak resins rolled with hexamethylenetetramine, as a result of greater cross linking than is found in resins rolled with fillers, give hardening curves of the same form as are given by molding powders of the resole type. The well defined horizontal region, characterizing softening of the resin, is lacking in these curves also. The viscosity of resins rolled with urotropine is two to three times as high as the viscosity of the molding powders, as the result of greater structurization during rolling. The same applied to other grades of resin rolled with hexamethylenetetramine .

TABLE 2

Technological Properties of Thermosetting Molding Powders Made with Different Rolling Times

Molding powder grade	Viscosity coefficient in centipoises	Drop temperature, °C	Rolling time, min	Plastometer data at 170°					
				Duration of viscofluid state in sec.	hardening time in sec.	complete hardening time in sec.	shearing stress at final hardening state, kg/cm²	mechanical properties	
								shearing stress, kg/cm²	relative deformation e
К-17-2	76	96	1.0	40	122	272	55.5	—	—
	76	96	1.5	36	112	270	62	50	0.9
	76	96	2.0	36	110	260	56.5	—	—
К-17-2	155	103	1.0	28	84	210	117.5	117.5	1.25
К-20-2	87	95	1.0	54	122	242	58.5	25.4	1.1
	87	95	1.5	50	122	254	71	63.5	1.1
	87	95	2.0	50	112	260	66.5	60.5	1.0
К-20-2	104	99	1.0	46	98	280	86	68.5	1.15
	104	99	1.5	42	92	272	95	68.5	1.05
	104	99	2.0	42	94	254	92.5	81.5	1.20
К-20-2	131	102	1.0	50	108	226	78	82.5	1.2
	131	102	1.5	42	100	210	79	86	1.2
	131	102	2.0	40	100	200	78	93	1.3

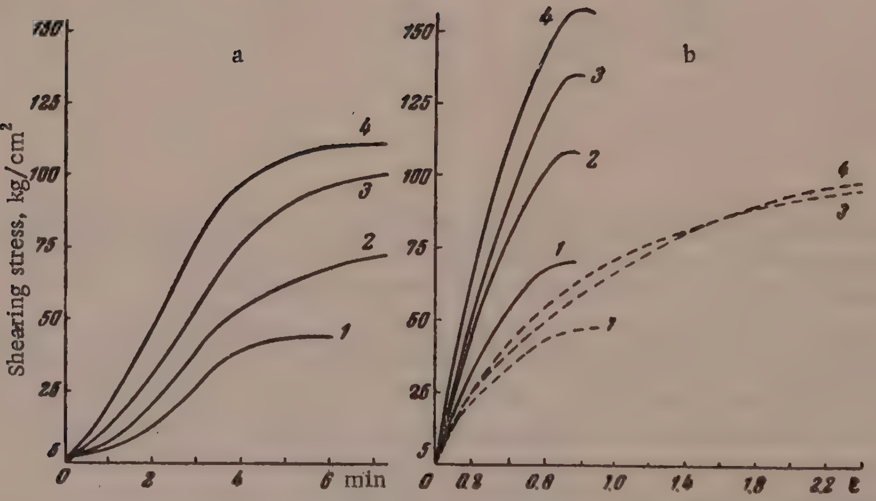

Fig. 2. Kinetics of the hardening at 170° of a molding composition of the resole type grade K-21-22 with different drying times (a), and the mechanical properties for the hardening time corresponding to a stress of 25 kg/cm² (b) (broken lines) and at the final hardening stage (continuous lines); 1) drying for 30 seconds, 2) 1.5 hours, 3) 2 hours, 4) 2.5 hours.

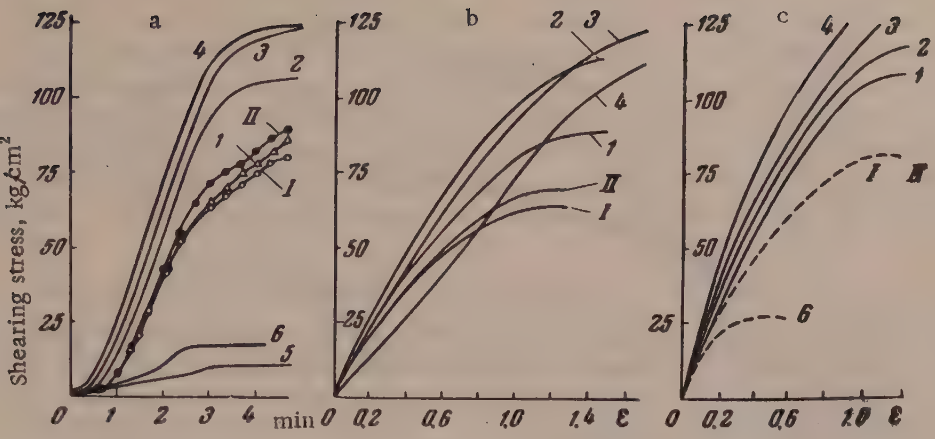

Fig. 3. Kinetics of the hardening at 170° of a molding composition of the Novolak type grade K-17-2 with different rolling times (a), the mechanical properties for the hardening time corresponding to a stress of 25 kg/cm^2 (b), and the mechanical properties at the final hardening stage (c): 1) rolling for 1 minute; 2) 2 minutes; 3) 3 minutes; 4) 4 minutes; 5) not rolled; 6) ditto, heated at 150° for 20 minutes; and I and II) from internal mixer .

TABLE 3

Average Data for Factory Grades of Molding Powders Made by the Roll (r) and Mixer (m) Methods .

Grade	Viscosity in centipoises	Technological properties		Mechanical properties	
		duration of viscofluid state in sec.	hardening time in sec.	shearing stress in kg/cm²	relative deformation, ε
K-18-2 (r)	119	33±8	83±14	86.2±16	1.0 ±0.1
K-18-2 (m)	99	29±3	87±4	61.0±4.5	0.85±0.05
K-15-2 (r)	95	40±5	96±9	68.7±10	1.1 ±0.15
K-15-2 (m)	97	39±6	99±5	67±10,7	0.99±0.1
K-20-2 (r)	97	41±9	106±13	67.7±10	1.1 ±0.15
K-20-2 (m)	101	44±12	109±14	64.5±6.7	1.0 ±0.04
K-17-2 (r)	100	13±10	106±17	74±12.7	1.2 ±0.2
K-17-2 (m)	100	55±14	128±21	67.3±9.7	0.95±0.1
K-17-23	—	71±14	153±14	21.2±3.7	0.65±0.04
K-21-22	552	38±21	189±27	72.2±12.5	1.8 ±0.7
K-211-2	—	92±13	566±81	29.5±5.0	1.0 ±0.07
K-220-23	—	83±6	300±36	29.7±3.2	1.2 ±0.22
K-214-2	—	91±14	208±35	78±12.5	1.6 ±0.4
"Voloknit"	—	28±5	60±6	121.2±11.7	0.86±0.13
K-103-2	—	42±11	117±19	—	—
K-111-2	—	50±9	145±32	—	—
K-15-2	—	67±3	113±6	56.2±8.5	0.95±0.1
K-17-2	—	85±5	140±7	51.2±3.5	0.93±0.02
Aminoplastic	—	60±8	102±8	84.5±16	1.3 ±0.2
K-F-3	—	56±9	79±9	87.0±16,5	0.89±0.17
"Monolit" No. 1	—	40±3	89±4	64.2±6.2	1.05±3.0
"Monolit" No. 7	—	54—60	120—128	45—65	1.0 —1.1
K-77-51	—	180±60	240±20	50±5	0.9 ±0.1

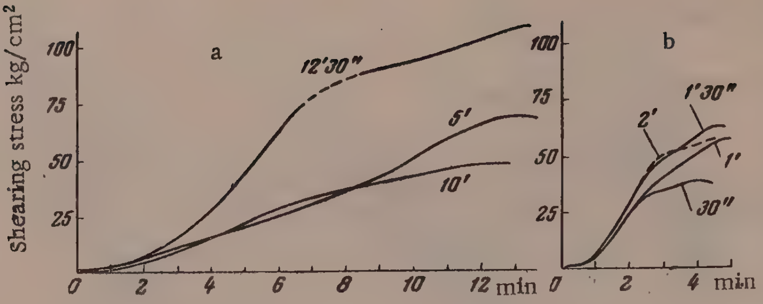

Fig. 4. Kinetics of the hardening at 170° of a Novolak resin grade 17 (a) without filler, rolled with 15% of hexamethylenetetramine, and molding powder K-17-2 (b) made from the same batch of resin. The numbers on the curves are the rolling times.

Variation of the contents of substances extracted by alcohol-benzene mixture in molding powders at different stages of rolling and drying. Thermosetting molding powders undergo changes with increasing rolling and drying times, resulting in a decrease of the duration of the viscofluid state, and a decrease of the content of substances extracted by alcohol-benzene mixture from 58 to 34%. Experimental data show that molding powders after 1 minute of rolling have an extractable content of about 50-58%, and at the last stage of rolling and drying this falls to 34-40%. It should be noted that at the last stage of rolling and drying the molding powders give hardening curves (Fig. 1) which ascend sharply without an appreciable horizontal region corresponding to the viscofluid state, although such powders contain 34-40% extractable matter. It follows from these experiments that a decrease of the amounts of extractable reactive resins in molding powders decreases the duration of the viscofluid state, and conversely.

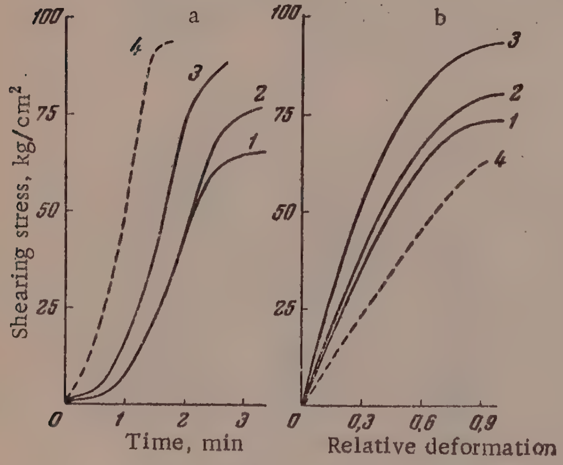

Fig. 5. Variation of the properties of a Novolak molding composition on heating: 1) without heating; 2) heating in oven at 80° for about one hour with decrease of volatiles from 3.5 to 2.5%; 3) high frequency or oven heating; 4) resin converted from resole into resite.

Influence of other components present in molding powders on their quality. Various substances of low molecular weight, such as hexamethylenetetramine, magnesium oxide, lime, organic fatty acids, etc., are added to molding powder compositions; in addition, moisture, free phenol, and resin fractions in the initial stages of polycondensation are introduced into the molding powders with the resins, while moisture and mineral impurities enter the composition with the fillers. To obtain a molding powder with predetermined properties it is necessary to know what effects the various substances present influence its technological properties and the properties of the material in the finished article.

The effects of moisture and volatile matter were studied on Novolak and resole molding powders. The experiments show that variation of the moisture content in the molding powder (from 1 to 12%) has no practical effect on the hardening rate, but the viscosity coefficient at the final hardening stage is approximately halved when the moisture content is increased to 12%. The same is found on variation of the volatile content. Fig. 5 gives data found for molding powders containing 3-3.5% volatiles, and for the same powders after drying for one hour at 70-80° . In the latter case the volatile content of the molding powder decreased by about one per cent. The curves in Fig. 5, representing the hardening of Novolak molding powders before drying (1) and after drying (2), coincide, but the shearing stress at the final hardening stage is less for the undried powders. Stronger heating by high frequency current or in an oven at a higher temperature changes the properties of the resin owing to conversion of the fractions of low molecular weight into higher stages of polycondensation [3], and conversion of the resin from stage A into stage B [4] . The mechanical and other properties deteriorate in the process; consequently, the duration of the viscofluid state and hardening rates of molding powders are practically unchanged by variations of their contents of moisture and volatile matter which do not react chemically with the resins.

Furfural, which reacts chemically with phenol-formaldehyde resins, is a characteristic plasticizer for thermosetting molding powders. Furfural was added to molding powders of the Novolak type in 5, 10, and 15% amounts. In contrast to the results of the preceding experiments, it was found that addition of furfural to Novolak molding powders results not only in plasticization of the material, i. e., a decrease of the shearing stress at the final hardening stage, but also increases the duration of the viscofluid state and retards the hardening rate (see Fig. 6). For example, molding powder K-18-2, after additions of 5, 10, and 15% furfural, has (instead of 50 seconds without additions) durations of the viscofluid state of 55,60 and 70 seconds respectively, while the time of hardening increases from 90 seconds to 100, 112, and 123 seconds respectively . Thus, furfural and extractable resins, which react chemically with the resin, have a different effect from moisture and other plasticizing additions on the technological properties of molding powders.

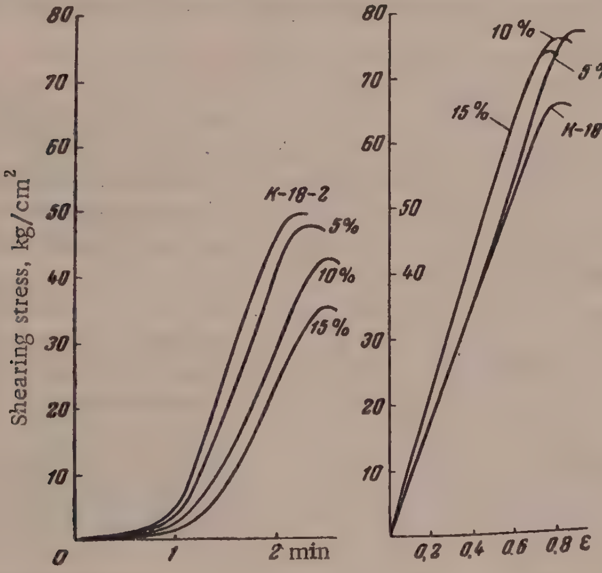

Fig. 6. Effect of addition of furfural (in %) during compounding on the technological properties of molding powder K-18-2.

The effects of hexamethylenetetramine, magnesium oxide, and lime on the technological properties of molding powders based on resins of the resole type are illustrated by the experimental results given in Fig. 7 . The molding powder represented by Curve 1 gives Curve 2 on addition of hexamethylenetetramine; this shows an increase of the duration of the viscofluid state and a lower viscosity in the initial hardening stage. Addition of magnesium oxide or lime (Curve 3) increases the viscosity and shortens the duration of the viscofluid state of the molding powder. Molding powders with added magnesium oxide, lime, and hexamethylenetetramine have higher viscosities or greater maximum shearing stresses than molding powders containing smaller amounts of these substances.

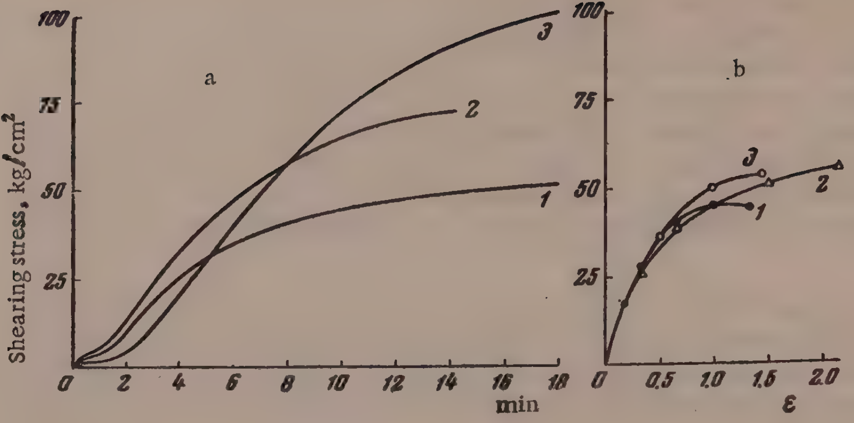

Fig. 7. Variation of technological and mechanical properties during an interval corresponding to a stress of 25 kg/cm² at 170°: 1) resole molding composition K-21-22 without additions; 2) with added hexamethylenetetramine; 3) with hardeners of the magnesium oxide or lime type.

Similar changes in the technological properties of molding powders are found with FFG phenol-furfural resin and the same resin with addition of hexamethylenetetramine. Experiments show that resin FFT, based on peat furfural, has a lower hardening rate than FFG resin based on hydrolytic furfural; probably owing to the presence of ~ 20-25 % of methyl-and oxymethylfurfural in peat furfural. Addition of hexamethylenetetramine to the Novolak molding powders shortens the duration of the viscofluid state and increases the hardening rate and shearing stress.

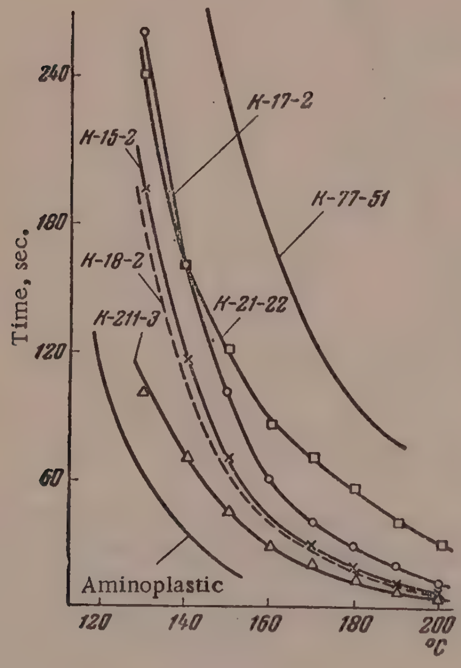

Fig. 8. Effect of temperature on the duration of the viscofluid state.

Effect of temperature on the duration of the viscofluid state and on the hardening rate. The data in Fig. 8 show that the effect of temperature on the duration of the viscofluid state of molding powders conforms to the law

$$\theta = Ae^{-u/kT}, \qquad (1)$$

where θ is the duration of the viscofluid state in seconds; u is the free energy of activation for the polycondensation reaction, in kcal./mole; T is the absolute temperature; k is the Boltzmann constant; A is a factor which depends on the amount of reactive substances in the molding powder.

The course of the hardening reaction with time is represented by the equation

$$\Delta\sigma_t = \frac{\Delta\sigma f}{1 + e^{-\lambda\theta}}, \qquad (2)$$

where σ_t — is the shearing stress at time t, in kg/cm²; σ_f is the shearing stress at the final hardening stage in kg/cm², and σ_0, at the initial instant, in kg/cm²;

$\Delta\sigma_t = \sigma_t - \sigma_0$; $\Delta\sigma_k = \sigma_f - \sigma_0$; $\theta = t - t_m$,

t_m is the time from the start of the experiment to the moment when the maximum hardening rate is reached.

The hardening rate K varies with temperature and time according to the equation

$$K = \frac{A_0 e^{-\lambda\theta}}{(1 + e^{-\lambda\theta})^2} \cdot e^{-u/kT}, \qquad (3)$$

where A_0 is a constant, λ is a factor which depends on the resin properties and the temperature, and the remaining symbols are as in Equation (1). Data on the hardening rates and other characteristics of the main grades of molding powders are given in Table 3.

DISCUSSION OF RESULTS

According to the modern theories, hardening of thermosetting resins occurs as the result of chemical reactions between the functional groups in the macromolecular chains. The physicochemical properties of the resultant plastics depend not only on the chemical structure of the reacting molecules but also on the shape and dimensions of the macromolecules formed in the reactions. Good quality thermosetting molding powders should soften but not melt on heating, and should remain for some time in the softened or viscofluid state. This time is used for molding the articles. The softening power is determined by the state of the resin in the molding powder; this should be intermediate between stages A and B *. The duration of the viscofluid state is determined not by the physical properties of the resins, as has been believed hitherto, but by the rate of chemical conversion of low-molecular fractions and reactive substances into products of higher molecular weight. This is shown by the decrease in the content of extractable resins in molding powders with decreased duration of the viscofluid state, and its increase on addition of furfural. If the resin in the molding powder is at stage A, the molding powder is not suitable for conversion into articles owing to extrusion of resin from the filler and faulty external appearance of the articles. If the resin has reached stage B, the molding powder is not suitable because the articles are gray and incompletely molded.

The hardening rate of thermosetting molding powders depends not only on the degree of condensation but on the resin structure; it increase regularly with increasing degree of condensation from 60 to 150 centipoises (measured by the coefficient of viscosity in solution) if the resin, near to linear in structure, has been made from crystalline phenol (see Table 1, K-18-2). Molding powders made from cresol, xylenol, aniline-formaldehyde, and other resins with a complex branched structure may have a lower hardening rate despite a higher average viscosity coefficient for the resins in solution. Resins based on raw materials containing different amounts of isomeric phenols of different reactivity have a complex branched structure and contain large amounts of low-molecular fractions and products at the initial condensation stage. Such resins have high average viscosity coefficients in solution, and molding powders made from them have increased duration of the viscofluid state and a lower hardening rate(seeTable1moldingpowdersK-17-2,K-20-2, and Table 3). Therefore the viscosity coefficient of resins in solution (determined by the technical specification methods for molding powders) does not provide a characteristic evaluation of resin quality.

A more correct evaluation of resins is by viscosity in melts and by molecular weight distribution. The melt viscosity can be determined by the plastometric method, while instead of molecular weight distribution resins may be evaluated by the duration of the viscofluid state of the molding powders, directly related to the duration of the reaction whereby the low-molecular resins are converted into resins of high molecular weight. Attention must be drawn to the low shearing stress values (down to one tenth) for nonrolled resins with hexamethylenetetramine and for molding powders even after thorough mixing of the ingredients in a ball mill and after rolling on cold rolls. The fact that Novolak resins rolled with 15% of urotropine have a considerably lower hardening rate than molding powders made from the same batches of resins and at the same rolling temperatures confirms that resin quality should be evaluated in molding powder compositions made up by the usual procedure, as the duration of rolling and drying needed to give a molding powder with particular technological characteristics depend on the molecular weight distribution in the resin and the contents of low-molecular fractions. In such experiments carried out by accelerated methods [3, 4] on samples taken during rolling, data are obtained on the resin hardening rate, on the quality of the molding powder, on the rolling conditions, etc., and therefore such evaluation is less laborious and more complete than the procedure adopted at present.

---

* Stage A resins are fusible and soluble, at stage B resins do not melt but soften and swell in solvents, and at stage C they do not melt or dissolve.

The duration of the viscofluid state, the effective viscosity coefficient, and the hardening rate are the most characteristic values for establishing the optimum temperatures and rolling and drying times of molding powders, and also for evaluating the quality of the finished products. An under-rolled molding powder will have a longer, and an over-rolled powder a shorter duration of the viscofluid state (in comparison with the normal). The duration of the viscofluid state gives the most correct evaluation of the state of the resin in the molding composition, ensuring the correct flow properties in the molding powder during processing. This very important characteristic can be determined only by the plastometric method [3, 4]. The exponential decrease of the duration of the viscofluid state with temperature indicates the statistical nature of the law governing the conversion of resin from stage A into stage B in molding powders. The exponential course of the reaction as represented by Equations (1) and (2) is a general law for processes determined by the probability of surmounting potential barriers. We showed earlier [4] that conversion of thermosetting resins from stage B into stage C also obeys a statistical law. It was then pointed out that the kinetics of the hardening of phenol-formaldehyde resins and of molding powders made from them obeys the same law for the conversion from stage B to stage C, and is described by an equation of the form of Equation (2), which applies to degenerate explosion reactions. Therefore molding powders with a low duration of the viscofluid state harden rapidly on contact with the hot mold, which leads to rejects in production owing to grayness.

Because of the polycondensation reaction which takes place at various stages of molding powder production according to a statistical law, the resin gradually becomes less polydisperse or more homogeneous in composition because the lower fractions, being more mobile, react more rapidly than the fractions of higher molecular weight. This accounts for the improved mechanical properties of the material in articles molded from powders taken at later rolling and drying stages. In the experiments described (Figs. 1-3) each successive sample taken during rolling and drying is, in a sense, made from a resin more homogeneous than the preceding one in fractional composition, and of higher molecular weight.

It follows from the theory of reaction rates that the factor which determines the rate of a reaction is not the heat of activation (H) but the free energy of activation (u), which enters Equations (1) and (2).

Taking θ as constant in Equation (3), we find that the rate of the hardening reaction as a function of temperature obeys the Arrhenius law

$$K = Be^{-u/kT}. \tag{4}$$

Korshak [7], on the basis of literature data, gives the activation energy of the chain growth process as 12 kcal./mole for polyesters and 24 kcal./mole for polyamides. For phenol-formaldehyde resins, as determined in molding powders, $\underline{u}$ lies in the range of 7.2-16.6 kcal./mole, H from 18.8 to 23.8 kcal./mole, and the entropy of activation from 17 to 52 cal./mole. degree [1, 3].

In the reactions occurring according to Equations (2 and 4) between complex molecules in resins rolled with urotropine or resins of the resole type in molding powders, considerable redistribution of energy between all the degrees of freedom takes place. This leads to a decrease of the entropy of activation, i. e., a decreased probability of the formation of an activated complex, and hence to retarded hardening. The data in Table 3 show that molding powders of grades K-21-22, K-220-23, and K-211-2, which have more complex structure than Novolak resins, harden more slowly. The complex structure of these resins is confirmed experimentally by the absence of a clearly defined horizontal region on the curve in the initial stage of hardening.

The hardening process may be accelerated in the part of it which depends on the entropy of activation either by the use of resins of less branched structure, or by increase of temperature. In either case the probability of collision between the reacting particles will be increased, favoring acceleration of the hardening reaction.

The influence of steric hindrances, caused by the loose structure of xylenol and aniline-formaldehyde resins, on the hardening rates of molding powders K-112-2 and K-211-2 is confirmed by experiments illustrated by Fig. 9. The hardening rate of these molding powders increases with increase of shearing rate and rise of temperature. We believe that the reason for this is that shearing deformations destroy the loose structure of the resins and so remove the steric hindrances which prevent entry of the unreacted components into the reaction, and not an agitation effect [9, 10, and 11]; if the agitation effect prevailed over destruction, this effect would be greater at lower temperatures and it could be observed by deviations between the curves representing the variation of hardening rate with temperature. The experimental results shown in Fig. 9 indicate that these curves are almost parallel for different temperatures.

The experimental results given above show that, despite the great diversity of the chemical and physical composition of the substances contained in molding powders, they may be divided into two characteristic groups, depending on whether they react chemically with the resins or not. Depending on this, they have different effects on the technological properties of molding powders and the mechanical properties of the materials in the finished articles. The substances which react chemically with the resins influence the duration of the viscofluid state and the hardening rate of molding powders. If they react to form initial or intermediate resin products, the molding powder remains longer in the viscofluid state and has a lower viscosity coefficient, while the hardened material has a higher maximum shearing stress and relative deformation, indicating growth of the polymer chains as the result of the reaction. An example of this effect is provided by hexamethylenetetramine in molding powders of the resole type (Fig. 7), or furfural in Novolak molding powders (Fig. 6). If, however, cross linking of the polymer chains predominates in the reaction, the duration of the viscofluid state decreases, the viscosity coefficient in that state increases, while the maximum shearing stress in the hardened material increases and the relative deformation changes little or diminishes. An example of such cross linking of the polymer chains is provided by the action of magnesium oxide or lime when added to molding powders of the resole type (Curve 2 in Fig. 7 lies above Curve 1 along its entire length). Substances which do not react with the resins only cause an increase in the plasticity of the material at all stages of hardening and have practically no effect on the duration of the viscofluid state or the hardening rate (Fig. 5).

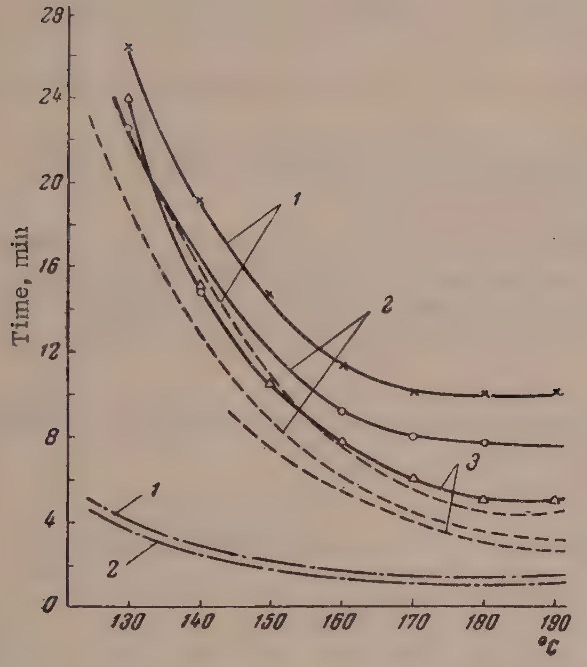

Fig. 9. Effect of shearing rate on the hardening time of molding compositions K-18-2 (dot-dash line), K-112-2 (broken line) and K-211-2 (continuous line): 1) full turn of the mold T = 2698 seconds; 2) T = 1350 seconds; 3) T = 295 seconds.

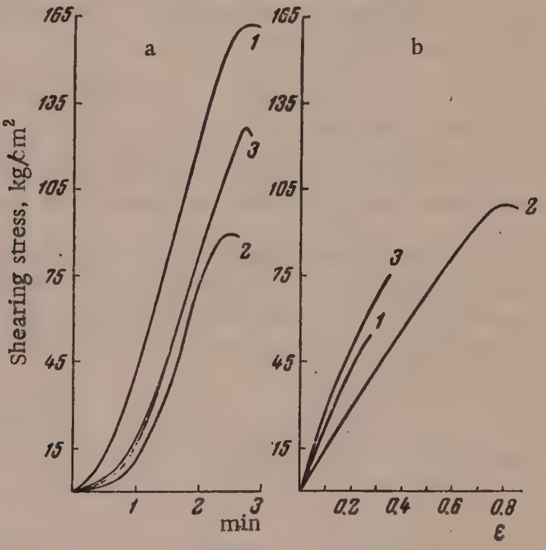

Fig. 10. Kinetics of the hardening reaction (a) and mechanical properties (b) of a Novolak molding powder at 170° made from oxidized resin: 1) molding composition based on oxidized resin; 2) K-18-2 (normal) molding composition; 3) molding composition based on oxidized resin with addition of furfural.

Oxidized resins have a loose structure, and molding powders made from them lose their viscofluid properties in the same rolling time as unoxidized resins (Fig. 10). Shearing deformations produce a strength increase (Curve 1 in Fig. 10, a); the mechanical properties of the material are inferior to those of the normal material (Curve 2, Fig. 10, b). Addition of furfural increases the duration of the viscofluid state and improves the mechanical properties (Curve 3, Fig. 10).

The relationships which have been found between the technological and mechanical properties of molding powders and the nature of the substances present in them can be used for studying the physicochemical processes occurring in resins at various stages in the production and processing of molding powders, and facilitate control of the technological processes. The choice of the optimum technological characteristics of molding powders must be made in relation to the technology of molding them into articles. Molding must take place while the material is in the viscofluid state. For example, despite the fact that a powder rolled for 230 seconds (Curve 4, Fig. 1) has a higher hardening rate (40 seconds) than a molding powder rolled for 210 seconds (63 seconds), it is not suitable for ordinary molding, as it has lost its viscofluid properties and a considerable higher pressure and greater time are required to attain the same density of the material in the finished article as is obtained from samples rolled for a shorter time, in which the duration of the viscofluid state is of the order of 30-40 seconds. Experience shows that molding powders having a viscofluid state lasting 30-40 seconds are of good quality and can be used for production of articles of complex form and large dimensions (radio receiver bodies) if molded with preheating. Small articles can be molded from powders with a lower duration of the viscofluid state. For example, electric bulb sockets of the best heat resistance, electrical properties, and external appearance are molded from powders the duration of the viscofluid state of which is ~ 10 seconds.

SUMMARY

1. The influence of physicochemical factors on the plasticity and reaction kinetics of thermostatting plastics during production of molding powders and their conversion into articles has been studied, and the structural changes occurring in the plastics during these processes have been elucidated.

2. The duration of the viscofluid state in molding powders is determined not by physical factors but by the rate of chemical conversion of low-molecular resin fractions and of reactive materials into substances of higher molecular weight.

3. The hardening rate of molding powders depends not only on the degree of condensation of the resins, but also on their structure.

4. The quality of thermosetting resins should be evaluated by their viscosity and molecular weight distribution, which are directly related to the duration of the viscofluid state.

5. The various components of thermosetting molding powders influence the kinetics of their hardening and other technological properties. The ingredients of molding powders can be classified into two groups according to whether they react chemically with the resins or not. The former influence the duration of the viscofluid state, the hardening rate, and the mechanical properties of the hardened material, while the latter act only as plasticizers.

6. For the production of articles with good and stable physical and mechanical properties, the molding powder must be molded when it is in the plastic or viscofluid state.

Scientifc Research and Planning Institute of the Plastics Industry
Moscow

Received March 2, 1956

LITERATURE CITED

[1] I. P. Losev and G. S. Petrov, Chemistry of Synthetic Resins (State Chem. Press, 1951).*

[2] A. A. Vansheidt, J. Chem. Ind., No. 7 (1954).

[3] I. F. Kanavets, Proc. Acad. Sci. USSR, 95, No. 6 (1954); Org. Chem. Ind., No. 7 (1940).

[4] I. F. Kanavets, Proc. 7th Conf. on High Mol. Compounds (Acad. Sci. USSR Press, 1952). *

[5] P. P. Kobeko, Amorphous Substances (Acad. Sci. USSR Press, 1952). *

[6] S. Glasstone, K. Laidler, H. Eyring, Theory of Rate Processes (Foreign Lit. Press, Moscow, 1948).*

[7] V. V. Korshak, Organic Chemical Methods in the Chemistry of High Polymers (1953).

[8] I. P. Mikheev, Molding Materials Based on Phenol-Formaldehyde Resins (State Chem. Press, Moscow, 1955).*

---

* In Russian.

[9] G. L. Slonimsky, V. A. Kargin, and L. I. Golubenkova, Proc. Acad. Sci. USSR, 93,2 (1953).

[10] L. A. Igonin, N. A. Krasulina, and V. A. Kargin, Colloid J., 17,4 (1955).

[11] G. L. Slonimsky, B. M. Kovarskaya and S. I. Klaz, Colloid J. 16,5 (1954).

ELECTRON-MICROSCOPE STUDIES OF COLLOIDS

1. MINERALS OF THE KAOLINITE – HALLOYSITE GROUP

M. I. Kuadzhe

The main mass of finely dispersed clay materials consists of kaolinite, halloysite, montmorillonite, illite, and other closely related minerals. These clay minerals usually compose the fine fractions of clays, muds, soils, etc. (0.005 – 0.001 mm and less), and therefore study of them presents considerable difficulties.

Detailed analysis of clay minerals necessitates the use of a number of modern physicochemical methods of investigation. One such method is electron microscopy, which has been widely used in recent years for studying the mineral composition of various clays [1-3].

Methods of investigation. A 1-3 g sample was soaked in distilled water in a porcelain basin; after ~~kneading with the fingers and stirring~~ it was transferred to a beaker 200-300 ml in capacity. After 24-48 hours the top layer of the suspension (10-15 cc) was carefully poured off and the suspension was diluted with distilled water to a slight opalescence. A drop of the suspension was transferred onto a collodion film on a wire screen fixed in the specimen holder, and dried in air or in a thermostat at 20-25°. The quality of the specimen was checked by examination under the microscope to confirm that the film is suitable for the work, i. e., that it is not too thick, not torn, and not warped. The dried specimen was examined under the electron microscope. After evacuation, an image of the object was examined on a fluorescent screen and characteristic regions of the specimen were photographed.

EXPERIMENTAL DATA

Certain electron micrographs of fine clay fractions are given below; these are mainly of the kaolinite and halloysite groups and their mixtures (the photographs were taken by V. M. Lukyanovich and A. V. Bogdashevsky, to whom the author is deeply grateful).

The plate shows electron micrographs (1, 2, 3, 4, 5) of fine fractions ($<1\ \mu$), of typical kaolinite minerals of Glukhovets, Balai, Kumak, and Prosyanaya clays, which clearly show hexagonal plates of kaolinite of various thicknesses and sizes, with internal angles from 106 to 140°, similar to those found in coarser fractions of kaolinite minerals. Careful examination of the micrographs reveals, in addition to these particles, also mica-like scales of various thicknesses and sizes, irregular in shape, and thinner at the edges. Fragments of kaolinite of these varieties are also seen, with their primary form partly retained and partly lost. Allowing for maximum accumulation of the plates, the thickness of the plates is estimated at about 20 $m\mu$, which agrees with x-ray estimations. The diameter of the plates is $0.1 - 0.5\ m\mu$. Electron micrographs of Kavpov (6), Pologoe (7) and Yantsensk (8) clays show that these clays consist mainly of kaolinite with small amounts of halloysite.

Examination of the electron micrograph of the fine fraction ($< 1\ \mu$) of white Zhuravlinsk clay (9) reveals halloysite crystals of acicular form, elongated, narrow and thin plates, and possibly also tubes evenly sheared off at the ends, sometimes grown together as twins at an angle. The specimen of clay (9) examined contained little or no kaolinite, and therefore Zhuravlinsk clay can be regarded as a typical halloysite. This is in good agreement with results obtained by the thermal, x-ray, and other methods of analysis. Thus, visible crystals of halloysite were first found by us in 1948 in Zhuravlinsk, Yantsensk, Pologoe and Karpov clays.

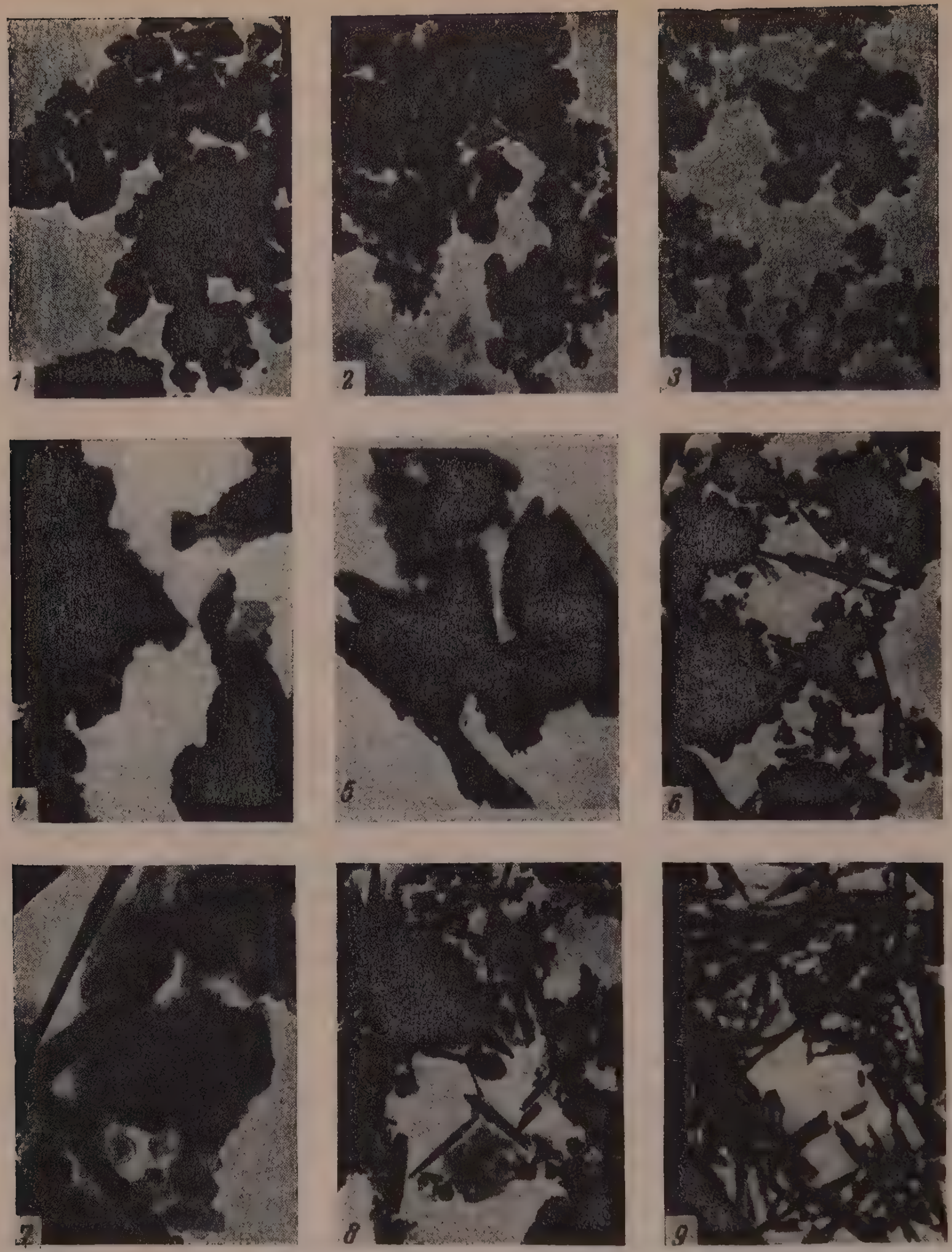

Electron micro graphs of fine clay fractions: 1) Glukhovets kaolinite (x 8000); 2) Balai kaolinite (x 8000); 3) Kumak clay (x 8000); 4) Prosyanaya kaolinite (x 17000) 5) ditto, after heating to 700° (x 20000); 6) Karpov kaolinite with halloysite (x 8000); 7) ditto, Pologoye (x 25000); 8) ditto, Yantsensk (x 8000); 9) Zhuravlinsk halloysite (25000).

Halloysite forms clearly defined cryptocrystals,closely resembling nontronite crystals * but differing from the latter in having smooth and even edges. Burton and Kohl [1] report that, under a magnification of 44,000 most of the plates are ~ 1 μ long and 1 / 20 μ wide. This distinguishes halloysite from kaolinite, the crystals of which are hexagonal plates.

Changes of the particle shape of clay minerals on increase of temperature are of considerable interest, as the adsorptive and catalytic properties of clays depend on these to a considerable extent. A typical Prosyanaya kaolin was chosen as an example. The specimens were kept at a definite temperature in a thermostat, and then examined under the electron microscope. It was found that a specimen heated at 200° showed no appreciable changes of particle shape. The same specimen, heated at 700° in a thermostat for

---

* According to Bakulova [2], nontronite consists of a mass of elongated splinterlike thin crystals up to 0.3 μ long with sharp and splitting ends of thicker and larger grains or aggregates of irregular and isometric form with diffuse edges.

4-5 hours (Micrograph 5) changed appreciably, and acquired the shape of montmorillonite particles. The adsorptive and catalytic properties of the substance changed also.

Thus, the electron microscope can be used to distinguish the shape, dimensions, and relative thicknesses of particles and to estimate the degree of homogeneity and dispersion of the substance under investigation. The main grounds for assigning a clay substance to a given mineral class are the particle shape and the sharpness of the particle outlines. Kaolinite and halloysite minerals have particles with sharp contours, while minerals of the montmorillonite group usually have particles with diffuse contours.

Kaolinite, halloysite, montmorillonite and others are relatively easily identified in finely dispersed clay fractions under the electron microscope. It is very difficult to distinguish montmorillonite from beidellite, while the latter may be confused with hydromica, which forms elongated plates.

SUMMARY

1. The specimen of fine Zhuravlinsk clay fraction examined was halloysite. White Karpov, Yantsensk and Pologoe clays consist of kaolinite and halloysite.

2. Specimens of fine fractions of Glukhov, Glukhovets, Prosyanaya, Balai and Kumak clays were found to be typical kaolinites and did not contain halloysite.

3. When Prosyanaya kaolinite is heated at 200° its crystal form is unchanged; heating kaolinite at 700-800° alters its original crystal form and also the adsorptive and catalytic properties.

The M. V. Lomonosov State University
Moscow
Faculty of Chemistry

Received October 19, 1955

LITERATURE CITED

[1] M. Arden, K. Endell, U. Hofmann, Betrich Keram. Gesel., Bd. 21, No. 6, (1940); F. Burton, W. Kohl, The Electron Microscope,(New York , 1942).

[2] B. N. Vertener, Factory Labs., No. 6 (1945); M. F. Vikulova, Soviet Geology, No. 39 (1949); Trans. All-Union Sci. Res. Geol. Inst., No. 2 (1950); Electron Microscopy of Clays (State Geological Press, 1952).

[3] M. I. Kuadzhe, Questions of Petrography and Mineralogy, vol. II (Acad. Sci. USSR Press, Moscow, 1953); Trans. Mineral. Museum, No. 5 (1953); V. T. Bykov, V. M. Lukyuanovich, L. V. Radushkevich, Bull. Acad. Sci. USSR, Div. Chem. Sci., No. 3 (1952).

THE MECHANISM OF PROTEIN DENATURATION

10. EFFECT OF FATTY ACID ANIONS ON THE STABILITY OF GLOBULAR PROTEINS TO DENATURATION

A. L. Loseva and A. S. Tsyperovich

During the last 8-10 years the view has become established in the literature that salts of organic fatty acids with small nonpolar radicals ($C_4 - C_9$), are effective stabilizers of globular proteins, especially serum albumin. There have been several investigations [1, 2] of the stabilizing effects of such salts as sodium caprylate, heptylate, caproate, and valerate on globular proteins. These investigations were related with the need of certain states to provide their armed forces, operating in tropical conditions, with thermostable blood protein preparations [3]. It was found that salts of fatty acids raise the coagulation temperature of serum albumin and prevent viscosity increases and turbidity in its solutions on heating [4]. These observations were directly related to aggregation phenomena, and are therefore not entirely convincing. It was possible, however, that in some instances strengthening of the macromolecular structure of the protein (inhibition of denaturation proper) does occur, as salts of fatty acids decreased the usual viscosity increase produced by 6 M urea in serum albumin, in conditions in which aggregation reactions are improbable [5]. The magnitude of the effect increased with lengthening of the hydrocarbon radical in the salt molecule. These and other facts [6, 7] led to the opinion that fatty acid salts exert a stabilizing effect on proteins.

Subsequently the binding of fatty acid anions by serum albumin was studied by various, including some direct, methods; it has been demonstrated by the ultrafiltration method [8], by the increase of the electrophoretic mobility of proteins in presence of these substances [9], and by equilibrium dialysis, whereby the reversible bonding of small amounts of salts with tagged carbon (C^{14}) in the carboxyl was detected [10]. It was established that the bonding was of a nonpolar character, and its stability increased with increasing length of the anion chain.

The principal defect of these investigations is that the true influence on denaturation was not studied in any of them. Observations of viscosity changes, turbidity, or coagulation in protein solutions would mainly indicate postdenaturation processes. Therefore the true nature of the action of salts on protein stability (on the course of denaturation proper) cannot be regarded as established.

In view of this, it was decided to study the influence of fatty acid anions separately on denaturation proper and on the postdenaturation aggregation of denatured molecules, with special attention to the main phase of the process (denaturation proper). This was the only possible way of determining the true influence of the substances studied on the stability of the macromolecular protein structure.

Materials and methods. Three globular proteins were used for the experiments: serum and egg alumins and edestin. The first two proteins were prepared by Baranovsky's method [11], with double recrystallization; crystalline edestin was prepared by Osborne's method [12]. The proteins were generally used at 2.3-2.8% concentrations in the experiments.

The action of the sodium salts of caproic and nonylic acids on the proteins was studied. The acids were converted into salts by neutralization with caustic soda, by a standard procedure described elsewhere [13]. In the experiments, to 10 ml of the protein solution 0.5 ml of 1 M phosphate buffer at pH 7.4 was added, followed by0.5 ml of 1 M solution of the fatty acid salt (sodium nonylate). The final salt concentration was 0.045 M.

This corresponded to the concentrations generally used in various investigations for stabilization of serum albumin. The amount of sodium caproate used was 2-3 times as large, to obtain a more pronounced action. The amount of salt to be used was generally determined by preliminary experiments. The same volumes of water were added to control specimens, containing the same amounts of protein and buffer.

The denaturation was effected by heating. The course of the process was determined by isolation of the denatured protein by isoelectric precipitation (denaturation proper) and finding its amount by the biuret reaction. The isoelectric precipitation tests for all three proteins did not differ from the usual tests [14, 15]. Variations in the course of aggregation processes were observed by the viscosity changes measured by means of the Ostwald viscosimeter. After addition of the salt or after its prolonged action on the samples the pH was always checked to determine whether the reaction of the medium had changed.

The experiments were started with studies of the action of salts on serum albumin, as this protein was the main material used in all studies of the stabilizing action of fatty acid anions. The first experiments were with sodium nonylate. The hydrocarbon radical of this salt differs by only one CH_2 group from the more frequently used caprylate. For comparison, a salt of a fatty acid with a shorter hydrocarbon radical, sodium caproate, was used.

After addition of the fatty acid salt, samples were immediately taken from the experimental and control mixtures and their contents of denatured protein determined. This gave the first point on the curve. The experimental and control mixtures were then placed in a water bath and the course of denaturation was followed by taking samples at definite time intervals (15 and 30 minutes, 1 hour, 2 hours, etc).

The basic fact described in all investigations was first reproduced. The experimental and control solutions were heated at various relatively high temperatures (80-90°). The solution containing nonylate remained without visible change, while in the control (without nonylate) the protein was completely denatured. It appeared that addition of the salt increases the stability of the albumin.

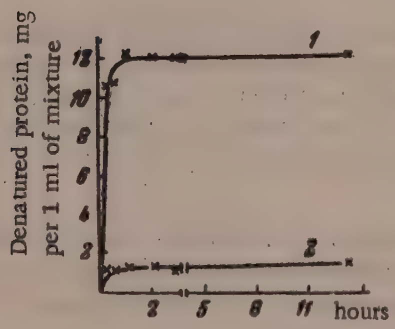

Fig. 1. Denaturation of serum albumin by heating at 50°: 1) with sodium nonylate; 2) without sodium nonylate.

The experiment was then performed with mild heating (50°), when neither solution changed in appearance, and the course of denaturation proper was followed by isolation of the denatured part of the protein by isoelectric precipitation. Even the first experiments yielded a clear and apparently unexpected result. It was found that addition of the fatty acid not only does not increase the stability of serum albumin but, on the contrary, diminishes it, sharply accelerating denaturation.

Figure 1 illustrates a typical experiment; this shows that addition of nonylate causes rapid formation of a considerable amount of insoluble protein, which is easily isolated from the outwardly unchanged "stabilized" mixture; it comprises ~ 12 mg of the 25 mg (in 1 ml of solution) taken for the experiment. The salt therefore acts as a denaturant. The reaction occurs only to a slight extent in the control sample.

Figure 2 represents an analogous experiment, but here the temperature was gradually raised, the protein being heated first at 50°, and then at 65, 75, and 85°. It is seen that in the sample with nonylate a considerable amount of denatured protein is formed very rapidly and this gradually increases with rise of temperature. Denaturation in the control sample followed the normal course; the amount of protein passing into the insoluble form increased with increase of temperature.

These results naturally suggest that the fatty acid anion acts on the protein only by preventing or weakening the aggregation of denatured molecules, i. e., postdenaturation changes. Since aggregation is the main cause of increased solution viscosity, this suggestion was verified by measurements of viscosity increases during denaturation in presence of sodium nonylate and under normal conditions (without the salt). The experimental conditions were chosen so that it was possible to study changes in the protein in solutions in which no coagulation occurred at all (pH ~ 7; temperature 72-75°; protein concentration 2.5%) .

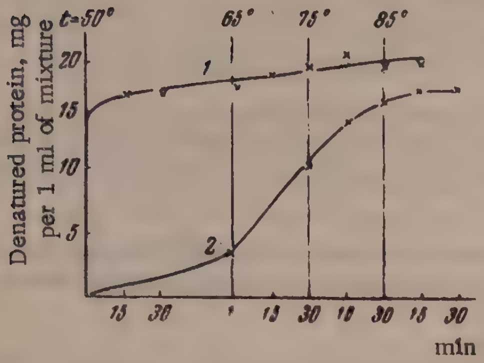

Fig. 2. Denaturation of serum albumin by heating at 50, 65, 75, and 85°: 1) with sodium nonylate; 2) without sodium nonylate.

A typical experiment is illustrated by Fig. 3, a, which shows the effect of nonylate on postdenaturation aggregation in serum albumin solutions. There is almost no increase of viscosity in the experimental mixture although, as is already known, denaturation occurs in it very rapidly. In the control (without nonylate) aggregation proceeds normally, and the viscosity increases. Both solutions changed little in external appearance, and only their opalescence increased slightly. On stronger heating (85-95°) the protein in the solution without nonylate coagulated, while in the experimental solution there was no visible change. These observations directly confirmed that the fatty acid salt retards secondary aggregative changes in the denatured particles, preventing or greatly weakening aggregation reactions.

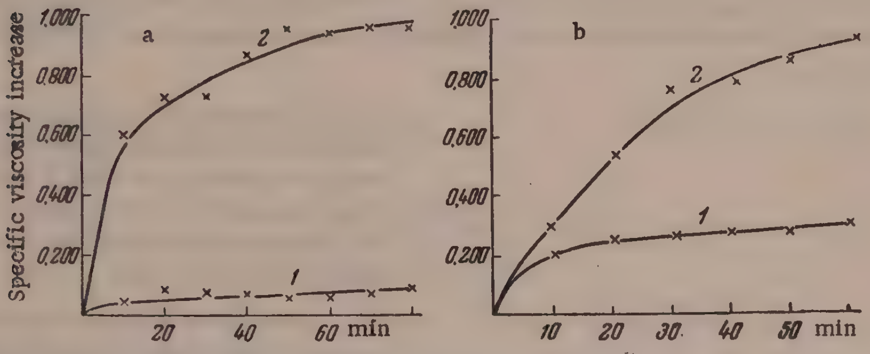

Fig. 3. Effect of sodium nonylate on postdenaturation aggregation in solutions of serum (a) and egg (b) albumins; 1) with nonylate; 2) without nonylate.

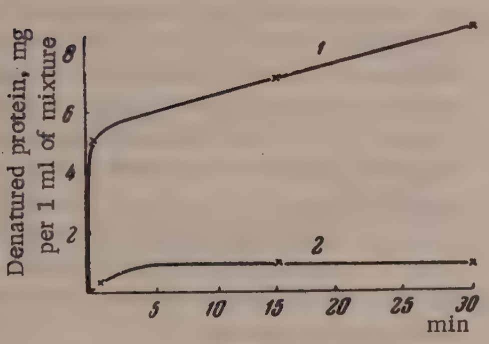

Fig. 4. Denaturation of egg albumin by heating: 1) with sodium nonylate; 2) without sodium nonylate.

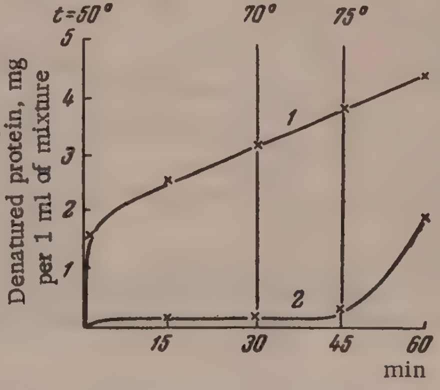

Fig. 5. Denaturation of edestin by heating at 50, 70, and 75°: 1) with sodium nonylate; 2) without sodium nonylate.

The facts established for serum albumin were fully confirmed in studies of the action of fatty acid anions on egg albumin and edestin. Figure 4 shows that denaturation is sharply accelerated immediately after addition of sodium nonylate to egg albumin. The process is so rapid that a considerable amount of denatured protein can be isolated by isoelectric precipitation immediately after addition of the salt solution; the amount increases on further heating. External changes in the experimental and control solutions may not occur if the heating is not very strong (50-55°). However, separate determinations of viscosity showed that the viscosity changes very little in presence of nonylate (the viscosity shows almost no increase throughout the process). The viscosity of the control solution increases rapidly in the same conditions (Fig. 3, b).

A sharp decrease of protein stability under the action of sodium nonylate was also found in the case of edestin. The experiments with this protein were carried out in salt solutions (10% NaCl) under normal conditions [15], but at higher temperatures, as in this case edestin is itself much more stable than the other proteins studied.

Figure 5 shows that addition of the fatty acid salt considerably decreases its stability to heat. Edestin, like the other proteins, was protected from coagulation (the postdenaturation reactions were diminished). The magnitude of this effect depended on the added salt.

The action of a fatty acid salt with a shorter hydrocarbon radical, sodium caproate, was then studied. As has been stated, this salt has appreciably less reactivity toward proteins. It seemed likely that the observed effect – decrease of the stability of the macromolecular structure to denaturation – will be much less pronounced with the use of sodium caproate. This was confirmed by experiments with two proteins.

In the case of serum albumin (Fig. 6, a) the amount of denatured protein after addition of the salt always exceeded the control value; however, it was considerably less than in the action of nonylate under the same conditions. An analogous result was obtained for egg albumin (Fig. 6, b). It was therefore shown, on the one hand, that caproate increases denaturation, and on the other, that the denaturing action of fatty acid salts diminishes with shortening of the hydrocarbon chain. Sodium nonylate increases denaturation to a much greater extent than sodium caproate.

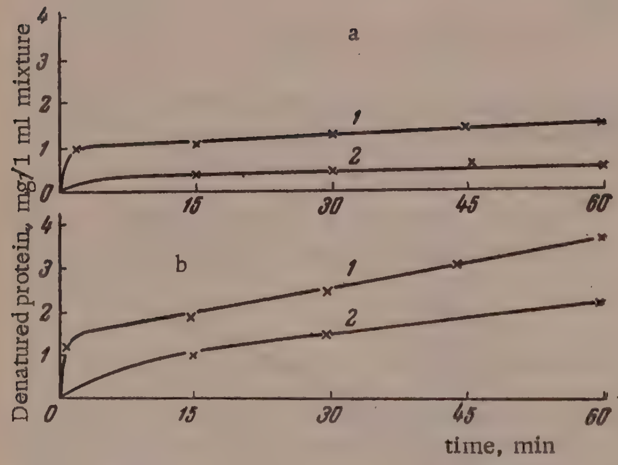

Fig. 6. Denaturation of serum (a) and egg (b) albumin: 1) with sodium caproate; 2) without sodium caproate.

It has been established by these investigations that, in the experimental conditions used, fatty acid anions do not have a stabilizing effect on globular proteins, but are denaturants. This has been demonstrated for serum and egg albumins and for edestin.

Fatty acid salts prevent or diminish secondary (aggregative) changes in denatured molecules, thereby giving the impression of protein stability. Their effect on the macromolecular structure of the protein is, however, such that the latter becomes less stable to denaturation under the action of fatty acid salts. Therefore, the view which has become established in the literature concerning the stabilizing effect of fatty acid salts on the molecules of globular proteins is incorrect. The workers in question observed directly the action of salts on aggregative changes in proteins without once investigating their influence on the course of denaturation as such. By separate investigation of these stages it was at once possible to clarify the true position and to establish that the observed effect was mainly anti-aggregative.

Both effects – the denaturing effect of the salt, and the protection of the denatured protein against aggregation – are apparently fairly easily explained. The anions are bound by the protein and decrease the stability of the macromolecular particle structure as the result of addition of a considerable number of negative charges (COO^- groups of the fatty acid), and also by interaction of the nonpolar radicals with the hydrophobic regions of the protein molecule. The first factor probably results in a stress in the macromolecular structure owing to repulsion of the negative charges, while the second weakens and even ruptures the stabilizing bonds in the hydrophobic regions owing to incorporation of long hydrocarbon chains. There are various possibilities, but it is clear that in any event the action of fatty acid anions must be similar to the action of detergents.

Addition of fatty acid anions leads to increase of the total negative charge on the protein molecules; forces of repulsion between them increase. This probably accounts for the decreased aggregation of the denatured particles in presence of nonylate, caproate, etc. In such cases fatty acid salts act as alkalies.

As we have shown, the denaturing effect of fatty acid salts increases sharply with increasing hydrocarbon radical chain length. It is known from the literature that the stability and extent of anion bonding by the protein increases in a similar way. The amount of butyrate is only 15-20% of the amount of caprylate bound under the same conditions. The number of anions attached to the protein will be much greater in the latter case. It is reasonable to assume that this is the reason for the greater labilizing action of salts containing radicals with longer hydrocarbon chains.

SUMMARY

1. Fatty acid salts ($C_4 - C_9$, of the sodium caprylate type) do not exert a stabilizing effect on serum albumin and other globular proteins.

2. Fatty acid anions decrease the stability of the macromolecular structure of serum and egg albumins and of edestin and intensify denaturation; i. e., they are denaturants, and they weaken the secondary (aggrevative) changes in the denatured molecules.

3. The denaturing action of fatty acid salts increases with the size of the hydrocarbon radical in the anion.

4. The mechanism of these effects is discussed.

Institute of Biochemistry, Acad. Sci. Ukrainian SSR
Kiev

Received May 12, 1956.

LITERATURE CITED

[1] F. Putnam, Proteins, v. 1, (New York, 1953) p. 825.

[2] W. Kausmann, The mechanism of enzyme action, (Baltimore, 1954) p. 70.

[3] J. Edsall, Adv. Protein Chem. 3, 383, (1947).

[4] P. Boyer, F. Lum, G. Ballon, J. Luck, R. Rice, J. Biol. Chem. 162, 181, (1946).

[5] P. Boyer, G. Ballon, J. Luck, J. Biol. Chem. 162, 199, (1946).

[6] F. Kendall, J. Biol. Chem. 138, 97, (1941).

[7] J. Hink, F. Johnson, J. Am. Pharm. Assoc., 40, 537, (1951).

[8] P. Boyer, G. Ballon, J. Luck, J. Biol. Chem. 167, 407, (1947).

[9] G. Ballon, P. Boyer, J. Luck, J. Biol. Chem., 159, 111, (1945).

[10] J. Teresi, J. Luck, J. Biol. Chem. 194, 823, (1952).

[11] T. Baranovsky, Proc. Acad. Sci. USSR, 28, 723 (1940); see also K. I. Strachitsky and A. Yu. Kologrivova, Biokhimiya, 11, 385 (1946).

[12] C. L. A. Schmidt (ed), The Chemistry of Amino Acids and Proteins, 2 ed., (1945).

[13] A. L. Loseva, "Investigation of Some Questions of Stabilization of Globular Proteins", dissertation (Acad. Sci. Ukrainian SSR, Kiev, 1956).

[14] A. S. Tsyperovich, Ukrain. Biochem. J., 20, 108 (1948); 21, 44 (1949).

[15] A. S. Tsyperovich and A. L. Loseva, Biokhimiya, 21, 53 (1956).

GELATION OF LATEXES ON POROUS FORMS

D. M. Sandomirsky

A number of processes for the production of rubber articles from latex are based on the formation of a rubber gel either by slow formation of various cations in the latex (gelation in the true sense) or by diffusion into the latex of cations from the surface of the form coated with a suitable solution (known as ionic deposition), or from a metallic anode (electrodeposition) [1-3].

In addition to these methods another process is used in practice, in which destabilization of the globules by the action of ions is not used. This is the production of articles in porous molds or forms, for example, made of plaster [4-6]. In this method the latex mixture is poured into a dry plaster form the inner cavity of which has the shape of the required article. After some time the latex mixture is poured out, and the gel remaining on the walls of the form is then dried and vulcanized.

The main cause of gel formation in this case is evidently the absorption of the dispersion medium of the latex by the pores of the form. Although the production of latex articles in porous forms is used fairly widely in the rubber industry abroad, it has not so far been systematically studied.

The present communication contains the results of an investigation of the influence of the nature and concentration of the latex, duration of deposition, and temperature, on the course of the deposition and on certain properties of the gel.

EXPERIMENTAL DATA*

The deposition was effected on cylindrical plaster of Paris forms 16-18 mm in diameter and with working portions 45 mm long, made from analytical grade calcium sulfate. Two types of natural latex were studied: unconcentrated latex with 34.6% dry content, and vulcanized "Revultex" concentrate (60.4%). Attempts to obtain deposits from Revertex (concentrate made by evaporation) and SKS-30 butadiene – styrene synthetic latex were unsuccessful owing to the looseness of the gel formed.

The dried plaster form was immersed to a definite depth in the latex and removed after a certain time; the gel was rinsed, removed from the form, weighed, and dried at 80° to constant weight. The amount of rubber deposited per 1 cm^2 of the form surface and the concentration of the gel were calculated. It should be noted that the gels formed on porous forms differ from gels produced by, say, ionic deposition, in being more loose and not having a clearly defined boundary with the latex.

The Figure shows the kinetics of deposition of rubber from Revultex and unconcentrated latex at different temperatures. The amount of rubber deposited and the rate of deposition increase with increasing latex concentration and temperature. It was observed during these experiments that the concentration of the gel formed is independent of the concentration of the original latex, of the duration of deposition, and of the temperature.

To test the effect of latex concentration on the amount and concentration of the gel formed, experiments were carried out on deposition of gel from Revultex, diluted with distilled water to various concentrations, for 15 minutes. The results are given in the Table.

---

* G. Baibakova and I. Shmurak, students at the Lomonosov Institute of Fine Chemical Technology, assisted in the experimental work.

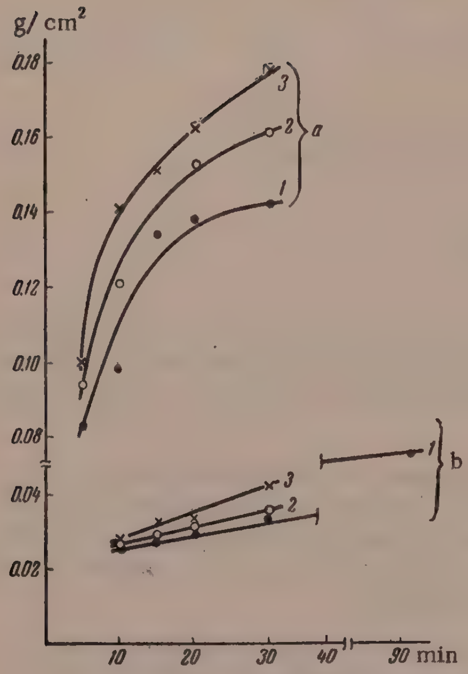

Kinetics of deposition of rubber on a plaster form from Revultex (a) and unconcentrated latex (b):
1) at room temperature; 2) at 40°; 3) at 60°.

DISCUSSION OF RESULTS

The processes which occur when the latex comes into contact with a porous surface (with pores smaller than the latex globules) may be represented as follows. When the latex comes into contact with the porous wall, the latter begins to absorb the dispersion medium. The concentration of the adjacent latex layer gradually increases, and a moment is reached when the globules come into continuous contact. Evidently this limiting concentration will not depend on the initial concentration of the latex, but will be determined by general geometrical considerations.

In fact, as is shown above, gels formed from Revultex at different dilutions and from unconcentrated natural latex differ relatively little in concentration, although the latex concentrations are very different. The gel concentration is close to the degree of space filling in close packing of spheres of equal diameters (74.05%). The absence of any appreciable influence of temperature on the gel concentration is explained by the same considerations. Increase of temperature accelerates the dehydration process, but the gel is always formed at practically the same concentration.

After a gel layer has been formed directly on the plaster surface, dehydration of the latex layers further from the form proceeds by diffusion of the serum through the gel layer. This retards the process somewhat, as is confirmed by the nature of the kinetic curves. Because of this, there is at any given instant a concentration gradient in the gel, from a greatest value at the form wall to greatest dilution at the opposite surface of the gel. It was stated above that gels formed by dehydration at a porous surface have no sharp boundary with the latex. There is rather a gradual transition from latex through a thick paste to the gel.

Effect of Latex Concentration on the Amount and Concentration of the Gel Deposited

Type of latex	Latex concentration in %	Amount of gel in g/cm²	Gel concentration in %	Average concentration of gel from Revultex, %
Revultex	60.4	0.092	69.0	70.5
	49.8	0.067	73.5	
	40.1	0.058	71.4	
	28.9	0.047	69.9	
Latex	34.6	0.014	64.1	

The above considerations are supported by the fact that the gel concentration decreases somewhat with increasing time of deposition. The existence of a limiting concentration in rubber gels was also found by us in the syneresis, in water, of a gel formed by gelation of a "Nairit" latex by means of zinc oxide [7]. The effect also occurs in the syneresis, in water, of natural latex coagulum in the production of rubber in plantations [8].

Thus the partial destabilization of latex globules, leading to formation of a gel with a network structure, occurs not only as the result of changes in the protective layer by interaction with electrolytes, but also by close contact between the globules. The strength of the gels so formed is a sign of breakdown of the layers and of contact between the rubber contained in the globules at these points. The presence of large amounts of protective substances in the latex (as in Revertex or SKS-30) prevents close packing and formation of a firm gel.

It seems likely that gel formation in consequence of close packing of the globules occurs not only when a rubber gel is dehydrated at a porous surface, but also when films are made from latex by drying the latter. Gel formation is probably the first stage of this process.

SUMMARY

1. The deposition of rubber from latex on a porous surface has been studied.

2. The amount of rubber deposited depends on the concentration of the latex, the duration of contact with the porous surface, and the temperature.

3. The concentration of the gel formed does not depend on the latex concentration or the conditions of deposition, and is close to the degree of space filling in close packing of spheres of equal diameters.

The M. V. Lomonosov Institute of Fine Chemical Technology
Moscow

Received May 31, 1956

LITERATURE CITED

[1] S. S. Voyutsky and B. V. Shtarkh, Physical Chemistry of Film Formation from High Polymer Dispersions (State Light Ind. Press, 1954), p. 110.*

[2] D. M. Sandomirsky and V. V. Chernaya, Trans. Sci. Res. Inst. Rubber Ind., No. 1, 20 (1954).

[3] B. Dogadkin and D. Sandomirsky, Trans. VI Mendeleev Conf., Vol. 2, No. 3 (1933).

[4] S. C. Stokes, Trans. I. R. I. 25, 407, (1950).

[5] N. J. Jarman, Rubber Age 67, 68, (1950).

[6] A. A. Round, Rubber Age a. Synth. 33, 169, (1952).

[7] D. Sandomirsky, in Symposium "Production and Applications of Synthetic Latexes" (State Chem. Press, 1953), p. 33.*

[8] Th. G. F. Schoon, Chem. Abstr. 48, 13255, (1954).

---

* In Russian.

~~THE~~ THIXOTROPIC PROPERTIES OF CERTAIN PRINTING INKS*

A. A. Trapeznikov and T. G. Shalopalkina

Printing inks are structurized colloidal systems with a complex combination of structural and mechanical properties, including fairly pronounced thixotropy.

These properties, including the thixotropy of disperse systems, have been studied by many workers [1-13]. A number of authors plotted hysteresis loops and evaluated thixotropy from the viscous properties only [4-8]. Others [9-11] studied strength properties only, without consideration of the viscous properties. There have been hardly any investigations covering methods for evaluating the thixotropy of systems at various stages of deformation, both by strength and by viscosity. In consequence, the role of each of these stages in evaluation of the complex combination of thixotropic properties has not been determined.

In work on oleophilic aluminum naphthenate gels [12], both strength and viscous properties were studied; after the maximum on the stress – deformation curve, corresponding to the strength of the structure, had been passed, a constant shearing stress became established, corresponding to steady flow, with a corresponding viscosity value.

Two samples of newspaper inks have been similarly studied in the present investigation. However, owing to some structural characteristics of these systems, their rheological properties were different from the corresponding properties of aluminum naphthenate gels. It was found that the shearing stress reached after the strength maximum (yield value) after not too long a time must be regarded as not a true equilibrium, but only a quasi-equilibrium value, which depends on the velocity gradients to which the system had previously been subjected. These characteristics can be represented by the so-called hysteresis loops. Thus by our investigations it was possible to elucidate more fully the thixotropic characteristics of different systems related to their structural differences, and also to combine methods for evaluating thixotropy based on strength and viscosity determinations.

The two newspaper inks, supplied by the Sci. Res. Inst. of the Polygraphic Industry and Technology, had the following compositions: No. 787 – furnace black 16%, fused induline 16%, black marine oil 68% (ink rated as nondusting); No. 788 – channel black 9%, fused induline 19%, black marine oil 72% (ink rated as dusting).

The structural and mechanical properties were studied by means of a compound elastoviscosimeter [12, 13] further modified in some details. The outer cylinder was rotated at a constant rate Ω = const. Cylinders of the following dimensions were used in systematic determinations: outer cylinder, radius $R_2 = 1.495$ cm, height $L_2 = 12.0$ cm; inner cylinder (longitudinally fluted, with a concave hemispherical base), radius $R_1 = 1.420$ cm, height $L_1 = 7.96$ cm. In some instances an inner cylinder was used with $R_1 = 1.404$ cm, with a thermocouple fixed flush with its fluted side surface for measurement of the cylinder surface temperature. An ultrathermostat was used to regulate the temperature of the instrument ($t = 20° \pm 0.1$). The torque at the inner cylinder arising at different velocity gradients in this series of experiments was measured with the aid of wires with elasticities C_0 from $10.13 \cdot 10^4$ to $12.9 \cdot 10^6$ dynes-cm/radian. This made it possible to measure shearing stresses from 10 to 30,000 dynes/cm^2; the velocity gradient was varied stepwise over a wide range by means of a gear box system. The angle of displacement of the inner cylinder was read off by means of a light spot reflected from a mirror. The outer cylinder was started and stopped by means of an electromagnetic clutch.

---

* The investigation was suggested by the Scientific Research Institute of the Polygraphic Industry and Technology.

RESULTS AND DISCUSSION

Since printing ink is used under high velocity gradients in printing, and undergoes considerable structural breakdown in the process, the properties of the inks were studied at relatively high velocity gradients.

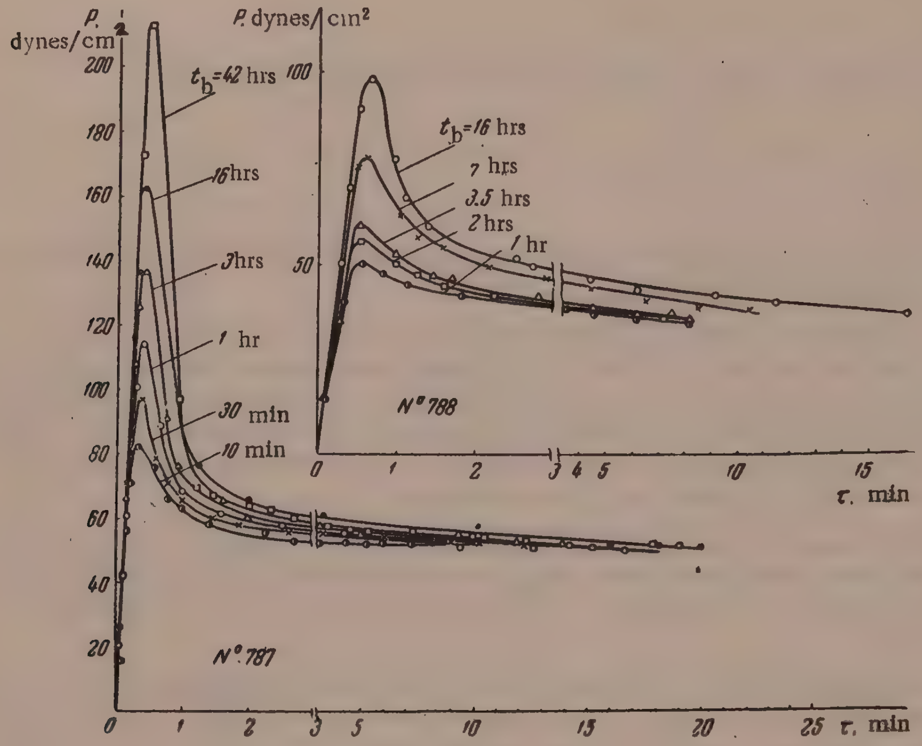

Fig. 1. $P - \tau$ curves for inks No. 787 and 788 at $C = 0.192$ sec.$^{-1}$.

A characteristic property of thixotropic systems is the formation, by the particles of the disperse phase, of structures with resistance to shear, which are broken down by mechanical forces and restored after a period of rest. Increase of the strength of the structure during rest is one of the characteristics of its restoration.

The inks studied in this work have clearly defined resistance to shear, as shown by the stress maxima P_r formed on the stress – time ($P - \tau$), curves plotted for a constant rate of rotation of the outer cylinder† (the Ω const. method).

Figure 1 shows $P - \tau$ curves for different times of restoration of the structure of inks No. 787 and 788 after prolonged deformation at a velocity gradient $G = 0.192$ sec.$^{-1}$.

A constant value of the shearing stress after the maximum $P = P_r$ and partial breakdown of the structure ought to correpond to equilibrium established between the structures additionally broken down and restored in flow, and determine the steady flow viscosity. However, it is seen (Fig. 1) that the shearing stress continues to decrease on prolonged rotation of the outer cylinder (τ). This slow decrease of the shearing stress was observed, for example, in ink No. 788 with longer rotation of the cylinder than that shown in Fig. 1 (see Table).

τ, min	1	5	10	30	60	90	120
P_s* dynes/cm²	44.0	39.0	38.4	36.4	35.9	35.4	34.9

---

†In these experiments, for easier measurement of changes of stress for short deformation times with an incompletely restored structure, a wire of relatively low rigidity $C_0 = 101300$ dynes · cm/radian was used. For this reason the initial regions of the $P - \tau$ curves refer to a not quite constant deformation rate, but to one becoming established only gradually.

Therefore a true equilibrium value of P_s is not reached in 2 hours. It is seen from the curves in Fig. 1 that when the system is at rest the increase of P_r is accompanied by increases in the values of P_s^*, which refer to the same periods of rotation of the cylinder, for example, to τ = 5 minutes (which is about 10 times as much as the time required to reach the maximum). These values of P_s^* we shall term quasiequilibrium, in distinction from the true equilibrium P_s. Fig. 2 gives curves representing structural buildup at rest, $P_r - \tau_b$ and $P_s^* - \tau_b$, where τ_b is the time of restoration or buildup of the structure. These curves show that the strength of the structure greatly increases during rest, but does not reach a completely constant value even after 42 hours.

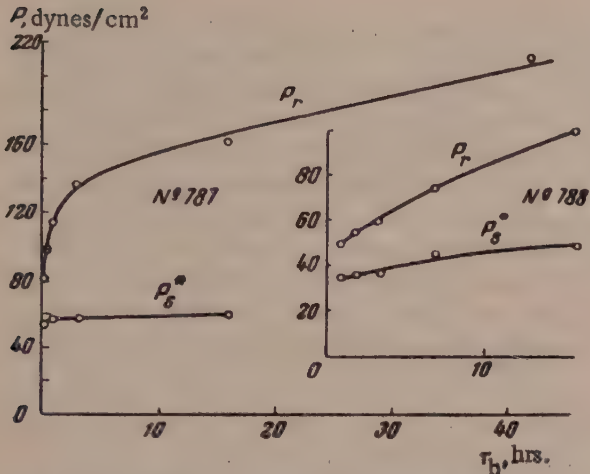

Fig. 2. Variation of P_r and P_s^* with the time of structural buildup in inks No. 787 and No. 788.

The descending part of the $P - \tau$ curve (Fig. 1) represents breakdown of the continuous structural network. The slow decrease of P far beyond the maximum on the $P - \tau$ curve indicates very protracted breakdown of the structure, which should be attributed to breakdown of separate aggregates of particles and fragments of the continuous network. It is natural to suppose that a certain true equilibrium value should be reached with much greater deformation times. At the same time we can obtain values for P_s^* at G = 0.192 sec.$^{-1}$ much lower than the true P_s by breaking down the system by a much greater velocity gradient. Then P_s^* will increase and approach the true value during restoration of the structure even from lower values of P_s^*. This is illustrated by ink No. 788, broken down at G = 433 sec.$^{-1}$, and then measured at G = 0.192 sec.$^{-1}$ or after every 15 minutes of rest (Curve 1, Fig. 3) or with continuous rotation of the outer cylinder (Curve 2, Fig. 3). In the latter case the experiment was continued for only 3.5 hours and during this time P_s^* rose continuously and tended to a certain limit, reaching only 18.2 dynes/cm^2, a value considerably lower than the value of P_s^* reached at the same value of G in 2 hours rotation in a system with an undestroyed structure (34.9 dynes/cm^2)(see Table). Therefore the true equilibrium P_s lies between the values of 34.9 and 18.2 dynes/cm^2, reached during decreasing and increasing P_s^* within this time of rotation.

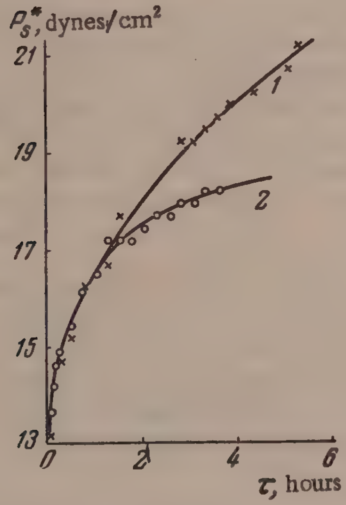

Fig. 3. Restoration of structure in ink No. 788, broken down at G = 433 sec.$^{-1}$ Description in text.

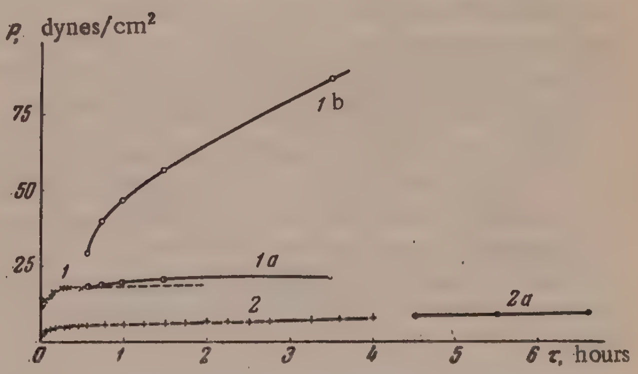

Fig. 4. Restoration of structure in ink No. 787 (1, 1a, and 1b), and No. 788 (2 and 2a). Description in text.

The explanation of the difference between Curves 1 and 2 in Fig. 3 is that during each 15 minutes of rest (Curve 1) the structure is restored appreciably, possibly even to a greater extent than would correspond to the true equilibrium value of P_s. For this reason Curve 1 ascends continuously. Therefore curves of the type of Curve 2 in Fig. 3 are of special significance for finding and establishing the true value of P_s. It is evident that such a curve for structure restoration with continuous rotation in principle represents only the value of P_s^*, as in such conditions of deformation a continuous network, determining P_r, cannot be formed. Any $P-\tau$ curve, however, obtained even after a minimum period of rest and structural buildup in static conditions, could in principle have a maximum P_r, relating to breakdown of the rapidly restoring elements of the structural network.

The curves in Fig. 4 (in these measurements the radius of the inner cylinder R_1 was 1,201 cm) show increases of P_s^* on continuous rotation of the outer cylinder ($G = 0{,}052$ sec.$^{-1}$) and also increases of P_s^* and appearance of P_r after rest in inks No. 787 and No. 788, the structure of which was broken down at $G = 115$ sec.$^{-1}$. Curve 1 shows the increase of P_s^* with continuous rotation of ink No. 787 for 30 minutes, in which time P_s^* reaches an almost constant value (the broken line represents the presumed very slight further increase of P_s^*). After this the system was rested for five minutes, and then a $P-\tau$ curve was plotted at the same $G = 0{,}052$ sec.$^{-1}$. In this case a distinct maximum appears on the $P-\tau$ curve, after which a value of P_s^* somewhat higher than before is reached. Further similar measurements performed after 10, 15, 30 and 120 minutes of rest show that P_r increases especially rapidly (Curve 1b) and P_s^* decreases to a lesser extent (Curve 1a). The same Fig. 4 also shows curves for the increase of P_s^* with continuous rotation for 4 hours for ink No. 788 (Curve 2), and after rests of 30, 60, and again 60 minutes for the same system (Curve 2a). We note that P_r does not appear at all in this ink during this resting time.

This comparison shows that the structure is restored much more rapidly in ink No. 787 than in No. 788, and the formation of a network is more pronounced in ink No. 787, as indicated by the values of P_r. In ink No. 788 P_s^* increases slowly, while P_r probably appears only when the structure has been restored to a considerable extent. It should be noted that here again there is still a considerable difference between the values of P_s^* found in the "down" and "up" curves (35 and 18.2 dynes/cm^2 for ink No. 787, 24 and 8.2 dynes/cm^2 for ink No. 788).

Thus, in farily complex systems, P_r may appear on the $(P-\tau)_G$ curve and may increase during rest to some extent independently of the increase of P_s^* and of the attainent of true P_s. The maximum P_r may be the consequence of the formation of a structural network from a part of especially rapidly restoring elements of the structure. Consequently, the true value of P_s can be correctly determined only from the coincidence of the ends of the $(P-\tau)_G$ curves for a restored and a strongly broken down structure. Hence the maxima of P_r relate to deformation and breakdown of the continuous network, and the increase of P_r during rest to its strengthening. The prolonged decrease of P_s^* during deformation of the undestroyed structure (at a certain value of G) and the prolonged increase of P_s during continuous rotation of the system (at the same G) after considerable structural breakdown, relate to breakdown of network fragments and individual aggregates of particles, and to their restoration respectively. Consequently, the whole thixotropic effect can be regarded as consisting of two parts: strength thixotropy, relating to breakdown and restoration of the continuous network; and viscosity thixotropy, involving breakdown of network fragments and individual aggregates of particles, and their restoration (this also includes the orientation component of thixotropy). Viscosity thixotropy is associated with the duration of the time required for reduction of the size of the particles in the structure, which depends on their slippage through the liquid medium.

In addition to the experiments described above, the effects of strength and structural thixotropy appear in $P-\tau$ curves (Fig. 5, for ink No. 787) obtained for the same value of $G = 0.192$ sec. $^{-1}$ (cylinder with $R_1 = 1.42$ cm) after deformation of the inks at various higher values of G (10 minutes of rest between the measurements). The curve for $G = 0{,}192$ sec. $^{-1}$, taken for repeated deformation after 10 minutes of rest, represents a certain initial state of the system. The subsequent curves show that after deformation of the ink at increasing values of G both the height of the maximum P_r on the curve and the quasiequilibrium stress P_s^* diminish.

The effect of the magnitude of the "destroying" velocity gradient on the values of P_r and P_s^* is seen in the curves in Fig. 6 . These show that the greatest structural breakdown occurs up to values of G of 50-60 sec. $^{-1}$, which represent a certain critical value of the " destroying" velocity gradient for the given type of structure. Increase of G to 430 sec.$^{-1}$ leads to only a very slight further structural breakdown.

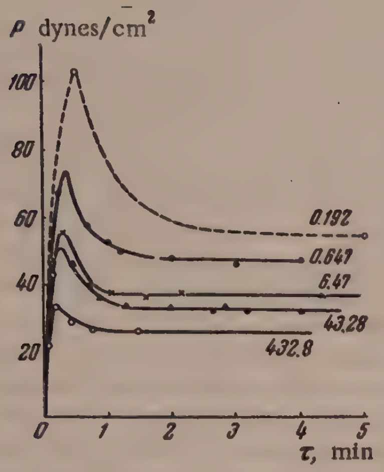

Fig. 5. $P-\tau$ curves for G = 0,192 sec.$^{-1}$, after deformation of ink No. 787 at higher G (shown on the curves in sec. $^{-1}$).

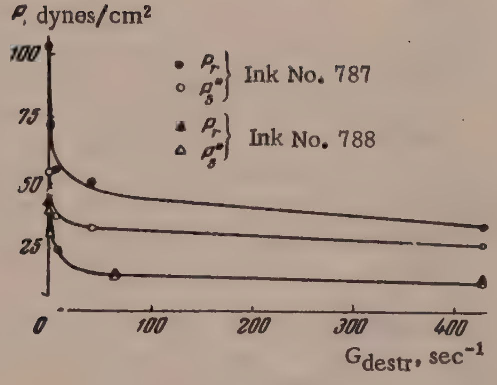

Fig. 6. Variation of P_r and P_s^* at G = 0.192 sec. $^{-1}$ with the value of the destroying G (curves based on data in Fig. 5).

The variation of G with P_s gives an idea of the rheological curve (flow curve). Such a curve would be conclusive only for true equilibrium values of P_s, corresponding to true steady flow. However, as we have seen, in practice true values of P_s are difficult to attain at low G. Therefore quasiequilibrium values of P_s^* can be used to plot at least an approximate rheological curve. Fig. 7 shows a rheological curve of this kind, based on values of P_s^* found from $P-\tau$ curves (at different values of G). In conjunction with this curve it is possible to calculate the effective viscosity of the system, curves for which (as a function of P_s^*) are given in Fig. 8 in two different scales. These curves show that a rapid viscosity increase with decreasing shearing stress begins for both inks at $P_s^* \approx 200-300$ dynes/cm^2 and at G $\approx 2-3$ sec.$^{-1}$.

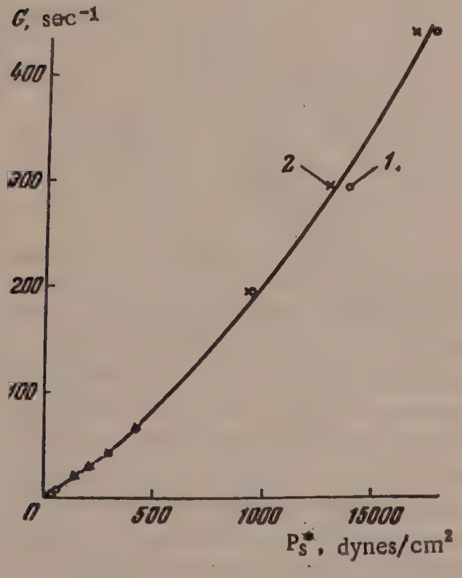

Fig. 7. Rheological $G-P_s^*$ curve for inks No. 787 (1) and No. 788 (2).

As we pass from higher to lower values of G, the values of P_s^* obtained are lower than would correspond to a gradual increase of G and even lower than the true equilibrium values of P_s. These values of P_s^*, found for increasing and decreasing G, may be used to plot hysteresis loops, as shown in Fig. 9 for G < 7 sec. $^{-1}$ (based on the curves in Fig. 5).

A great variety of conditions has been used in different investigations for plotting hysteresis loops, and therefore none of these loops is quite conclusive. Moreover, often it is not known how steady is the value of the shearing stress used in plotting the hysteresis loop. By means of our $P-\tau$ curves, which include the initial deformation region, it is possible to determine the principle of the correct construction of hysteresis loops and to show more clearly which particular stress values give the widest loop, i. e., show its outermost branches.

Further, these data demonstrate the relationship between the hysteresis loop and the rheological curve, and demonstrate the difference between anomalous viscosity and viscosity thixotropy.

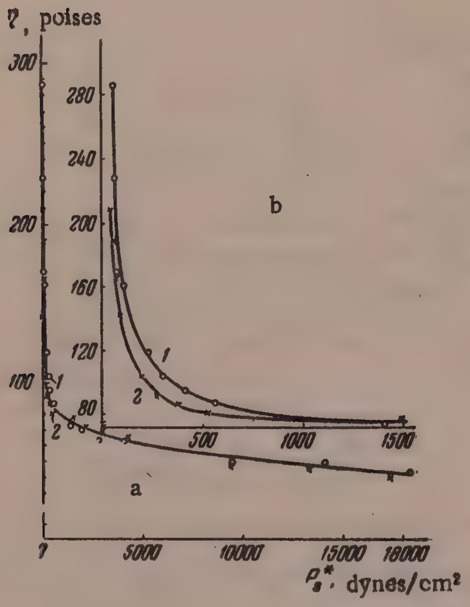

Fig. 8. Viscosity as a function of the shearing stress for inks No. 787 (1) and No. 788 (2): a) on small scale, b) on large scale.

According to Figs. 1 and 2, the $P-\tau$ curves for different τ_b lie one above the other, and hence all values of P_s^* (chosen for any value of τ) increase with τ_b. In general it may be taken that the increases of P_s^* and P_r with τ_b are not necessarily parallel, but may be independent. Therefore the outside, ascending branch of the hysteresis loop should, strictly speaking, be based on values of P_s^* found for each G for a completely restored structure, namely, P_s^* from the highest $P-\tau$ curve. These values of P_s^* will give the furthest (to the right) branch of the hysteresis loop. The left (return) branch of the hysteresis loop should be plotted by means of a rapid transition from the velocity gradient corresponding to a completely destroyed structure (theoretically, from the upper linear region of the rheological curve, but in practice possibly from a smaller gradient) to each given gradient, as shown schematically in Fig. 10 by the curved arrows (a continuous transition from a higher to lower velocity gradients cannot give the correct left branch of the hysteresis loop owing to the continuous restoration of a certain part of the structure during progressive decrease of G).

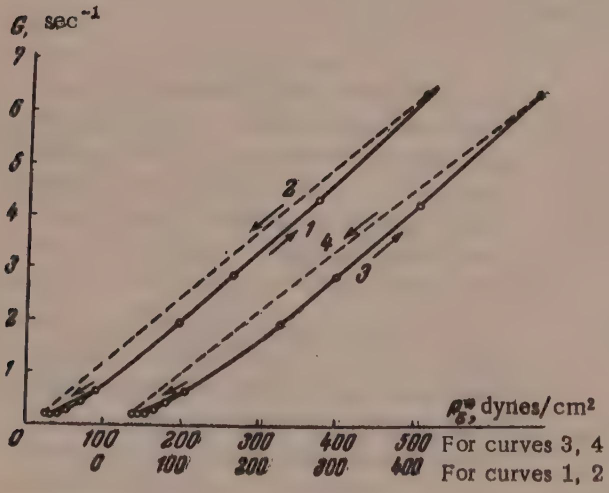

Fig. 9. Examples of hysteresis loops for ink No. 788 (1 and 2), and No. 787 (3 and 4).

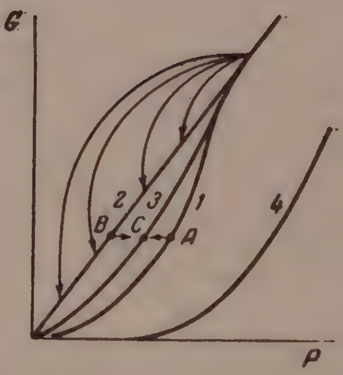

Fig. 10. Schematic $G-P_s$ curves with hysteresis loop (1, 2, 3) and $G-P_r$ curve for a completely restored structure (4).

The choice of the value of P_s^* on the continuous $P-\tau$ curve remains somewhat arbitrary, both in deformation of the undisrupted structure, i. e., in passing "downward", and in deformation of a strongly broken down structure, i. e., in ascent "upward". Clearly, this value of P_s^* must lie somewhere at the end of the steeply descending branch of the $P-\tau$ curve at its transition from the maximum region into the "horizontal" part. In our investigation, the quasiequilibrium P_s^* characterizing the transition from the strength region to the viscosity region was taken to be the value of P_s^* at a distance $10\tau_r$ (τ_r is the time to reach maximum P_r) from the start of the $P-\tau$ curve. The values of P_s^* for the left branch of the loop should be taken from the start of the $P-\tau$ curve corresponding to the establishment of the given G after total breakdown of the structure. This arbitrariness, however, does not invalidate the division of thixotropy into strength and viscosity components, as the mechanism and character of the structure which determine them are different. Moreover, the practical significance, and the possibility of the appearance, of each of these kinds of thixotropy may also differ. For example, if the ink is being continuously agitated on the machine rollers, the most probable manifestation of thixotropic properties will be viscosity thixotropy. Conversely, in the intervals between individual stages of rotation of the ink on the rollers, i. e., when the system is at rest (at $G = 0$), a continuous structural network may be formed in the ink, characterized by the appearance and increase of P_r. However, the viscosity component may greatly increase at the same time, and this determines the subsequent ability of the ink to flow. There is no doubt that the state of the ink on the printing form is closely associated with its viscous properties, and therefore with viscosity thixotropy. At the present time it is still difficult to say whether such thixotropic properties are necessary or detrimental for good printing ink quality. There is no doubt, however, that detailed study of these properties is necessary for a better understanding of the printing process.

In all investigations which use hysteresis loops for evaluation of thixotropy, these are usually represented as two branches, representing the forward (Curve 1, Fig. 10) and the reverse (Curve 2, Fig. 10) course of changes in the deformation rate. On the basis of our data it is possible to trace a third line (Curve 3, Fig. 10†), lying between the two extreme lines, and corresponding to equilibrium values of P_s, reached both in breakdown of the restored structure on prolonged deformation, and in restoration of a strongly broken down structure during continuous rotation at a given G. In Fig. 10 the horizontal arrows show the variation of P_s^* with time (during flow at a given G) in the transition from the restored quasiequilibrium (A) and maximally broken down (B) state of the system to the true equilibrium state (C). During rest of the system, restoration results in transition from the state represented by the point B in Curve 2 to the state represented by the point in Curve 1, i. e., a jump across the true equilibrium viscosity to a quasiequilibrium, higher viscosity of the system.

The middle Curve 3 with the point C represents anomaly of viscosity only. Goodeve [2, 3] determined thixotropy from the rheological curve, thus taking anomaly of viscosity to be thixotropy. In that case it would be impossible to distinguish between anomalously viscous and thixotropic systems. Moreover, a characteristic feature of thixotropy is the variation of the rheological properties of the system with time. Thixotropy must therefore be evaluated from changes of the strength and viscosity properties with time. Strength thixotropy is characterized by variation of the strength P_r with time in relation to the quasiequilibrium P_s^* existing at the given instant of structure restoration. Viscosity thixotropy is characterized by increase, with time, of the quasiequilibrium P_s^* in relation to the minimum P_s^* found for conditions of maximum structural breakdown and corresponding to the extreme left branch of the hysteresis loop. The relationship between the strength and viscosity components of thixotropy is illustrated by the diagram for the variation of these quantities during rest (Fig. 11). The lower line, designated P^*_{SB}, represents the minimum shearing stress, after maximum breakdown, required to maintain a given G at which the strength and viscosity thixotropies are measured (it is interesting to note that measurement of even only the strength component of thixotropy from the values of P_r, as has been done by various workers, must be based on the use of a definite G).

Figure 11 shows curves for the increase of P_s^* and P_r with time for a certain value of G used in the determination, and the curves showing the approach to a true equilibrium P_s "downward" and "upward" with continuous rotation of the outer cylinder. The difference $(P_r - P_s^*)$ gives the strength thixotropy. Complete thixotropic buildup is given by the maximum difference $(P_r - P_s^*)$, (P_r and P_s^* const., independent of τ_b). Such curves may be obtained for different G in accordance with the hysteresis loop. It is evident that the greatest difference $(P_s^* - P^*_{SB})$ in Fig. 11 corresponds to the maximum width of the loop for the given G. On the other hand, the maximum difference $(P_r - P^*_{SA})$ in Fig. 11 corresponds to the abscissa between the line representing P_r as a function of G (Curve 4, Fig. 10) and the right branch of the loop in the same Fig. 10. The full $P_r - P^*_{SB}$ ordinate (Fig. 11) represents the total thixotropic effect, the sum of the strength $(P_r - P^*_{SA})$ and viscosity $(P^*_{SA} - P^*_{SB})$ components. It is clear that if the system has practically no viscosity thixotropy, as is the case for many systems with aluminum naphthenate, the line representing P_s^* as a function of τ_b in Fig. 11 will be absent, and the system will be characterized by strength thixotropy only, represented by $(P_r - P^*_{SB})$, and then $P^*_{SB} = P_{SC} = P^*_{SA}$. In this case there will be no hysteresis loop (Fig. 10), and only Curve 3, representing anomaly of viscosity, will remain. Systems in which the viscosity component of the structure reaches its equilibrium value practically "instantaneously" on change of G evidently have such properties.

---

† Curve 2 is represented as a straight line in accordance with literature data [6, 7]. However, it cannot be assumed that this branch of the loop must always be linear, even with maximum breakdown.

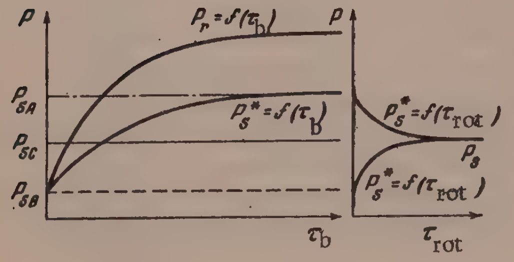

Fig. 11. Variation of P_r and P_s^*, measured at definite G, with the time of structural buildup τ_b (at rest) after maximum (or sufficiently great) breakdown of the structure.

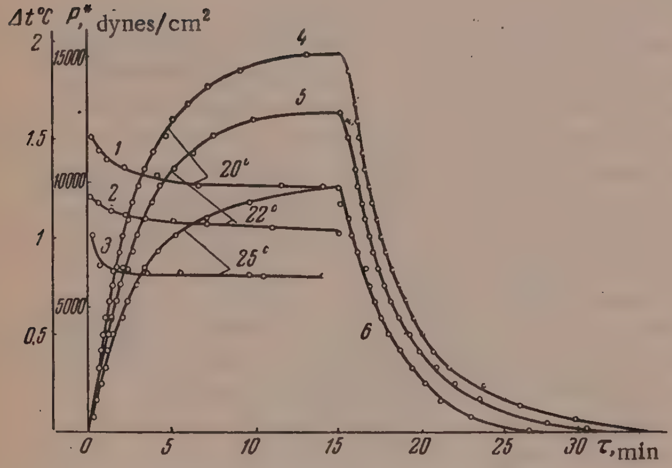

Fig. 12. Curves for $P = f(\tau)$ (Curves 1, 2, and 3) and $\Delta t = f(\tau)$ (Curves 4, 5, and 6) for ink No. 787 at G = 253,9 sec. $^{-1}$ and at initial temperatures of 20, 22, and 25°.

Since, according to our experimental data on printing inks, P_s^* decreased continuously during prolonged deformation, the suggestion arose that this may be related to some extent to a decrease in the viscosity of the system owing to the increase of temperature as the result of rotation. To verify this, the increase in the temperature of the system at the surface of the inner cylinder was measured by means of a thermocouple attached to it. Fig. 12 gives $P = f(\tau)$ and $\Delta t = f(\tau)$ curves for three initial temperatures (20, 22, and 25°) for rotation of ink No. 787 at G = 288.5 sec. $^{-1}$. These curves show that the gradual increase Δt of the ink temperature reaches maximum and constant values after 15 minutes of rotation of 1.94, 1.64 and 1.26° at 20, 22, and 25° respectively.

Consequently, after 15 minutes of rotation of the cylinder thermal equilibrium is established in the system and any further change of viscosity cannot be ascribed to changes of the ink temperature. When the outer cylinder is stopped, the temperature difference falls to zero also in 15-17 minutes. At a low value of G = 0.192 sec. $^{-1}$ there was practically no temperature effect.

In our experiments, in studies of the consecutive influence of large and small values of G, breakdown in the system at large G lasted for not more than 1 minute (30 seconds in a number of experiments), and therefore, according to Fig. 11, the temperature could not rise by more than 0.5°.

Moreover, before measurements at low G (0.192 sec. $^{-1}$), the intervals were 10 minutes, which was evidently quite enough for almost complete equalization of temperature. It follows from these experiments that variation of P_s^* with time can be assumed to be practically independent of the heat effect, and to be the consequence of mechanical breakdown of the structure only.

Mills and Gates [8] found that heat effects may necessitate a certain correction to the hysteresis loop, but did not determine its value.

Thus, the two inks studied, of different composition, are very similar in viscosity at sufficiently high velocity gradients, in the region of almost complete structural breakdown: at G ≈ 433 sec. $^{-1}$ the value foı both inks is $\eta \approx 41$ poises (at 20°). However, they show an appreciable viscosity difference in the region of small velocity gradients of thixotropic buildup, and they differer in the properties of the restored structure and in viscosity after extensive breakdown. Thus, the viscosity measured 10 minutes after passing from $G = 433$ sec.$^{-1}$ to $G = 0.192$ sec.$^{-1}$ is 158 poises for ink No. 787, and 63 poises for ink No. 788. Ink No. 787 quickly regains its properties, and has a relatively high structural network strength and higher P_s, especially in the initial resting stages. This shows that the particles in this ink have greater mobility and are able to interact fairly strongly with each other.

SUMMARY

1. The strength and viscosity of two printing inks, studied by means of an apparatus based on the coaxial cylinder principle, are independent and mutually complementary characteristics of the state of their structure, which vary both with variations of the velocity gradient and during rest of the system or during its continuous deformation. These properties are manifested in different ways in the two inks studied.

2. The thixotropic effect of a system is composed of two components: the strength and the viscosity components. The strength component characterizes breakdown and restoration of the structural network in the colloidal system, and is evaluated by the difference between the maximum strength and the quasiequilibrium shearing stress corresponding to quasistationary flow. The viscosity component, which reflects the breakdown and restoration of separate aggregates of particles, is evaluated by the difference between the quasiequilibrium shearing stresses corresponding to deformation of a structure restored to the limit (or partially) and of a structure broken down to the limit (or partially), and determining the complete (or incomplete) width of the hysteresis loop. It is pointed out that viscosity thixotropy is not identical with anomaly of viscosity.

Institute of Physical Chemistry Acad. Sci. USSR
Moscow

Received March 22, 1956

LITERATURE CITED

[1] M. P. Volarovich, Symposium, Physicochemical Principles of Printing Processes and Investigation of Printing Inks, Trans. Sci. Res. Inst. State United Press, No. 5 (1937).

[2] C. F. Goodeve, G. Whitfield, Trans. Far. Soc. 34, 511, (1938).

[3] J. E. Arnold, C. F. Goodeve, J. Phys. Chem. 44, 652, (1940).

[4] H. Green and R. Weltmann, Physical Chemistry of Clay Suspensions (Translated from English) (State Fuel Tech. Press, 1947).

[5] K. F. Zhigach and D. E. Zlotnik, Factory Labs., No. 5, 542 (1949).

[6] M. P. Volarovich and M. F. Nikishina, Colloid J., 12,169 (1950).

[7] V. L. Valdman, Trans. All-Union Conf. Colloid Chem. (Acad. Sci. Ukrainian SSR Press, Kiev, 1952).

[8] C. C. Mills, E. R. Gates, Analyt. Chem. 25, No. 9 (1953).

[9] N. N. Serb-Serbina and P. A. Rebinder, Colloid J., 9,381 (1947).

[10] E. E. Segalova and P. A. Rebinder, Colloid J., 10,233 (1948).

[11] L. A. Kozarovitsky and S. Ya. Shalyt, Colloid J., 15,437 (1953).

[12] A. A. Trapeznikov and V. A. Fedotova, Proc. Acad. Sci. USSR, 81, 1101 (1951); 82, 97 (1952); 95, 595 (1954).

[13] A. A. Trapeznikov and E. M. Shlosberg, Symposium, New Methods of Physicochemical Investigation of Surface Phenomena, Trans. Inst. Phys. Chem. (Acad. Sci. USSR Press, Moscow-Leningrad, 1950) p. 39.

[14] B. N. Shakhkeldyan, Colloid J., 18, 111, (1956).

EFFECT OF AN ACTIVE FILLER AND A SOLVENT ON THE STRUCTURAL AND MECHANICAL PROPERTIES OF BITUMENS

S. Ya. Shalyt, N. V. Mikhailov, and P. A. Rebinder

The preceding paper [1] gave the results of an investigation of the structural and mechanical properties of various oxidized petroleum bitumens in the temperature range of 40-160°. The temperature limits for the transition of the bitumen from one rheological state into another were determined from the relationship between the limiting viscosity values and the temperature. The region of the fluidlike state was studied in particular detail. Complete S-shaped rheological curves were obtained, from which a number of important characteristics could be determined: η_0, the maximum viscosity of the practically intact structure; η_m, the minimum viscosity of the structure broken down to the limit; and values of P_r', the conventional strength limit (the start of appreciable breakdown) and P_m', the limit of maximum structural breakdown.

It was of considerable interest to study the effect of an active disperse filler, which reinforces the bitumen structure, and a solvent which plasticizes it, as we had shown that by additions of filler and solvent in certain proportions it is possible to obtain a new system with a predetermined fairly high maximum viscosity η_0, with a simultaneous decrease of thermosensitivity, i. e., of the temperature coefficient of viscosity. The results of this investigation are presented in this paper.

Effect of active filler. The active filler used was fine calcium hydroxide powder, slaked lime. When anhydrous calcium oxide (quicklime) is made to react with the exact stoichiometric amount of water by the chemical dispersion method [2], the hydration reaction yields highly disperse slaked lime powder; from 2 to 25% of the total volume of this mixture was introduced into the bitumen. The hydrophilic surfaces of the filler particles form surface chemical compounds, calcium soaps, with the asphaltogenic acids of the bitumen; these compounds render the filler surface hydrophobic and improve its wetting by the bitumen. Diffuse structurized bitumen layers are thereby formed around the filler particles (Fig. 1), with highest viscosity in the layer directly adjacent to the particle surface owing to adsorption of the high molecular weight components and adhesion of the colloidal components of the bitumen.

To prepare the mixture, the bitumen was heated to 120-130° until moisture was completely removed, and the lime powder was then introduced into the hot bitumen. The mixture was thoroughly stirred and heated again until its surface became glossy. The hot mixture was poured into the space between the coaxial cylinders.

It was shown in the preceding paper that the maximum viscosity η_0 of the bitumen is its fundamental physicochemical property which reflects the characteristics of the intact structures formed by the bitumen micelles. Therefore we used the values of the maximum initial viscosity η_0 of the undestroyed structure to characterize the structural and mechanical properties of bitumen — filler systems.

For this, the initial regions of the ϵ (P) rheological curves were plotted for temperatures of 65, 75, and 85°. A sharply defined critical degree of volume filling was found (Table 1), evidently corresponding to the formation of a new spatial structure involving the active filler grains [3]. The explanation for this is that, at low filler contents, the particles with the structurized bitumen layers do not interact and no interlayers of more highly structurized bitumen are present between them (Fig. 2a). In such a case the viscosity variation may be represented by a linear equation of the Einstein equation type $\eta_0(\varphi) = \eta_0(0)(1 + \alpha\varphi)$, where $\eta_0(\varphi)$ is the viscosity of the mixture; $\eta_0(0)$ is the viscosity of the medium, α is the shape and solvation factor for the particles, and φ is the volume content of filler in the mixture:

$$100\varphi = \frac{c_1}{D_1} \cdot \frac{100}{100 + c_1/D_1},$$

where c_1 is the amount of filler in grams per 100 g of bitumen, and D_1 is the density of the filler.

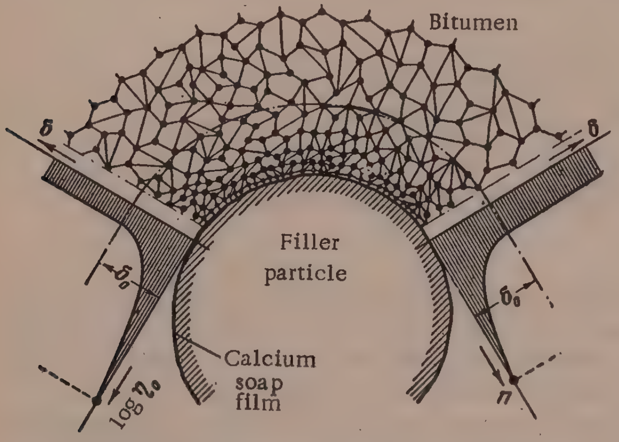

Fig. 1. Formation of a diffuse structurized bitumen layer on a filler particle.

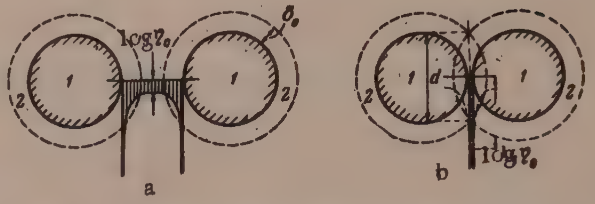

Fig. 2. Interaction of filler particles at low (a) and high (b) contents of filler in the mixture: 1) filler particles; 2) diffuse structurized layers on the filler particles.

TABLE 1

Maximum Viscosity η_0 and Thermosensitivity Coefficient K for a Mixture of Grade III Bitumen with Different Filler Concentrations (c_1 in g/100 g of bitumen) at Various Temperatures

c_1	100φ	65°			75°			85°			$K \cdot 10^3$ for 65—85°
		$\eta_0 \cdot 10^{-3}$ poises	$\log \eta_0$	$\frac{\eta_0(\varphi)}{\eta_0(0)}$	$\eta_0 \cdot 10^{-3}$ poises	$\log \eta_0$	$\frac{\eta_0(\varphi)}{\eta_0(0)}$	$\eta_0 \cdot 10^{-3}$ poises	$\log \eta_0$	$\frac{\eta_0(\varphi)}{\eta_0(0)}$	
0	0	4.15	3.62	1.00	1.25	3.11	1.00	0.470	2.67	1.00	4.50
5	2.33	4.76	3.68	1.14	1.58	3.20	1.26	0.540	2.73	1.15	4.50
10	4.55	5.30	3.72	1.28	1.78	3.25	1.42	0.610	2.79	1.29	4.50
15	6.68	6.00	3.78	1.44	1.86	3.27	1.48	0.680	2.83	1.44	4.50
20	8.70	6.50	3.81	1.56	2.10	3.32	1.68	0.750	2.87	1.59	4.50
30	12.5	7.95	3.90	1.91	2.69	3.43	2.15	1.02	3.01	2.17	4.50
40	16.0	11.5	4.06	2.77	3.90	3.59	3.12	1.29	3.11	2.75	4.50
50	19.2	25.5	4.41	6.15	8.00	3.90	6.40	2.30	3.36	4.90	5.20
60	22.2	62.0	4.79	4.9	14.0	4.15	11.2	3.00	3.48	6.39	6.50
70	25.0	76.0	5.88	183	115	5.06	92.3	20.4	4.31	43.5	7.80

With a higher content of filler the particles with their structurized bitumen layers interact and a contact region of diameter h, consisting of highly structurized bitumen, is formed between them (Fig. 2,b).

The coefficient α was found to be 7.5 for different bitumens and temperatures (Fig. 3), both because the particles were not spherical and because of solvation — the presence of structurized layers of bitumen on the surfaces.

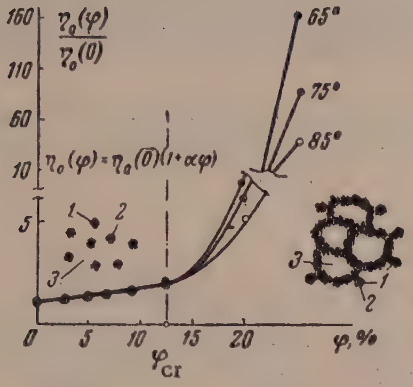

Fig. 3. Change of relative viscosity $\frac{\eta_0(\varphi)}{\eta_0(0)}$ of bitumen as a function of the volume content of $Ca(OH)_2$ filler at temperatures of 65, 75, and 85°: 1) filler particles; 2) diffuse structurized bitumen layers on the filler particles; 3) dispersion medium – bitumen; 4) contact between two filler particles, consisting of highly structurized bitumen.

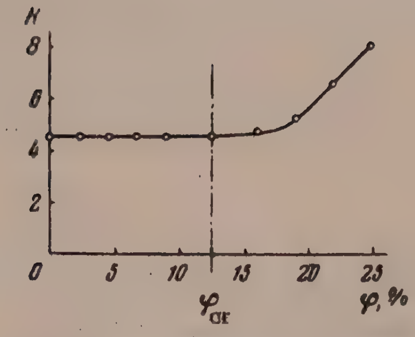

Fig. 4. Thermosensitivity coefficient of bitumen as a function of its volume content of active filler.

Figure 3 shows the variation of the relative viscosity of the mixture of bitumen and filler ($\eta_0(\varphi)/\eta_0(0)$) with the volume content of the filler at 65, 75, and 85°. Fig. 3 shows that at a volume content above the critical value, corresponding to 12.5-16% by volume of the active filler, the viscosity η_0 increases sharply owing to interaction of the active filler particles by their diffuse structurized outer layers (Fig. 2b). A new coagulation structure is formed, with the active filler grains acting as centers of structure formation. The calcium soaps of the asphaltogenic acids, which must be considered as the natural activators of the added filler, evidently play an important part in the formation of the continuous structural network. The structurizing action of the filler, as was to be expected, rapidly weakens with increase of temperature. Thus, with 25% by volume of the filler in the mixture, the viscosity of grade III bitumen is increased 183-fold at 65°, 92-fold at 75°, and 43-fold at 85° (Fig. 3 and Table 1).

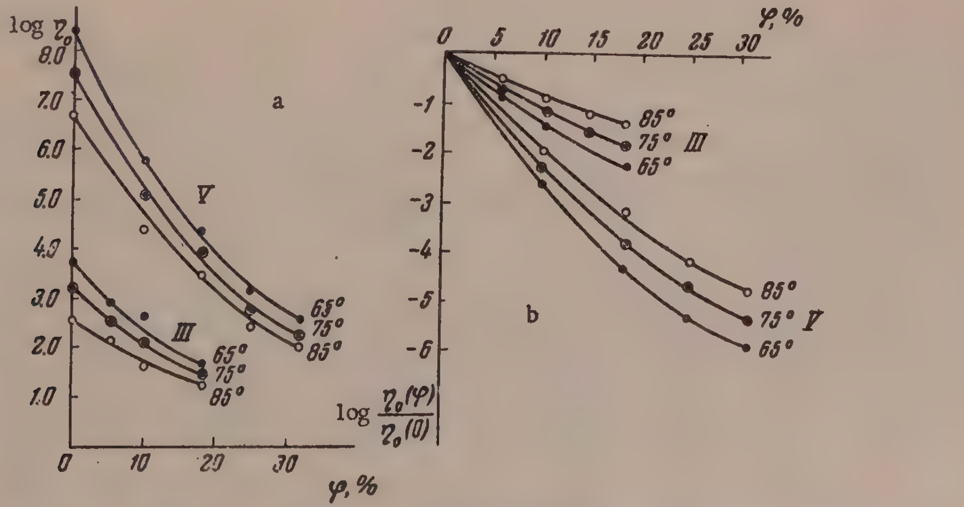

Fig. 5. Variation of maximum viscosity (a) with volume content of solvent in grade III and V bitumens at 65, 75, and 85°, and variation of the maximum relative viscosity $\log\frac{\eta_0(\varphi)}{\eta_0(0)}$ of grade III and V bitumens (b) with content of solvent φ.

The log η_0 (t) relationship found was used to calculate the thermosensitivity coefficients $K = -d\log\eta_0/dT$. It was found (Table 1 and Fig. 4) that, below the critical degree of filling, the thermosensitivity coefficient does not differ from that for the pure bitumen. Further increase of the filler content produces a sharp increase in the thermosensitivity coefficient owing to formation of a secondary structure. Thus, for grade III bitumen, K increases from $4.5\cdot10^{-2}$ to $7.8\cdot10^{-2}$, which is a 1.7-fold increase.

Effect of solvent. The effect of a solvent on the structural and mechanical properties of grade III and V bitumens was studied. The solvent used was a nonvolatile technical solvent, green oil, which is the usual plasticizer for bitumen. Green oil consists mainly of aromatic hydrocarbons of high molecular weight, and at room temperature is a true-viscous (Newtonian) liquid.

5, 10, 15, and 20 g of green oil per 100 g of pure bitumen was added to grade III bitumen, and 10, 20, 30, and 40 g to grade V bitumen. The volume content φ of green oil in the system was defined as

$$100\varphi = \frac{c_2}{D_2}\cdot\frac{100}{100+\frac{c_2}{D_2}},$$

where c_2 is the amount of solvent in grams per 100 g of bitumen, and D_2 is the density of green oil ($D_2 \approx 0{,}90$).

The values of the maximum viscosity η_0 of the practically undestroyed structure were used to characterize the systems. For determination of the values of η_0, the initial regions of the rheological $\dot{\varepsilon}$ (P) curves were studied at 65, 75, and 85°.

The results are given in Table 2. Fig. 5,a shows the variation of the maximum viscosity (η_0) with volume content of filler in bitumens III and V at 65, 75, and 85°. Fig. 5,b shows the variation of the maximum relative viscosity $\left(\log\frac{\eta_0(\varphi)}{\eta_0(0)}\right)$ of bitumens III and V with the amount of solvent present (φ). The effects of the solvent are enormous even with relatively small amounts of solvent present. The viscosity decrease is especially great for the most structurized bitumen (grade V) at lower temperatures (65°). As was to be expected, the solvent effect is greatest for the strongest, i. e., the most viscous, bitumen structures, where this effect is used in practice for plasticization. Thus, addition of 20% of green oil to bitumen produces a 100-fold decrease of viscosity in grade III bitumen and 10,000-fold in grade V bitumen.

The thermosensitivity coefficient of bitumen also falls considerably with increasing solvent content (Fig. 6); for grade III bitumen from $4.5\cdot10^{-2}$ to $0.85\cdot10^{-2}$, and for grade V bitumen from $9.1\cdot10^{-2}$ to $1.9\cdot10^{-2}$. The variation of the thermosensitivity coefficient with solvent content can be represented by the linear relationship $K(\varphi) = K_0 - \beta\varphi$, where K_0 is the thermosensitivity coefficient of pure bitumen, while the coefficient β, which represents the degree of decrease of K on addition of solvent, can be termed the coefficient of solution.

TABLE 2

Maximum Viscosity η_0 and Thermosensitivity Coefficient for Mixture of Grade III and V Bitumens with Green Oil

Bitumen grade	c_2 of solvent per 100 g bitumen	100φ	65°		75°		85°		$K\cdot10^2$
			$\eta_0\cdot10^{-3}$ poises	log η_0	$\eta_0\cdot10^{-3}$ poises	log η_0	$\eta_0\cdot10^{-3}$ poises	log η_0	
III	0	0	4.15	3.62	1.25	3.11	0.470	2.67	4.50
	5	5.25	0.783	2.90	0.312	2.50	0.145	2.16	3.70
	10	10.0	0.240	2.38	0.110	2.04	0.0570	1.76	2.90
	15	14.3	0.0700	1.85	0.0460	1.66	0.0330	1.52	1.60
	20	18.2	0.0330	1.52	0.0280	1.45	0.0223	1.36	0.85
V	0	0	300000	8.48	39000	7.59	4500	6.65	9.10
	10	10.50	1020	6.01	180	5.26	36.0	4.56	7.25
	20	18.2	25.0	4.40	12.0	4.08	4.50	3.65	4.55
	30	25.0	1.46	3.16	0.760	2.88	0.360	2.56	3.05
	40	30.1	0.265	2.42	0.150	2.18	0.110	2.04	1.90

Combined effect of active filler and solvent on the structural and mechanical properties of bitumens. The investigations show that it is possible to control the structural and mechanical properties of bitumens by plasticization of the spatial structure by means of green oil followed by structurization by addition of active filler to the previously plasticized system.

We investigated, at 65, 75, and 85°, grade III bitumen diluted with 20% of green oil with subsequent additions of 30, 50, 60, and 70% of lime powder, and grade V bitumen diluted with 40% of green oil with subsequent addition of 20, . 40, and 50% (by weight of the mixture) of lime powder.

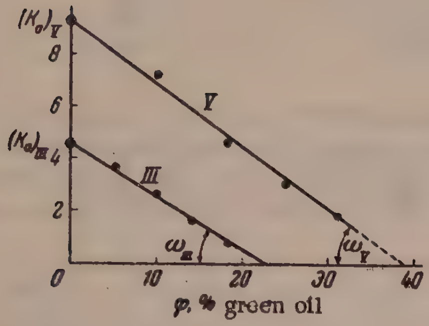

Fig. 6. Variation of the thermosensitivity coefficient of grade III and V bitumens with solvent content.

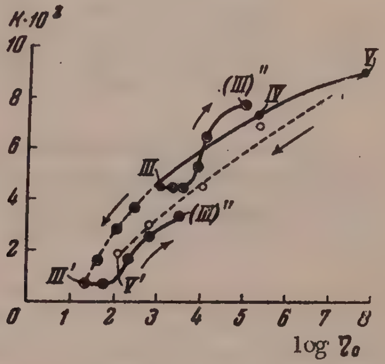

Fig. 7 . Variation of the maximum viscosity η_0 and thermosensitivity coefficient by the simultaneous action of active filler and solvent at 75° . Roman numerals indicate the grade of bitumen; primes represent dilution by green oil; double primes represent addition of active filler.

The volume content of active filler in the system was defined as

$$100\varphi = \frac{(100+c_2)\,c_1'}{D_1} \Bigg/ \left[100 + \frac{c_2}{D_2} + \frac{(100+c_2)\,c_1'}{100D_1}\right],$$

where φ is the degree of filling of the system by the active filler; D_1 and D_2 are the densities of the filler and solvent respectively; c_1 is the amount of filler added per 100 g of the solution of bitumen and green oil; c_2 is the amount of solvent added per 100 g of bitumen.

The initial regions of the rheological curves were investigated, and the systems were characterized by the values of the maximum initial viscosity η_0 for the practically undestroyed structure. The results are given in Table 3.

Thus it is seen that the combined action of solvent and filler is of special practical importance, as it makes possible the production of a new bitumen system with a decreased thermosensitivity coefficient (decreased from $K = 4.5 \cdot 10^{-2}$ to $K = 3.6 \cdot 10^{-2}$ for grade V bitumen) in comparison with pure bitumen and with values of the viscosity η_0 for the practically undestroyed structure increased about tenfold (from 312 to 3340 poises) (Fig. 7) . This interesting result depends on the different effects of the solvent on the structures of bitumens with different maximum viscosities. The higher the maximum viscosity of the bitumen system without filler, the greater will be the liquefying effects of added solvent and increase of temperature. However, when the increase of maximum viscosity is caused by a secondary structure formed by the filler particles, additions of solvent or increase of temperature produce much smaller decreases of viscosity. Thus, by adding solvent to the bitumen and then thickening the system to the original value of the maximum viscosity by addition of active filler, it is possible to lower the thermosensitivity coefficient.

TABLE 3

Maximum Viscosity η_0 and Thermosensitivity Coefficient K for Mixtures of Different Grades of Bitumen with Green Oil, at Different Contents of Active Filler

c'_1	100φ	65°			75°			85°			$K\cdot 10^{6}$
		η_0 poises	log η_0	$\frac{\eta_0(\varphi)}{\eta_0(0)}$	η_0 poises	log η_0	$\frac{\eta_0(\varphi)}{\eta_0(0)}$	η_0 poises	log η_0	$\frac{\eta_0(\varphi)}{\eta_0(0)}$	
Grade III bitumen + 20 g of green oil per 100 g of bitumen											
30	12.3	62.50	1.80	1.89	45.00	1.65	1.60	35.00	1.54	1.56	0.850
50	19.0	354.0	2.55	10.7	220.0	2.34	1.85	158.0	2.20	1.10	1.75
60	21.8	1350	3.13	40.9	724.0	2.86	25.8	390.0	2.60	17.5	2.69
70	24.6	7300	3.86	221	3340	3.52	119	1590	3.20	71.8	3.31
Grade V bitumen + 40 g of green oil per 100 g of bitumen											
20	9.2	400	2.60	1.51	227	2.36	1.51	150	2.18	1.36	1.90
40	15.6	750	2.88	2.85	386	2.56	2.57	220	2.34	2.00	2.66
50	18.7	1750	3.24	6.62	759	2.88	5.03	399	2.60	3.64	3.21

SUMMARY

1. When slaked lime powder, an active filler, is added to bitumen, a sharply defined critical region of volume filling is found, corresponding to the formation of a new spatial structure involving the active filler grains. When the degree of volume filling is above the critical value, the viscosity η_0 and the thermosensitivity coefficient both increase sharply with increasing filler content.

2. Addition of green oil solvent to bitumen causes plasticization effects in the spatial structure, opposite to the effects of the active filler, and both the viscosity η_0 and the thermosensitivity coefficient decrease rapidly with increasing solvent content.

3. By combined addition to bitumen of an active disperse filler, which reinforces its structure, and a solvent, which plasticizes it, in definite proportions, it is possible to attain a required high viscosity η_0 with a simultaneous decrease of the heat sensitivity of the mixture.

Scientific Research Institute for Building
Ministry of Construction USSR
Moscow

Received November 28, 1956

LITERATURE CITED

[1] N. V. Mikhailov and S. Ya. Shalyt, Colloid J., 18, No. 5, 609 (1956).

[2] P. A. Rebinder and G. I. Loginov, J. Acad. Sci. USSR, 10, 47 (1951); G. I. Loginov, P. A. Rebinder, and V. P. Sukhova, Proc. Acad. Sci. USSR, 98, 2, (1954).

[3] P. A. Rebinder, G. A. Ab, and S. Ya. Veiler, Proc. Acad. Sci. USSR, 31, 5, 444 (1941); Ya. B. Aron and P. A. Rebinder, Proc. Acad. Sci. USSR, 52, 3, 235 (1946); A. S. Kolbanovskaya and P. A. Rebinder, Colloid J., 12, 3, 208 (1950).

LETTER TO THE EDITOR

POSSIBLE DIFFERENCES IN THE COMPOSITION AND VISCOSITY RATIO OF A TWO-SIDED FILM AND A SURFACE LAYER OF A SOAP SOLUTION

A. A. Trapeznikov

The question of the structure and properties of two-sided soap (and similar) films is of great interest. It has been repeatedly studied by various methods: optically [1, 2, 3, 4, 5], conductometrically [6], by the froth method [7, 8], etc. Our method of measurement of the surface viscosity or strength (or other mechanical characteristics) is especially effective.

It is generally assumed that the composition and structure of the adsorption layers in foam films and in the surface of the solution from which the foam is formed are identical. If the solution contains more than one component, the components with the greatest surface activity pass into the adsorption layer of the solution surface and into the foam. It is usually supposed that such components are transferred equally in both cases, and consequently the composition and properties of the adsorption layers in the foam films and the solution surfaces are assumed to be the same. For example, this assumption is the basis of the frequent verification of the Gibbs equation by analysis of the composition of the destroyed foam from a solution. Similar assumptions are made when the surface tensions of solutions obtained from destroyed foams and the original solutions are compared.

Of interest in this connection are our experiments which show a difference in composition and properties of the adsorption layers in two-sided films and in the surface of the solutions from which the films are formed. The differences are cause by different rates of adsorption and with differences in the kinetics of layer formation from different components.

Differences of surface activity in such cases are seen not only in different degrees of surface tension lowering in equilibrium conditions, which is how surface activity is usually determined, but also in different mobilities of the solution components, and the special ability of some of them, evidently the more mobile, to migrate two-dimensionally and to pass into two-sided films as they become detached. This also shows that the mechanism of formation of a two-sided film involves a natural fractionation of different surface-active components, a sort of filtration of them at the instant when the two-sided film is detached from the solution surface.

A solution of a mixed soap, consisting of sodium palmitate and oleate in 1:9 ratio, was studied. The solution was warmed to 40° and cooled rapidly to 18° . In these conditions, after complete solution of the soap and cooling of the solution, sodium palmitate is held in solution for some time and then begins to separate out as a fine precipitate (apparently as an acid soap, which disappears on addition of alkali).

If, during aging of such a solution, two-sided films and adsorption layers on the solution surface form from such a solution, and their resistance to shear is measured between concentric horizontal platinum wire rings by a method described previously [9], the shearing deformation curves shown in Fig. 1 can be obtained. Here the serial numbers represent the sequence of formation and measurement of the surface layers or films, formed anew each time by raising and lowering the solution level, i. e., after stirring the solution. Therefore consecutive measurements reflect, not the aging of adsorption layers or films, but the aging of the solution in bulk and the precipitation of palmitate from the solution, i. e., changes in the composition of the solution.

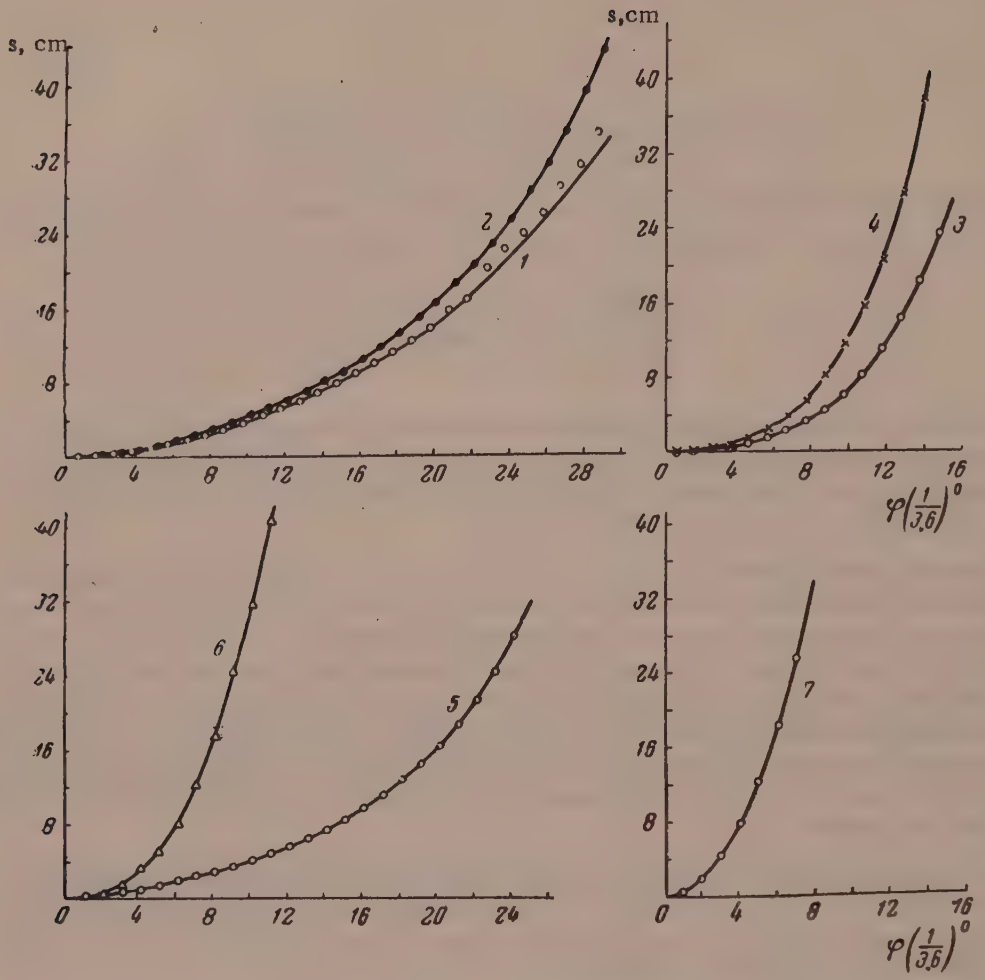

Fig. 1. Deformation S vs. angle of rotation ρ for the solution surface and two-sided films, measured in the sequence shown by the numbers, in a 1:9 palmitate — oleate soap solution; c_{total} = 2.7 millimoles / liter; 1 and 2) surface; 3 and 4) two-sided film; 5) surface; 6) film; 7) surface.

Fig. 2 shows curves for variation of the deformation rate with the torque $dS/d\varphi = f(\varphi - \theta)$. Although these curves are not linear (they indicate the existence of a structure in the films), and were obtained for conditions of not quite steady flow, the viscosity in surface poises (η_s , g / second) can be approximately calculated from their lower regions. The values of η_s are given in the Table and are shown graphically in Fig. 3 in order of the measurements.

It follows from the curves in Fig. 3 that the surface layer of a rapidly cooled solution has a high surface viscosity, ~ 7.0 surface poises, which persists during the first stages of aging of the solution, corresponding to the first 5 measurements (~ 1 hour), after which the high surface viscosity rapidly decreases to negligibly small values [10].

The viscosity of two-sided films (calculated on the full thickness) is even at the start 1.75 times less than the viscosity of the surface layer of solution (it must be remembered that a two-sided film has 2 adsorption layers, and therefore the difference for one layer is a factor of 3.5), while with aging of the solution (increasing number of the determination) it decreases to values of the order of $3 \cdot 10^{-5}$ surface poises.

It is significant that while the viscosity of the surface layer of the solution remains for some time at the same level, the viscosity of the films formed from the same solution decreases fairly rapidly and systematically.

The viscosity of the surface layer decreases extremely rapidly somewhat later, and practically overtakes the film viscosity. Thus, throughout the aging and decomposition of the solution, accompanied by deposition of the precipitate, the ratio of the viscosities of the film and the surface, if it is calculated from the ordinates of the curves, varies continuously. It decreases at first, and then increases again. Thus, for unstable solutions of this type the ratio of the viscosities of the two-sided film and the solution surface is not constant.

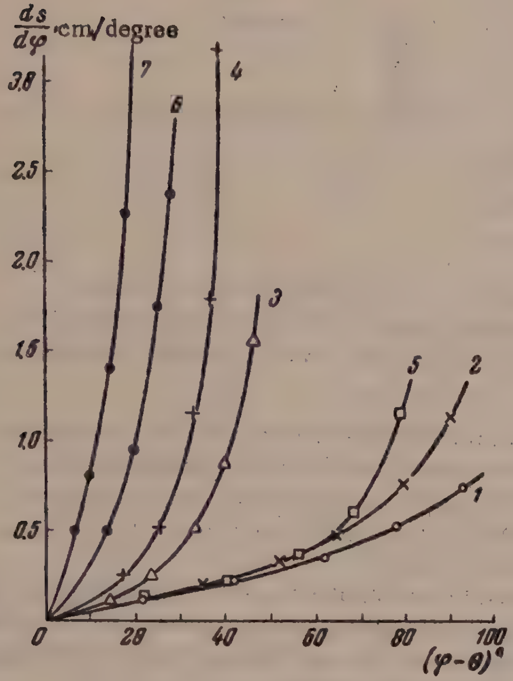

Fig. 2. Curves for the deformation rate as a function of the torque $dS/d\varphi = f(\varphi - Q)$, based on the $S-\varphi$ curves of Fig. 1. Numbering of the curves is the same as in Fig. 1.

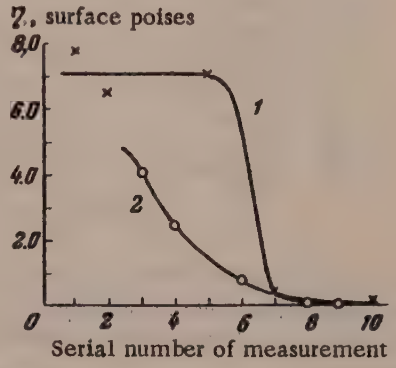

Fig. 3. Variation of the viscosity of the surface layer of solution and the two-sided films in the sequence of measurements, for a 1:9 palmitate – oleate solution.

These results show that the composition of the adsorption layers in two-sided films and at the solution surface may differ. During formation of the film, as it becomes detached from the solution surface, the more mobile components probably pass into it. In this instance they are less viscous and consist mainly of sodium oleate, while the more viscous component – sodium palmitate – remains in the bulk of the solution. However, it cannot be said in general that the less viscous components will always pass into the two-sided film. In a number of cases the reverse probably occurs, when the total viscosity of the 2-sided film is more than double that of the adsorption layer on the solution surface; this difference should be attributed to differences in the composition of the adsorption layer, and not to the additional high viscosity of the intermediate "volume" part of the two-sided film, although the role of this factor is not, of course, excluded in principle. It may be that in the mixed sodium palmitate and oleate soap solution mixed micelles are formed, which persist unchanged at first after the solution is cooled. However, during adsorption these micelles may break up into their components, the process being more intensive in the two-sided film.

These results show that adsorption at the foam films is selective in comparison with adsorption at the solution surface, and that the composition of the adsorption layers in both cases greatly depends on the adsorption kinetics of all the components and probably on the rate of film formation.

The viscosity differences between the film and the surface layer of solution are especially prominent in the case under consideration, when different components are present. In solutions of individual soaps, such as sodium myristate or palmitate, the two-sided film and solution surface differ less in composition and structure [10]. In such cases differences in the adsorption of the solution components may be attributed to formation of dissociated and undissociated soap micelles, formation of free acid or acid soap, etc., with different adsorptions and mobilities in the bulk of the solution and in the surface layer.

Viscosities of Two-Sided Films and Surface layer of a Mixed 1:9 Palmitate – Oleate Soap Solution; c_{total} = 2.7 millimole/liter*

Serial number of measurement	Object of measurement	η_s in surface poises		$\eta_{s_{film}}/\eta_{s_{surf}}$ calculated from curves in Fig. 3	State of solution
		surface	film		
1	Surface	7.7	—	--	—
2	Surface	6.4	—	---	—
3	Film	--	4.05	0.58	Turbidity
4	Film	—	2.42	0.346	»
5	Surface	7,0	—	0.214	»
6	Film	—	0.75	0.15	»
7	Surface	0.24	—	0.90	Copious turbidity
8**	Film	—	0.0063	—	» »
9	Film	—	0.0005	--	» »
10	Surface	0.00005	—	—	» »
11	Film	—	0.000029	—	» »

---

* Radii of the rings R_1 = 2.738 cm, R_2 = 2.995 cm; wire diameter 0.1 cm; elasticity constant of wire C_0 = 2.81 dynes·cm/radian, its diameter d = 0.005 cm; moment of inertia of the system M = 84.9 g cm^2.

** The values of η_s for the films and surface were obtained by the torsional vibration method, starting with measurement No. 8.

It follows from the foregoing that, in the general case, complete identity of composition and properties of the adsorption layers at the solution surface and in two-sided isolated films or in foam cannot be expected, even if their formation time is (macroscopically) the same. This applies especially to systems of complex composition, many of which are good foaming or wetting agents, used in practice, but it probably holds to a certain extent for all cases, even the simplest "individual" foaming agents.

It is often throught that, at concentrations above the critical concentration of micelle formation, complete soap micelles are adsorbed at once. Apparently it is necessary to take into account the possibility of their decomposition in the course of adsorption, especially at a two-sided foam film, and the possibility of extraction of the most surface-active and mobile components from the micelles in the process.

Institute of Physical Chemistry Acad. Sci. USSR
Moscow

Received January 9, 1957

LITERATURE CITED

[1] J. Perrin, Ann. de phys. 10, 160, (1918).

[2] P. V. Wells, Ann. de phys. 16, 39, (1921).

[3] K. S. Jochonott, Phil. Mag. 47, 501,(1899); 11, 716, (1906).

[4] S. Spierer, Koll.-Z. 54, 17, (1931).

[5] B. V. Deryagin and A. S. Titievskaya, Colloid J., 15, 416 (1953).

[6] W. Rikenbacker, Koll. chem. Beih. 8, 139, (1916).

[7] M. E. Laing, Proc. Roy. Soc. A109, 28, (1925).

[8] A. P. Brady, J. Phys. Coll. Chem.53, 56 (1949); A. Brady, and A. Brown, article in Symposium "Monomolecular Layers," translated from English (Foreign Lit. Press, Moscow, 1956).

[9] A. A. Trapeznikov, Symposium, Viscosity of Liquids and Colloidal Solutions, 1,67, 87,(1941).

[10] P. A. Rebinder and A. A. Trapzenikov, Proc. Acad. Sci. USSR, 18, 421 (1938).

COLLOID JOURNAL OF THE U.S.S.R. IN ENGLISH TRANSLATION

March-April, 1957

TABLE OF CONTENTS

	Page	Russ. page
1. On the Fiftieth Birthday of Valentin Alekseevich Kargin	139	129
2. The Structure of Linear Polymers. V. A. Kargin, A. I. Kitaigorodsky, and G. L. Slonimsky	141	131
3. Molecular Configuration and Structure Formation in Polyacrylate Solutions. V. A. Kargin and N. F. Bakeev	143	133
4. The Formation of Crystalline Aluminosilicates. Z. Ya. Berestneva, M. B. Konstantinopolskaya, and V. A. Kargin	149	138
5. Study of the Transition of Amorphous and Crystalline Polymers from the Solid into the Fluid State on Addition of Substances of Low Molecular Weight. V. A. Kargin, G. L. Slonimsky, and L. Z. Rogovina	153	142
6. Adsorption of Polystyrene Latexes in Relation to the Sign of the Particle Charge and the Sorbent. E. M. Aleksandrova and N. S. Razumikhina	159	148
7. The Relationship Between the Structure of Emulsifiers of the Alkylaromatic Acid Type and the Polymerization of Unsaturated Compounds. 4. Salts of Di-Sec-Butylnaphthalenesulfonic Acid with Univalent Cations. N. P. Apukhtina and A. M. Lyagalova	165	154
8. Investigation of the Aqueous Properties of Peat by Means of Radioactive Isotopes. M. P. Volarovich, N. V. Churaev, and B. Ya. Minkov	171	159
9. Heats of Swelling and of Solution of Nitrocellulose. D. I. Galperin and L. I. Moseev	179	167
10. Investigations of the Physical Chemistry of Agar. 1. Method for the Determination of the Intrinsic Viscosity of Agar. S. A. Glikman and I. G. Shubtsova	183	172
11. Aggregative Stability of Pigment Suspensions in Hydrocarbons, Alcohols, and Esters of Low Molecular Weight. Ya. M. Gurevich	189	178
12. Dependence of the Exchange Adsorption of Ions on their Structure. 2. Adsorption of Bivalent Amines. A. T. Davydov and R. F. Skoblionok	193	183
13. The Influence of Structure on the Chemical Activity and Vulcanizability of Butadiene Polymers. B. A. Dogadkin, A. V. Dobromyslova, F. S. Tolstukhina, and N. G. Samsonova	199	188
14. The Use of High Frequency Analysis in Colloidochemical Investigations. V. I. Ermakov, V. N. Maslov and O. G. Stolyarov	207	198
15. The Structure of Gels. 9. Effect of the Nature of the Plasticizer on the Physicomechanical Properties of Divinyl-Styrene Rubber. M. P. Zverev and P. I. Zubov	211	201
16. The Hardening Mechanism of Thermosetting Plastics (Molding Powders). I. F. Kanavets, L. G. Batalova, and A. G. Romashova	215	204

COLLOID JOURNAL OF THE U.S.S.R. IN ENGLISH TRANSLATION

March-April, 1957

TABLE OF CONTENTS (Continued)

	Page	Russ. page
17. Electron Microscope Studies of Colloids. 1. Minerals of the Kaolinite-Halloysite Group. M. I. Kuadzhe	229	219
18. The Mechanism of Protein Denaturation. 10. Effect of Fatty Acid Anions on the Stability of Globular Proteins to Denaturation. A. L. Loseva and A. S. Tsyperovich	233	222
19. Gelation of Latexes on Porous Forms. D. M. Sandomirsky	239	228
20. The Thixotropic Properties of Certain Printing Inks. A. A. Trapeznikov and T. G. Shalopalkina	243	232
21. Effect of an Active Filler and a Solvent on the Structural and Mechanical Properties of Bitumens. S. Ya. Shalyt, N. V. Mikhailov, and P. A. Rebinder	253	244

Letter to the Editor

	Page	Russ. page
22. Possible Differences in the Composition and Viscosity Ratio of a Two-Sided Film and a Surface Layer of a Soap Solution. A. A. Trapeznikov	259	252

JOURNAL OF

ANALYTICAL CHEMISTRY

OF THE USSR

in complete English translation

The top Russian journal in this field, dealing with all phases of analysis, organic and inorganic, including metallurgy, petroleum, spectrochemistry. Sample articles: A simple rational design for the elementary cell of a counter current distribution apparatus; a potentiometric method of determining saponification numbers in solutions of petroleum resins; potassium tetraborate as a primary standard in acidimetry. Translation began with the 1952 volume. Annual subscription, 6 issues, approximately 800 pages, $80.00.

CONSULTANTS BUREAU, INC.

227 WEST 17th STREET, NEW YORK 11, N. Y.

JOURNAL OF

APPLIED CHEMISTRY

of the USSR ***(Prikladnoi.)***

in complete English translation

Covers all aspects of applied research: New porcelain glazes; ozone production by silent electrical discharge; hydrogen fluoride as a cracking catalyst; effect of gelatin on the optical sensitization of photographic emulsions. Of particular interest to chemical engineers, due to its extensive coverage of applications in methods and equipment. Translation began with the 1950 volume. Annual subscription, 12 issues, approximately 2000 pages, $95.00.

Single articles available—Tables of Contents on request.

CONSULTANTS BUREAU, INC.

227 WEST 17TH STREET, NEW YORK 11, N. Y. ALGONQUIN 5-0713